THE STRENGTHENING OF SOME HIGH ALLOY STEELS BY RAPID AUSTENITIZING

A thesis submitted for the

degree of Doctor of Philosophy

in the University of London

by

NARINDER KUMAR NAGPAUL

February 1968

Department of Metallurgy,
Royal School of Mines,
Imperial College of Science
and Technology,
London, S.W.7.

CONTENTS

			Page No.
		Abstract.	7
		Introduction.	9
Chapter I.		Previous Work.	11
1.1		General.	12
1.2		Previous Work.	14
	1.21	Effect of rapid austenitizing on the strength of S.T.A. austenite.	15
	1.22	Effect of rapid austenitizing on the structure of S.T.A. austenite.	18
Chapter II.		Experimental Procedure.	26
2.1		Alloy composition and preparation.	27
2.2		Determination of martensite-austenite reversion temperature.	31
2.3		Rapid heating techniques.	32
2.4		Reversion.	34
	2.41	Austenitizing of powdered samples for x-ray study.	34
	2.42	Magnetic balance.	35
2.5		Mechanical properties.	37
	2.51	Hardness.	37
	2.52	Tensile tests.	37
		a. Test piece geometry.	38
		b. Testing technique.	38

			Page No.
	2.53	Formation of martensite during mechanical testing.	39
	2.54	Standardization of initial martensitic structure.	39
2.6		Metallographic procedure.	41
	2.61	Light microscopy.	41
	2.62	Interferometry.	42
	2.63	Electron microscopy.	43
	2.64	Dislocation density measurements.	44
Chapter III.		Results.	46
3.1		Strength and structure of S.T.A. austenite.	46
3.11		Presentation of results.	47
3.12		Initial structure.	48
		a. M_s temperatures and the amount of martensite at liquid nitrogen temperature.	48
		b. Structure and hardness of S.T.A. austenite.	48
3.13		Effects of austenitizing time and temperature on properties of S.T.A. austenite.	51
3.14		Effect of initial amount of martensite on the yield stress of S.T.A. austenite.	65

		Page No.
3.15	Structural changes.	
	(i) Optical microscopy.	68
	(ii) Electron microscopy.	69
	(iii) Crystallographic relations.	72
	(iv) Dislocation structure of S.T.A. austenite.	75
	(v) Shear-type nature of reversion.	80
3.16	Tempering during reversion.	82
3.17	Changes with time and temperature of austenitizing - recovery.	85
Chapter III.	Results (continued).	
3.2	Structure and properties of martensite produced from S.T.A. austenite.	88
3.21	Synopsis.	88
3.22	Effect of time of austenitizing on the hardness of martensite.	89
3.23	The two martensites - strength and plate size.	91
3.24	Properties of S.T.A. martensite and conventional martensite after tempering.	96
3.25	"Tempering" of S.T.A. austenite.	106
3.26	Structural observations of tempered martensites.	108

			Page No.
3.27		Sites for S.T.A. martensite formation.	113
3.28		Orientation relationship and coherency between precipitate and the matrix.	115
Chapter IV		Discussion.	119
4.1		Strength of S.T.A. austenite.	120
4.2		Characteristics of structure of S.T.A. austenite.	120
	4.21	Ghost structure.	120
	4.22	Dislocation density.	122
		Sources of dislocations in S.T.A. austenite.	
		(i) Structural volume changes.	124
		(ii) Inherited defects.	126
		(iii) Anisotropy of thermal expansion of martensite crystals.	127
		(iv) Vacancy condensation.	128
	4.23	Reversal twins and sub-boundaries.	129
		(i) Twin coalescence.	130
		(ii) Cross slip during reversion.	131
	4.24	Tempering during reversion.	132
4.3		Contribution of various strengthening mechanisms.	133
4.4		Mechanism of reversion	141

			Page No.
4.5		Effect of annealing time and temperature.	142
	4.51	Hardness changes.	142
	4.52	Structural changes and activation energy.	143
4.6		S.T.A. and conventional martensite - tempered and untempered.	148
	4.61	Factors contributing to the increased strength of the untempered S.T.A. martensite.	150
	4.62	Tempering and the strength of S.T.A. martensite.	154
		Conclusions.	159
		Some suggestions for future work.	162
		Acknowledgements.	163
		Appendix.	164
		References.	170

Abstract.

A study has been made of the strengthening by rapid austenitizing of iron-26% nickel-0.3 - 0.4% carbon and iron-23% nickel-2.9% molybdenum-0.4% carbon alloys which are austenitic at room temperature and in which a substantial amount of martensite can be formed on quenching below room temperature. Samples, initially in the martensitic state, have been austenitized to 600 - 850°C in salt bath for about one minute and quenched in water. The reverted austenite (S.T.A. austenite) has a strength 3 - 4 times higher than that of the conventionally annealed austenite. Factors contributing to the increased strength of the S.T.A. austenite have been discussed on the basis of microstructural observations. A high density of dislocations ($\sim 10^{11}$ lines/cm^2) is a characteristic structural feature. Interferometric techniques have established that for heating rates obtainable with a liquid salt bath, the reverse transformation is of martensitic nature.

With increasing time of austenitizing in the case of iron-nickel-carbon alloys, the yield stress and hardness of the S.T.A. austenite decrease slowly at first and, for relatively longer austenitizing times, attain nearly the same values as that of conventionally annealed austenite. This behaviour is attributed to a recovery process involving an activation energy of about 150 Kcal/mol. In iron-nickel-

molybdenum-carbon alloys, however, prolonged austenitizing results in phase changes.

The martensite produced from S.T.A. austenite (i.e. S.T.A. martensite) has a slightly higher strength than the conventional martensite - both in the tempered and untempered conditions. The difference in the strength ($\sim$ 6%) of the untempered martensite results from refinement in the S.T.A. martensite plate size and a change in its defect substructure.

The effects of tempering the two martensites (viz. S.T.A. and conventional) in the range 190 - 550^{o}C for times up to 100 hours have also been studied in relation to secondary hardening in the iron-nickel-molybdenum-carbon alloys. The tempered S.T.A. martensite (peak hardness) has a higher strength ($\sim$ 10%) than that of the tempered conventional martensite (peak hardness) and this is explained on the basis of the relatively fine size of alloy carbide (Mo_2C) particles in the case of S.T.A. martensite. Precipitation of alloy carbide along the twins and at the dislocations has been observed.

General Introduction

When austenite transforms on cooling, its grain size and defect structure are important factors to be considered in relation to the micro structure and properties of the transformation product. One of the ways of controlling the austenite structure, with a view to improving the mechanical properties, is to use short-time austenitizing treatments. Such treatments strengthen the austenite, and this effect has been demonstrated particularly well in alloys which are austenitic at room temperature and in which substantial amounts of martensite can be produced by quenching below room temperature. The terms S.T.A. austenite and S.T.A. martensite have been introduced to designate the austenite produced by short-time rapid austenitizing treatments and martensite produced therefrom.

Heating the martensite structure, using relatively low austenitizing temperatures, can increase the yield strength of the reverted austenite by a factor of about three; this type of strengthening has been termed 'phase hardening' by some authors.(A1). Using iron-nickel alloys (33.5 percent nickel)*, Krauss(A2) showed that the reverted austenite was characterized by a very high density of tangled dislocations and suggested that this structural feature resulted from the

* All compositions given in weight percent.

volume change accompanying the reverse martensite transformation. Some work has also been reported by Phillips and Duckworth (A.3; A.4) on the effect of short-time austenitizing treatments on the properties of martensite; working with a plain carbon steel containing 0.4% carbon, they showed that such treatments significantly increased the hardness and tensile strength.

There is a likelihood of similarity between the effects of short-time rapid austenitizing treatments and ausforming treatment in that both produce a high density of lattice defects in the austenite. The structure and properties of the martensite, produced from S.T.A. austenite, may be influenced in various ways e.g. the size, shape and sub-structure of the martensite crystals may be affected and also the sub-structure may play an important role in carbide precipitation during the tempering of the martensite.

The experiments reported in this investigation form part of a study of strengthening by means of short-time rapid austenitizing including the strengthening of martensite, both in the tempered and untempered conditions. Iron-nickel-carbon and iron-nickel-molybdenum-carbon alloys, austenitic at room temperature, were used.

CHAPTER I

PREVIOUS WORK

CHAPTER I

Previous Work

1.1 General

Our present day technology is forcing a demand upon metallurgists for alloys with higher yield stress and ductility and much of the work in ferrous metallurgy is concerned with methods of improving the strength attainable with martensitic and tempered martensitic structures. Among the relatively new ways of strengthening ferrous alloys that have attracted considerable attention are: ausforming, maraging and short-cycle rapid austenitizing.

Ausforming: Details of the ausform process have been described elsewhere (A.5 to A.7). Briefly, the process may be defined as the plastic deformation of metastable austenite and the subsequent transformation to martensite. The deformation is carried out at a temperature in the so-called 'bay' that exists in the T-T-T diagrams of certain alloy steels between the transformation bands of pearlite and bainite. The ultra-high strength of ausformed steel has been shown to be directly proportional to the carbon content (A.8). McEvily et al (A.6) have concluded that the attainment of ultra-high strengths in ausformed steels is dependent upon the development of a uniform dispersion of fine carbides. Earlier investigations of Raymond

and Reuter (A.9), and of Thomas et al (A.10) have illustrated that the strength increase in ausformed steels is due not only to the carbide dispersion but also to the increase in dislocation density.

Maraging: Relatively recently precipitation hardened high alloy steels have been developed by the International Nickel Company as the result of many years work by Bieber (A.11) on aluminium-titanium-niobium hardened iron-nickel alloys. As a result of intensive research and development the earlier steels have been superseded by the 18% nickel-Co-Mo steels which show better notch toughness. The yield/tensile strength ratio of these steels is very high but they have a good ductility - about ten percent. A typical composition is iron-18% nickel-(0.2 - 0.6%) titanium - 0.07% aluminium - 8.0% cobalt - (3 - 4%) molybdenum.

The cycle of treatment for the maraging steels involves mechanical treatment at about 920°C followed by solution treatment at 820°C and, after cooling to room temperature, ageing at about 480°C. It has been found (A.12) that the ageing effects depend upon the product of the percentage of cobalt and molybdenum. The reason for the very high strength (90 tons/in^2 - 135 tons/in^2) is believed to be associated with the precipitation of intermetallic compounds and there is some indication that the cobalt has an ordering effect (A.12).

Short-cycle rapid austenitizing: The short-cycle austenitizing method involves rapid heating, holding briefly at, and rapidly cooling from the austenitizing temperature. The enhancement in the mechanical properties of the short-time rapidly austenitized structure has been demonstrated by a few investigators (e.g. A.2, A.13 and A.14). The ultimate commercial benefits achieved by short-time rapid austenitizing methods may be limited since rapid heating of thick sections would be a problem in itself. However, the strengthening of austenite by rapid reversion might be of practical interest from the point of view of austenitic steels, provided that some martensite can be formed in them prior to rapid austenitizing. Furthermore, if the strength of the parent austenite has any effect on the subsequent formation of martensite, the structural features of the S.T.A. martensite may be of interest from the point of view of strengthening.

1.2 Previous work.

The physical effects of the martensite to austenite transformation were described, in principle, as long ago as 1932 by Wassermann (A.15). Studying an iron-30% nickel alloy after the direct and reverse martensitic transformation he observed X-ray line broadening, indicating the presence of a hardening process. He concluded that the reverse transformation is characterized by the random formation and

growth of crystal nuclei of the newly formed phase (i.e. austenite). Wassermann's work was concerned with the annealing behaviour of the reverted austenite and it is not clear from his report whether a high rate of heating was employed or not. This may be a critical feature to mention since the nature of reversion is likely to depend upon the heating rate. With a slow heating rate the reverse transformation is expected to be diffusion controlled.

1.21 Effect of rapid austenitizing on the strength of S.T.A. austenite.

During recent years, the study of the transformation of martensite to austenite, and its effect on strength and structure has attracted the attention of both Russian and American investigators. Russian workers, in particular, have shown considerable interest and have been investigating the structural features of the reversed austenite using alloy steels and iron-nickel alloys. One of the difficulties of studying the reverse transformation in carbon-containing ferrous martensites is that during the heating for austenitizing some tempering is likely to occur. It is probably for this reason that in the last decade, almost all the American investigators have studied reversion in iron-(30 - 34%) nickel alloys which are austenitic at room temperature.

The strengthening of austenite by the reverse martensitic transformation in iron-(30 - 33%) nickel alloys, with heating rates comparable to that used in the present investigation, was studied by Krauss and Cohen (A.13) who found that the reversed austenite was significantly altered in strength, microstructure and annealing characteristics. With increasing number of transformation cycles the strength of the reverted austenite was slightly enhanced but the major strengthening effect occurred in the first cycle. The structure of the reversed austenite was greatly distorted. Krauss (A.2), using an iron-33.5% nickel alloy, found that the reversed austenite contained a high density of tangled dislocations.

Following the hardness changes of the reversed austenite, Krauss and Cohen (A.13) employed various annealing temperatures (600°C - 700°C) and found that the plot of hardness 'vs' time of annealing at a particular temperature takes the sigmoidal form similar to that obtained when a cold-worked structure is recrystallized on annealing. Their conclusion, supported by optical micrography, was that the reverse martensite transformation, on prolonged austenitizing, involves recovery and recrystallization. Gridner et al (A.16) in their earlier work had shown similar sigmoidal changes in hardness with increasing time of annealing. However, no study of the reverted structure was made and the authors did not comment on the nature of the annealing behaviour.

The reversion of high-carbon austenitic alloy steels under conditions of rapid austenitizing treatments, with reference to their mechanical properties, has been studied by Gorbach and Malyshev (A.14). They have reported strengthening of the austenite (reversed austenite) by 300 percent. In comparison with the martensitic steels, the austenitic steels, from the point of view of yield stress, were shown to be more responsive to rapid austenitizing treatments. They have also demonstrated that there is a critical heating rate which must be exceeded if maximum strengthening is to be achieved. With a heating rate of about 1000°C per minute the martensite to austenite transformation (in iron-14.0% nickel-0.88% carbon alloy) resulted in a substantial increase in the strength of the reversed austenite. Reduction in the heating rate for austenitizing gradually raised the Ms temperature of the alloy, indicating thereby that the solid solution is being depleted of carbon and that the reversion is occurring by diffusion controlled tempering phenomena. In their view the yield stress of the reversed austenite due to rapid austenitizing increases in proportion to the initial yield strength of the annealed austenite. Exceptionally high strengthening in austenitic iron-nickel-(1-2%) titanium alloys, by rapid austenitizing treatments, has been reported by Malyshev and Borodina (A.17); but it appears that because these alloys belong to an ageing

system, the exceptionally high strength may be due to the development of dispersion hardening.

1.22 Effect of rapid austenitizing on the structure of S.T.A. austenite.

Most of the Russian investigators have made a detailed investigation of the structural features of the reversed austenite obtained by rapid austenitizing and the term "phase hardening" has been used to denote the strengthening that can be achieved. Their investigations have included the aspect of stabilization of the reversed austenite relative to the subsequent martensitic transformation. Gridnev et al (A.16) made a study of both the direct and reverse martensitic transformations. Using 22.0% nickel-0.02% carbon - 3.0% manganese steel (Ms = 10°C) and with heating rates varying from 100°C to 10000°C/second, they found that as a result of the reverse martensitic transformation by rapid austenitizing the maximum stabilization effect was observed after the first cycle of heating and cooling; the reverted structure (martensitic) showed an increase in the tensile strength of about 13 percent. These workers found that an increase in the heating rate from 100°C to 10,000°C per second had very little effect on the temperature at which reversion began in the case of the alloy studied. Krauss and Cohen, using molten salt for rapid heating, (A.13) have achieved complete reversal of the

martensitic transformation in iron-nickel alloys at a temperature within the ($\alpha + \gamma$) region of the phase diagram, indicating thereby that with relatively high rates of heating there is an apparent lowering of the transformation temperature. The study of the effects of heating rate on the reverse transformation in an iron-18% nickel-8% cobalt-0.6% titanium maraging steel by Goldberg and O'Connor (A.18) has supported the view that a decrease in reversion temperature is obtained with increase in heating rate. With relatively high rates of heating to certain austenitizing temperatures, the reversed austenite can be unstable relative to equilibrium ferrite + austenite mixtures. Depending upon the time of holding at the temperature of austenitizing, fully reversed austenite can be generated even though the structure tends to decompose to ferrite and austenite.

Gorback and Butakova (A.19) made an optical metallographic study of the reversed austenite in alloys (austenitic at room temperature) containing 28% nickel - 0.5% chromium - 0.3% manganese - 0.04% carbon. They reported that the transformation of a martensite crystal to austenite proceeds gradually and extends over a temperature range of 400 - 500°C. It is important to point out that in their investigation, a relatively low heating rate (10°C per minute) was employed and it can be expected that the reversion was

diffusion controlled, at least partly. It appears from their work that the reverse transformation did not develop over the entire martensite crystal to form a single plate (crystal) of reversed austenite.

Gorbach and Butakova (A.19) observed that the reversed austenite needles appeared at the martensite-austenite interface; the initial martensite boundaries disappeared on reversion, and the fragments of the reverted austenite formed a continuous structure with the retained austenite. Dash and Brown (A.20) working on an iron - 32% nickel alloy have reported similar observations. The observations also indicated that the reverse transformation takes place through layer by layer dissolution at the interface. However, the authors have not indicated the rate at which the specimens were heated. In a recent publication, Jana and Wayman (A.21), using an iron - 34% nickel alloy, have reported that with a heating rate of 1°C per minute and an austenitizing temperature of 320°C (very close to the $(\alpha + \gamma)/\gamma$ boundary), martensite to austenite reversion occurs by the martensite/austenite interface sweeping through the interior of the original martensite plate. It is likely that with this rate of heating, a perceptible amount of diffusion is occurring.

Kessler and Pitsch (A.22) have studied reversion in an iron - 32.5% nickel alloy using heating rates of 10°C per minute and 100°C per second. They found that the reverse transformation proceeded with the development of small austenite plates along the martensite-austenite interface and these plates were differently oriented within each martensite crystal. After heating to about 420°C, complete reversion was observed. On lowering the rate of heating to 0.3°C per minute an appreciable rise in the temperature at which transformation to austenite began was noticed and the reversion was completed at 550°C. Kessler and Pitsch's observation (heating rate 0.3°C per minute) of the sphere-like formation of reversed austenite in some regions was indicative of diffusion controlled processes.

Surface relief studies of the reverse transformation were pioneered by the Russians in the late thirties. It was Golovchina (A.23) who, later in 1951, reported that the reverse martensitic transformation (both in brasses and in iron alloys) was the result of coherent translations similar to those in the direct austenite to martensite transformation.

Edmondson and Ko (A.24) in their study of the martensitic transformation in an iron - 34% nickel alloy have shown the occurrence of plastic deformation in the austenite during both heating and cooling. When a partly martensitic

specimen, unpolished after transformation, was austenitized at 400°C (heating rate not mentioned) there was a residual tilting of the areas originally occupied by the martensite and some rippling effect was also observed. Such observations indicate that the reversion may be of martensitic nature. Since the specimen surface already showed tilts (due to the direct transformation), it is difficult to decide whether the final tilt of the surface after reversion included tilts due to the actual reversion. Sokolov et al (A.25) noted that the relief arising during the reversion is more complicated than a simple mirror reflection of the relief in the direct transformation and have suggested that a large number of fragments of reversed austenite arise during reversion. Gorbach and Butakova (A.19) have supported this view on optical micrography evidence. They have observed (iron-nickel alloy, heating rate 10°C/minute) that as the reverse transformation develops the relief progressively extends over the entire martensite plate. Krauss and Shapiro (A.26), while working on the crystallography of the reverse martensitic transformation in an iron-nickel alloy, have shown that there is a certain relief effect, with each fragment of the reversal product (austenite) which intersects the surface of the sample. Their measurement of the tangent of the tilt angle yielded values varying from 0.08 to 0.51. The maximum value of the shear (i.e. 0.51) appears to be

appreciably higher than that of 0.20 reported for the direct transformation by Machlin and Cohen (A.27). Work by Dash and Brown (A.20) has suggested that the reverse transformation is primarily through a shear process but it is aided by atomic diffusion. In a recent publication by Kessler and Pitsch (A.22) the martensitic nature of reversion (iron-32.5% nickel alloy) has been clearly demonstrated. According to these authors, the reverse transformation takes place martensitically if the specimen is austenitized at relatively high heating rates. At low heating rates (0.3°C per minute) part of the reverse transformation occurs martensitically but, simultaneously, the diffusion of iron or nickel across the austenite/martensite interface appears to stabilize the rest of the untransformed martensite, thus raising the transformation temperature.

The orientation relationships between the martensite and the reversed austenite have been found (A.26 and A.28) to be the same as that for the direct transformation. This indicates that the crystallographic nature of the reverse transformation is basically the same as that of the austenite to martensite transformation. Kessler and Pitsch (A.28) have explained their crystallographic data by an application of the Wechsler, Liebermann and Reed theory of martensitic transformations (A.29) and assuming that the lattice invariant shear of reverse transformation takes place along the {111} planes

of the reversed austenite. By this they proved that the reverse transformation which occurred at high heating rates (100°C per second) was of pure martensitic nature.

The metallographic investigation of Edmondson and Ko (A.24) on an iron - 34% nickel alloy has shown that the plastic deformation in austenite after a complete cycle of cooling and heating transformations consists of (a) slipping in austenite, (b) severe deformation in the regions originally occupied by the martensite crystals. The structure after reversion was called a 'ghost' structure.

In subsequent work Krauss (A.2) showed by electron-microscopy that the reversed austenite (obtained by using heating rates comparable to the ones used in the present investigation) contained a high concentration of tangled and jogged dislocations. The dislocation density of the reversed austenite was about a factor of ten greater than that observed in the retained austenite of directly transformed specimens. Dash and Brown (A.20) have also reported the tangled nature of the dislocations in the reversed austenite. Krauss (A.2) suggested that the increase in the density of dislocations is a result of vacancy generation during the sudden structural volume change occurring during the transition from the martensite (b.c.c.) to austenite (f.c.c.). Kuhlmann-Wilsdorf et al (A.30) have stressed the importance of excess vacancies

in the formation of jogged dislocations. The high dislocation density of the reversed austenite was considered to strengthen the reversed austenite.

Krauss (A.2) has also reported the presence of relatively large islands of reversed austenite and has identified these islands as twin related. He has referred to these twins as 'reversal' twins. Some of these twins have been reported (A.2) as being about five microns in width and appear to have slightly curved boundaries. Krauss (A.2) has observed the highly imperfect nature of the 'reversal' twins containing tangled dislocations. The mechanism by which the 'reversal' twins are formed has not been reported in the literature. However, Krauss (A.2) is of the opinion that these twins are formed on recovery after reversal. Breedis (A.31) has also shown the twinned nature of the reversed austenite in an iron - 16% chromium- 12% nickel stainless steel alloy.

A recent study of the structure of the reversed austenite in an 18/8 stainless steel alloy has been made by Thomas and Krauss (A.32). They have reported the formation of lathlike $M_{23}C_6$ precipitate particles in areas originally occupied by the martensite plates. The authors believe that the precipitation occurs prior to reversal, and affects the subsequent transformation to martensite on quenching. They have also shown a substructure of high density of dislocations in the reversed austenite.

CHAPTER II

EXPERIMENTAL PROCEDURE

EXPERIMENTAL PROCEDURE.

2.1 Alloy composition and preparation

As mentioned in Chapter I, the effects of short-time austenitizing are more marked in austenitic steels than in martensitic ones; the choice of steels for the present investigation was influenced by the requirement of producing a fully austenitic structure at room temperature while allowing substantial amounts of martensite to form on quenching to liquid nitrogen.

Steels, with composition (by weight) shown in table 2T-1, were chosen as suitable for the present investigation. For a study of the tempering behaviour of the steels, it was decided that some alloys should contain a strong carbide- forming element and molybdenum was chosen.

Preparation of materials.

All the alloys, except HP1, were obtained either from International Nickel Ltd. (Birmingham) or the British Iron and Steel Research Association (Sheffield).

Alloy HP1: This alloy was prepared by the author by high-frequency induction melting in vacuum, and cast in an argon atmosphere. After reheating to 1200°C in a hydrogen

TABLE 2T-1

Alloys used (with code numbers)	Composition (weight percent)													
	C†	Ni	Mo	Cr	Co	Ti	Al	Si	Mn	Zr	B	Mg	Cu	Fe
HP1	0.25-0.3	26 (nominal)	-	-	-	-	-	-	-	-	-	-	-	bala
PTWC (INN1)	0.37	25.6	<0.01	<0.05	<0.01	<0.01	<0.029	<0.05	<0.01	<0.01	<0.002	<0.01	<0.1	bala
N866 (INN2)	0.40	25.7	<0.01	<0.05	-	-	-	<0.01	<0.1	-	-	-	<0.1	bala
P14145 (INM1)	0.40	23.5	2.95	-	<0.1	-	-	<0.1	<0.05	-	-	-	<0.1	bala
S1013 (B1SM1)	0.41	23.7	2.95	-	-	-	-	-	-	-	-	-	-	bala

† See Appendix C.

atmosphere, the alloy was hot forged into plates of about $\frac{1}{4}$" thickness and air cooled.

Alloys INN1, INN2 and INM1: All these alloys, supplied by International Nickel Ltd., were vacuum melted and hot worked to $\frac{1}{2}$" or $\frac{1}{4}$" thick plates.

Alloy BISM1: This alloy, supplied by the British Iron and Steel Research Association, was manufactured by vacuum induction melting and casting using pure Swedish iron as melting base with the addition of graphite, nickel and ferro-molybdenum. With alternate annealing and hot-rolling, the ingot was reduced to about 0.2 inch thick plates.

All the alloys were scaled during the hot working and the plate was, therefore, surface-ground by an amount varying from 0.030" to about 0.060". Homogenizing was done in a vacuum furnace at 1200°C for 3-4 hours. This was followed by grinding the surface by about 0.02". An approximate calculation, Appendix 'A', shows that there was not likely to be any significant loss of carbon during homogenizing.

Rolling of the samples, with intermediate annealing, was carried out until the desired thickness was achieved.

Solution treatment: HP1, INN1 and part of INN2 alloys were solution treated in a vacuum furnace at 1000°C for 2 hours and were cooled slowly in the furnace. This resulted in an

austenite structure at room temperature.

The above method was found unsatisfactory for the solution treatment of iron-nickel-molybdenum-carbon alloys because of possible precipitation of carbides during slow cooling in the vacuum furnace. Samples of these alloys (INM1 and BISM1) and also of the remaining part of INM2, sealed in evacuated ($\sim 10^{-4}$ mmHg) transparent silica tubes, were heated to 1240°C for INM1 and BISM1 and to 1200°C for INM2 for 3 hours, after which the silica tube was dropped into a water bath and was broken immediately. The resulting structure was completely austenitic at room temperature. In the author's experience this method proved very satisfactory. An approximate calculation, Appendix A, shows that there was no significant loss of carbon during solution treatment. In addition, chemical analysis of the INM1 alloy after the solution treatment, showed that the amount of carbon was the same as in the as-received condition.

Samples of INM1 and BISM1 alloys, solution treated as described above, were used as the 'standard' (conventional) austenite. In the case of HP1, INM1 and INM2 alloys, samples, solution treated at 1000°C for 2 hours in the vacuum furnace, quenched to -196°C and reheated in the vacuum furnace at 800°C for one hour were used to produce 'conventional' austenite.

Mixtures of petroleum-ether and liquid nitrogen were used to obtain sub-zero temperatures ranging from $0^{o}C$ to about $-110^{o}C$. These mixtures, however, become 'pasty' below $-110^{o}C$ and alternative mixtures of iso-pentane and liquid nitrogen were used below this temperature down to about $-165^{o}C$. In both type of mixtures, the sub-zero temperatures could be easily maintained for about ten minutes.

2.2 Determination of martensite-austenite reversion temperature.

Experiments were made to determine the temperature at which austenite formed on rapid heating of martensite. Heating rates of about $40^{o}C$ per second were used and the transformation was studied by making use of the dilatometric property of the martensite-austenite transformation. The apparatus was that used by Ankara (B1). Martensitic strips (HP1 alloy), 7" x 0.01" x 2mm, were heated in a vacuum chamber by A.C. A continuous record of change in length of the strip showed that the transformation to austenite occurred between $532^{o}C$ and $550^{o}C$.

It should be noted here that some tempering of the martensitic structure occurs during the heating of the strip (see Section 2.54) and it is for this reason that the term 'reversion' temperature, rather than A_S temperature, has been

adopted. Also, use of the terms A_1 and A_3 temperatures is avoided as these refer to heating under equilibrium conditions of the phases concerned.

2.3 Rapid heating techniques.

Many methods of rapid heating are available. Each method has its own advantage and the choice depends on the size of the specimen, heat losses during heating and the subsequent observations to be made. It is necessary to keep in mind the need to avoid decarburization during heating.

One of the recent developments in this field is 'Laser' heating. With this technique, heating rates as high as 10^6 °C/sec have been reported (B2). This method has the following disadvantages for the present purpose of investigation.

a) As the specimen is heated in air, decarburization of the material, heated for relatively long times, is bound to occur.

b) Laser pulse heating is suitable for intervals of 0.001 - 0.1 second when no precautions are needed to avoid heat loss to the surrounding air. For times longer than this the temperature drop in the specimen becomes appreciable (B3).

Resistance heating. Some experiments were done using direct electric heating. This method of heating has the advantage that presumably the thermal diffusivity of the specimen does

not control the rate at which the centre of the specimen attains a given temperature. Direct electric resistance heating was, however, abandoned on the following grounds.

a) Martensite tensile specimens were tempered at the 'shoulders' of the test piece.

b) Buckling of the specimens, during the heating, invariably occurred.

Liquid bath immersion: Since, in direct electric heating, it was difficult to quench the specimen immediately after the rapid heating in the vacuum, use of a high temperature liquid-salt bath was found satisfactory. Simple manual immersion of the samples in these baths and subsequent removal can cover the time interval from a few seconds to longer times.

Two salts, supplied by I.C.I. under the commercial names Q.S.495 and N.C.660 were used. The former could be used up to 700°C and the latter up to 900°C. For austenitizing times longer than about 5 minutes, Regenerator "A" (supplied by I.C.I) was used. It is claimed that the use of the regenerator prevents decarburization during heating in the salt bath and some tests were carried out, Appendix B, to confirm this.

Heating in a liquid bath has the advantage that a constant temperature can be maintained throughout the bath thus giving a uniform heating rate of the specimen. The

temperature of the bath was controlled to within ± 3°C up to a temperature of 650°C and to within ± 5°C up to 850°C.

In view of the difficulties of obtaining accurate values of the co-efficient of heat transfer and the specific heat for the alloys employed in this investigation and of the thermal properties of the commercial salts used in the bath, approximate calculations suggest that it takes about 5 seconds for a specimen 0.01" thick to reach a bath temperature of 650°C.

2.4 Reversion

Experiments were aimed to determine the extent of reversion when a martensitic structure is austenitized for short-times. X-ray powder-study and the use of a magnetic balance were the two techniques used for this purpose.

2.41 Austenitizing of powdered samples for x-ray study.

Rapid heating of powdered samples, for the purpose of x-ray study, was carried out by enclosing annealed and quenched (-196°C) powder samples of INM1 alloy in aluminium-foil envelopes and immersing them in the salt bath at 640°C for about 40 seconds followed by quenching in water. No b.c.c. or b.c.t. diffraction lines were detected

on x-ray diffraction examination.

2.42 Magnetic balance.

Experiments, using a Sucksmith-type magnetic balance (B4), were carried out in the Metallurgy Department of Birmingham University. It should be pointed out here that, since austenite is paramagnetic, the recorded magnetic response, in fact, includes the paramagnetic contribution and the ferromagnetic contribution.

Under standard conditions of non-uniform field and constant field gradient the force on a ferromagnetic specimen, measured by displacement (D), is given by

$$D = Km\sigma.$$

where m is the mass of the specimen, σ is the average saturation intensity and K is a constant for the apparatus under standard conditions. This relationship does not yield an absolute value of σ but allows an accurate comparison to be made between the values of the two specimens; if σ for the material of one of these be known, then that of the other can be deduced. The apparatus can therefore readily be calibrated by measuring the deflection due to a specimen of known mass prepared from material of known σ. Pure nickel was used for this purpose since, besides its availability, its saturation magnetic intensity is accurately known (54.3 c.g.s

units). We have then

$$\frac{D_x}{D_{Ni}} = \frac{Km_x \sigma_x}{Km_{Ni} \sigma_{Ni}} = \frac{m_x \sigma_x}{m_{Ni} \sigma_{Ni}} \qquad \text{——} \qquad (1)$$

where the suffices 'Ni' and 'x' refer to nickel and the specimen of unknown σ, respectively. The calibration was checked immediately before and after every determination of σ and it was found that, provided the apparatus (particularly the optical system) was not disturbed, the deflection due to the standard nickel specimen varied only slightly.

The value of σ_x, containing M% equivalent amount of ferromagnetic content, can be obtained by

$$\sigma_x = \frac{\sigma_x(100\%) \times M\%}{100} \qquad \text{——} \qquad (2)$$

Thus using equations (1) and (2)

$$M\% = \frac{D_x \times m_{Ni} \times \sigma_{Ni} \times 100}{m_x \times \sigma_x(100\%) \times D_{Ni}}$$

It is claimed that the magnetic balance had ± 0.5% reproducibility provided the value of σ is accurately known. The calculations for σ_x (100%) were made using published data (B4) on the effect of nickel and molybdenum on the saturation intensity of iron assuming that these effects would be additive; the influence of carbon was assumed to be that of pure dilution. (B5)

The overall sensitivity is claimed to be 0.1% at ferromagnetic contents of 0% falling to about 0.2% for 100% ferromagnetic contents.

2.5 Mechanical properties.

2.51 Hardness: All samples used for the purpose of hardness testing (or for optical microscopical study), after austenitizing, were ground to remove any scale or surface layer formed during the heat treatment. The macrohardness of the polished specimen was determined using a Vickers testing machine with a pyramid indentor and a load of 2.5 or 5.0 kgm depending upon the thickness of the specimen. Either five or ten indentations were used on each specimen depending on the degree of reproducibility discovered.

Microhardness tests were carried out using a G.K.N. microhardness tester with a load of 30 gms. and a 4mm. objective.

2.52 Tensile tests. Tensile test specimens were prepared from rolled and annealed sheets. They were then solution treated as described earlier in this chapter. The dimensions of the tensile specimens (shown below) were in accordance with a British Standard Specification.

Overall width	Gauge width	Gauge length	Radius	Pin hole diameter
0.75"	0.25"	1.5"	0.25"	0.25"

The tensile tests were carried out on samples with different thicknesses (0.025" - 0.040") and the specimens contained about 6 - 10 grains across the thickness. All tests were carried out using an Instron testing machine which had a load range from 10 to 5000 kgm with the load cells. The extension was measured by marking two pairs of light scratches, with each scratch of a pair at a distance of 2.0 cms from the other. A cross-head speed of 0.2 cm per minute was used throughout the investigation.

Factors affecting the tensile tests.

a) Testing technique: The main feature of testing technique which affect the yield stress, other than rate of straining, is the axiality of loading and evenness of straining of the test piece. Care was, therefore, taken to ensure both proper gripping of the test piece and axial loading.

b) Machine characteristics: To determine the strain induced in the testing machine, a rigid bar was tested under the same conditions as the specimen (i.e. the same strain rate, temperature etc). Assuming the effect of loading is only in

the machine, the strain in the machine was calculated and subtracted from the recorded strain in the specimen.

2.53 Formation of martensite during mechanical testing.

The possibility of martensite formation in the austenite during hardness testing and tensile testing at room temperature was investigated by metallographic examination. No martensite was detected during hardness testing (Fig. 2.1). This figure, however, shows strained regions around the indentation. Fig. 2.2 is a micrograph of S.T.A austenite strained about 0.2% in tension. Dark etching regions, somewhat like slip bands in appearance, are, in fact, the characteristic structural feature of the S.T.A. austenite (see section 3.15).

2.54 Standardization of initial martensitic structure - tempering at room temperature.

It was found that when the martensite, produced by quenching iron-nickel-carbon alloys to -196°C, was heated to room temperature, a hardness increase of about 60 HV occurs during the heating. Annealed specimens of INV1 were kept at -196°C for about 15 minutes, and then polished and tested for hardness at room temperature. The polishing operation took about two minutes. After about 30 minutes the specimen

Fe-Ni-C(INN1) alloy

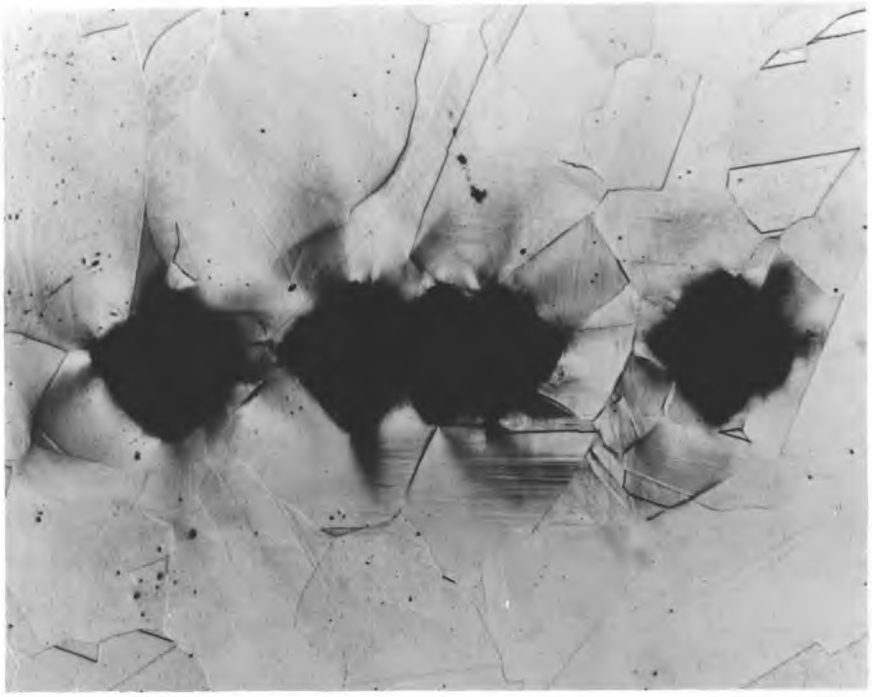

Fig. 2.1. Effect of hardness tests on formation of martensite in austenite. Etching indicates strained regions around an indentation. X96

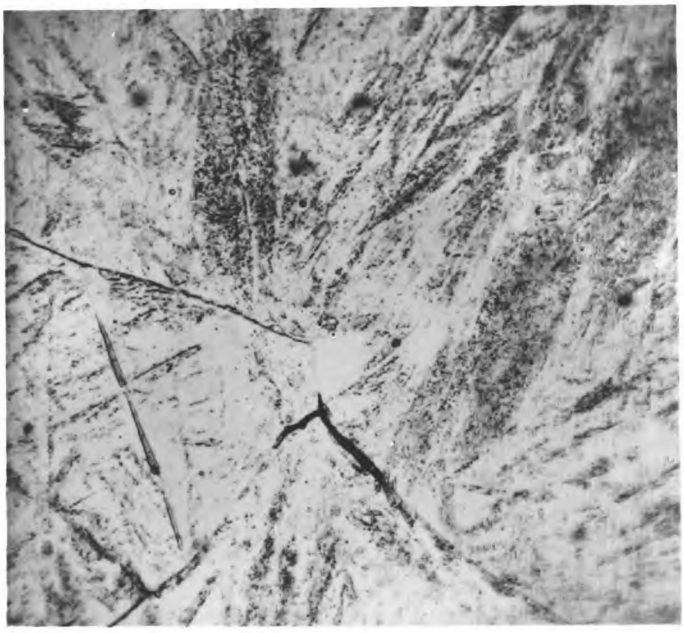

Fig. 2.2. Effect of 0.2% plastic strain on formation of martensite in austenite. Dark regions are 'ghost' structure. X600

achieved a maximum hardness of about 440 HV.

Thus, the martensite examined at room temperature was a slightly 'tempered' structure. The observed hardening is consistent with the results of Winchell and Cohen (B6). Specimens, after quenching in liquid nitrogen were therefore kept at room temperature for about half an hour to ensure that approximately the same hardness and degree of tempering were achieved prior to reversion or mechanical testing.

2.6 Metallographic Procedures.

2.61 Light Microscopy

All the specimens for metallographic examination were mounted in bakelite. The rough polishing on silicon carbide papers of various grades was followed by polishing on diamond wheels using diamond dust of seven and one micron fineness.

For structural observations of S.T.A. austenite, some of the specimens were chemically thinned by about 0.02" to ensure complete removal of any surface layer formed during the austenitizing treatment. The following etchants were found satisfactory.

Alloys	Structure	Etchant
Iron-nickel-carbon	Austenite	Alcoholic Ferric Chloride
	Martensite	2% Nital
Iron-nickel-molybdenum -carbon	Austenite	Alcoholic Ferric Chloride
	Martensite (Untempered)	Alcoholic Ferric Chloride + 2% Nital
	Martensite (Tempered)	30 c.c. HCl. 10 c.c. HNO_3 20 c.c. Glycerol

2.62 Interferometry: The study of surface relief accompanying reversion was made by an interferometric technique. The interferometer was in the form of a metallographic optical microscope (Reichert MeF) having a polarizer and an analyser in the crossed position.

Specimens of INM1 alloy, after quenching to just below Ms, were polished with $\frac{1}{4}$ micron diamond paste followed by electropolishing in chromic acid. To avoid touching the polished surface the specimens were put in a 'cradle' with narrow ends. The cradle was then put into the salt bath at 650°C and held there for about one minute. After austenitizing, a light polish on the $\frac{1}{4}$ micron diamond paste had no effect on the surface relief appearance. The same procedure was adopted for the preparation of specimens for making carbon replicas.

2.63 Electronmicroscopy.

The samples used for electronmicroscopy were in strip form about 0.75" wide and about 0.005" thick. The strip was heated from the martensitic state in the salt bath for various times and temperatures.

A two-stage Bollman technique (B7) was used for producing thin foils. In the first stage the electrothinning was fast and the thickness was reduced from 0.005" to about 0.001". The second stage of electrothinning was carried out in a different electrolyte. Success was achieved and after a little practice fairly large thin foils were obtained for observation in the electron microscope.

The electrolytes and conditions employed for electrothinning and polishing were:

Stage I.

Composition:	Ortho phosphoric Acid ---	60 mls
	Sulphuric Acid (conc) ---	40 mls
Conditions:	Temperature $\geq$	$50^{o}C$
	Current Density	--- 2.0A/sq".
	Cathodes --- Stainless steel (strip)	

Stage II.

Composition:	CrO_3	--- 100 gm.
	Glacial Acetic Acid	--- 540 c.c.
	Distilled Water	--- 28 c.c.
Conditions:	Voltage	--- 20-25V
	Current Density	--- 0.2A/sq".
	Temperature	--- 10 - 15°C
	Cathode --- Stainless Steel (Pointed)	

During the course of the research, both a Hitachi (HU 11) and an AEI (EM6G) microscope were used. Both the electron-microscopes can be operated at 100 KV. and have the facilities for tilting the specimen about one axis through an angle of 5^{o}.

Regions of interest in the foils were photographed together with diffraction patterns from selected areas. In addition a high resolution dark field technique was employed.

Analysis of diffraction patterns, obtained from areas of "reversal twins" and carbide precipitates, was done by standard methods, and orientation relationships were determined.

2.64 Dislocation density measurements.

The determination of the density of dislocations was done by the method of Smith and Guttman (B.8.).

It should be emphasized that accurate dislocation density measurement has not been possible because of the frequent occurrence of the unresolved and 'cloudy' dislocations scattered throughout the network in S.T.A. austenitic structures. However, the average dislocation density 'ρ' of areas of particular interest was estimated using the grid method which employs the expression

$$\rho = \frac{2N}{Lt}$$

where 'N' is the number of intersections made by the dislocation lines with the grid lines of total length 'L', 't' being the thickness of the foil and 'ρ' is the dislocation density. Two grids were used, one with a regular set of grid lines and the other with grid lines drawn at random. The foil thickness 't' was not determined but was taken as 2500Å.

In view of the fact that few electron micrographs, with resolved networks of dislocations in the S.T.A. austenite, were obtained, only about 600 counts were possible in the S.T.A. austenite structure. About 120 counts were made in the case of fully annealed austenite. The possibility of the introduction of dislocations by foil handling in the case of annealed austenite, (being softer than the S.T.A. austenite) must be taken as a source of error in the estimation of dislocation density. This error is difficult to estimate.

CHAPTER III

RESULTS

3.11 Presentation of results.

Using the high heating rates in liquid baths, it is aimed in this investigation to study the effects of rapid austenitizing on the mechanical properties of the austenite and to compare these properties with those of the austenite produced by conventional austenitizing-annealing. The observed enhanced strength has been explained on the basis of structural observations made both by optical and electron microscopical study.

The shear-type nature of the reverse transformation (martensite → austenite) is verified by the surface relief. Evidence for the relief effect, occurring during reversion, has been obtained by an interferometric microscopical study and also by electron microscopy using the direct carbon replica technique.

On the basis of the structural observations, an attempt has been made to explain the high activation energy for recovery of the austenite.

3.12 Initial structures

3.12a - M_S temperatures and the amount of martensite at liquid nitrogen temperature.

Approximate values of M_S for the alloys employed in the present investigation are tabulated below. One of the factors which influences the M_S is the prior austenizing temperature and this is also mentioned in the table (3T-1).

The amount of martensite formed after quenching to -196°C was calculated by the 'point counting' technique of quantitative metallography. An average of 1000 counts on each sample was made.

For all the iron-nickel-carbon alloys, the M_S temperature is in fair agreement with the results of previous workers' (C.1).

3.12b - Typical structure and hardness on short-time rapid austenitizing.

Short-time rapid austenitizing treatments result in an appreciable enhancement in hardness. The increase in hardness is dependent upon the time of austenitizing, the amount of martensite present prior to austenitizing and, for relatively long times, upon the temperature of austenitizing.

TABLE 3T-1

Code	Alloy composition (by weight)	Austenitizing Treatment	M_S	Approximate percent martensite on cooling in liquid nitrogen
HP1	26*% nickel-0.25% carbon balance-iron Other total impurities <.1%	800°C for one hour. Vacuum furnace cooled	-38°C	90
INN1 (PTWC)	25.6% nickel-0.4% carbon† balance-iron Other total impurities <.2%	As above	-65°C	85
INN2 (N866)	25.7% nickel-0.4% carbon† balance-iron Other total impurities <.2%	(a) As above (b) 1200°C for 3 hours in evacuated silica tube followed by direct quench in water	-20°C	95
INM1 (P1415)	23.5% nickel-2.95% molybdenum -0.4% carbon balance-iron Other total impurities <.2%	As (b) above but austenitized at 1240°C for 3 hours.	-130°C	70
BISM1 (S1013)	23.7% nickel-2.95% molybdenum -0.41% carbon, balance-iron Other total impurities <.2%	As above	-85°C	80

* Nominal Composition

† See Appendix C

Typical changes in hardness and structure may be illustrated by reference to the iron-nickel-molybdenum carbon alloy (INM1) solution treated, then cooled in liquid nitrogen and re-austenitized at 650°C for one minute followed by direct quenching in water. The following table shows the hardness of S.T.A. austenite. (i.e. austenite obtained after short-time austenitizing treatment).

Austenitizing Temperature = 650°C.

Amount of martensite after cooling in liquid nitrogen = 70 percent.

TABLE 3T-2

Hardness of conventional austenite(solution treated at 1240°C for 3 hrs. followed by quenching in water)	Hardness of S.T.A. austenite(austenitized in salt bath for one minute at 650°C)	Hardness of conventional martensite/ austenite mixture
135-145 HV	280-300 HV	360-370 HV

Optical metallographic examination of the S.T.A. austenite has shown (Fig. 3.1b) that the original martensite crystals on rapid austenitizing, are divided into a number of fragments. The structure, prior to reversion (Fig. 3.1a), consists of both twinned and untwinned platelets of martensite

crystals. Most of the martensite plates were internally twinned, and the untwinned plates showed no twin contrast on tilting the thin foil. Similar observations have been made by Kelly and Nutting (C.2). Fig. 3.1C is an electronmicrograph showing both types of martensite crystals.

One of the interesting features that emerged from the earlier experiments was that the size of the original grains of the austenite (with martensite crystals in the matrix) remains unaltered on rapid heating for relatively short times. (Figs. 3.1a and 3.1b).

Further effects of time and temperature of austenitizing on the strength, and the accompanying structural changes were studied in greater detail using both iron-nickel-carbon and iron-nickel-molybdenum-carbon alloys.

3.13 - Effects of austenitizing time and temperature on properties of S.T.A. austenite.

As has been mentioned in Chapter 2 (section 2.54), some tempering of the martensite can occur at sub-zero temperatures; therefore, all specimens, after cooling in liquid nitrogen, were maintained at room temperature for about half an hour to ensure that approximately the same hardness and degree of tempering were achieved prior to reversion or mechanical testing.

Fe-Ni-Mo-C (INM1) alloy

Fig. 3.1a. Conventional martensite and austenite structure X540

Fig. 3.1b. Structure after austenitizing at 650°C for one minute X540

Fig. 3.1c. Twinned and untwinned nature of martensite X40,000

Iron-nickel-carbon alloys.

Samples of the three iron-nickel-carbon alloys (HP1, INN1 and INN2) with different carbon content were rapidly heated from the martensitic state and austenitized in a salt bath at temperatures ranging from 600°C to 670°C for times varying from a few seconds up to about 80 hours. Figures 3.2, 3.3 and 3.4 show the variation of hardness with austenitizing time for various treatment temperatures.

In the early period of austenitizing, there is a slight decrease in hardness and this is later followed by a large drop. With prolonged austenitizing, the hardness reaches nearly the same value as that of the vacuum annealed austenite. The variation in yield stress[*] (Fig. 3.2) shows a similar effect of rapid austenitizing.

Table 3T-3 shows the effects of rapid austenitizing in the temperature range of 600 - 620°C for one minute on the hardness of the three iron-nickel-carbon alloys.

TABLE 3T-3

Alloy	Hardness of vacuum annealed austenite	Hardness of S.T.A. austenite	
		Austenitized in the range 600-620°C for one minute.	Prolonged austenitizing in the range 600-620°C.
HP1	95-105 HV	~210 HV	~100 HV
INN1	100-115 HV	~230 HV	~110 HV
INN2	135-145 HV	~265 HV	~140 HV

[*] Average of four tests.

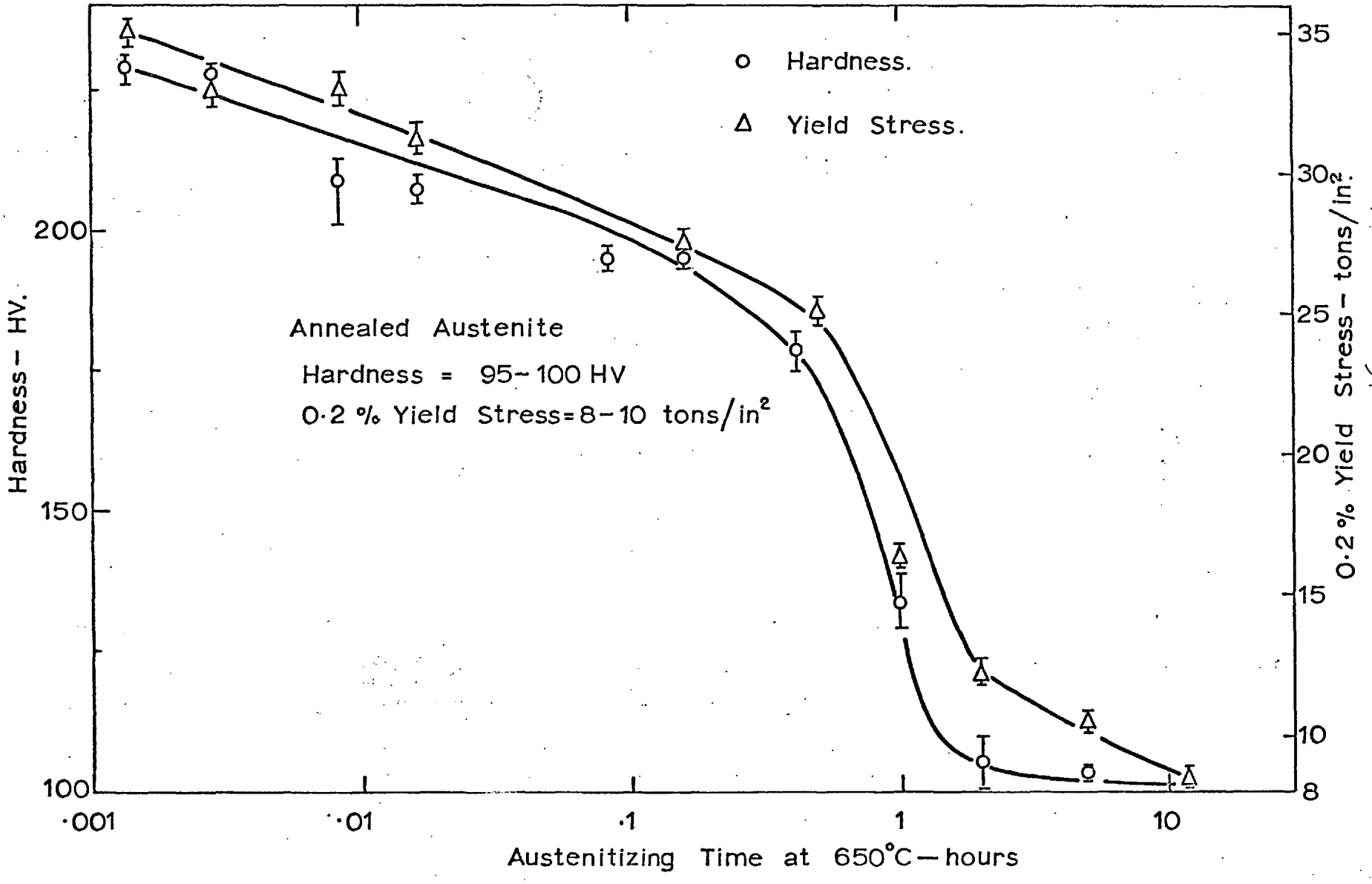

Fig. 3.2. HP1 alloy. Variation of hardness and yield stress with austenitizing time.

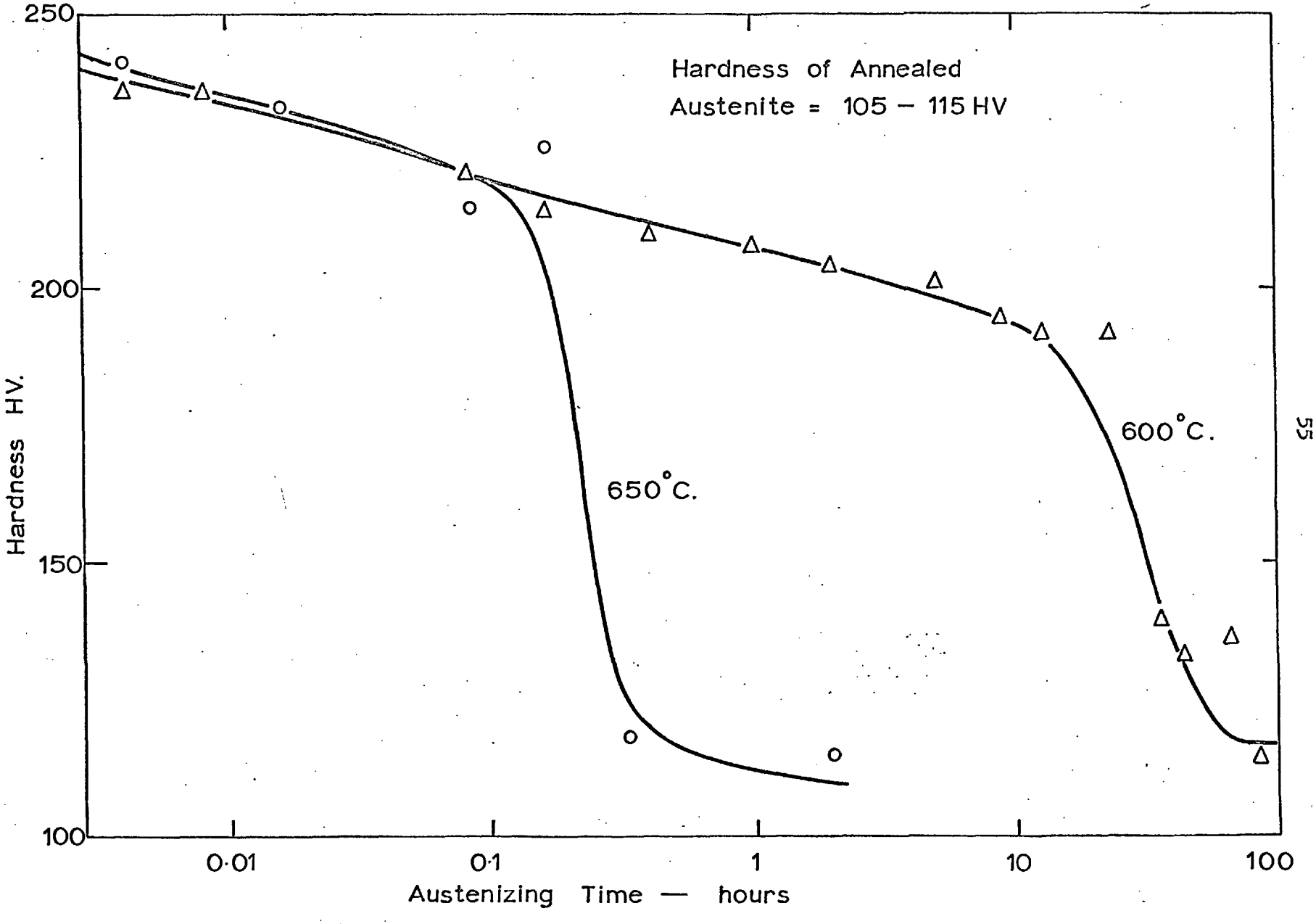

Fig. 3.3. INN1 alloy. Variation of hardness with austenitizing time at (a) 600°C (b) 650°C.

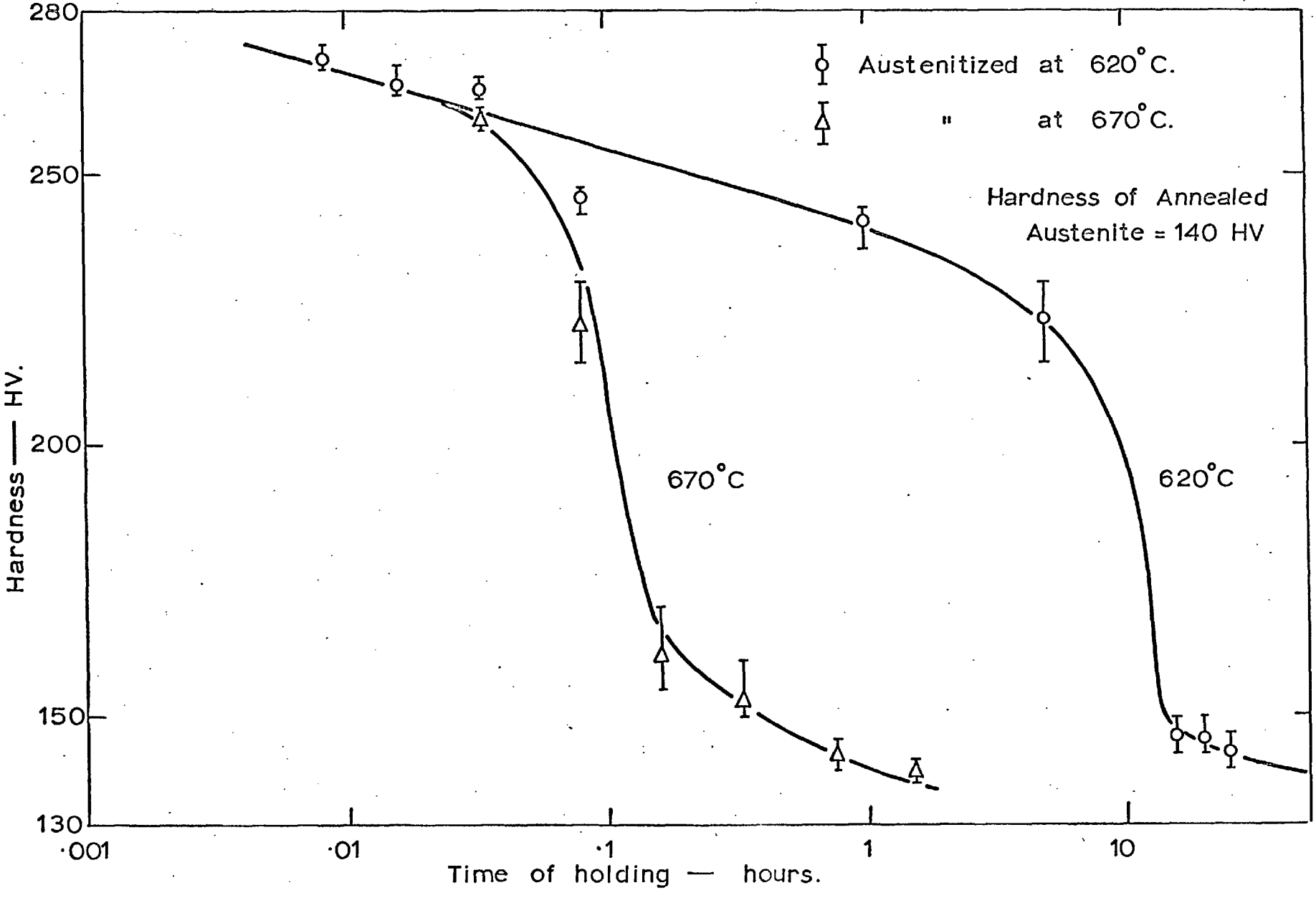

Fig. 3.4. INN2 alloy. Variation of hardness with austenitizing time at (a) 620°C (b) 670°C.

The results of the effects of rapid austenitizing on ductility and ultimate tensile stress have been plotted for the iron-nickel carbon alloy (HP1) in Fig. 3.5.

The tensile strength seems to be little affected by variation in the austenitizing time (at 650°C). In view of the wide scatter in the values of the T.S., it is difficult to make conclusive comments on the effects of rapid austenitizing (Fig. 3.5); however, there seems to be a small increase (up to about 10 tons/in^2) in the value of T.S. of S.T.A. austenite over the 'standard' austenite.

The accompanying loss in the ductility for an austenitizing time of about one minute at 650°C is relatively small - the value is approximately 80 percent for S.T.A. austenite in comparison with approximately 120 percent for annealed austenite. The wide scatter in the values of ductility indicates that the ductility of the S.T.A. austenite is a complex function of its internal structure - it probably depends upon the density of internal defects, such as dislocations, and their interaction.

Some of the scatter in the values of both ductility and T.S. is probably due to the fact that several different thicknesses of tensile specimens were used.

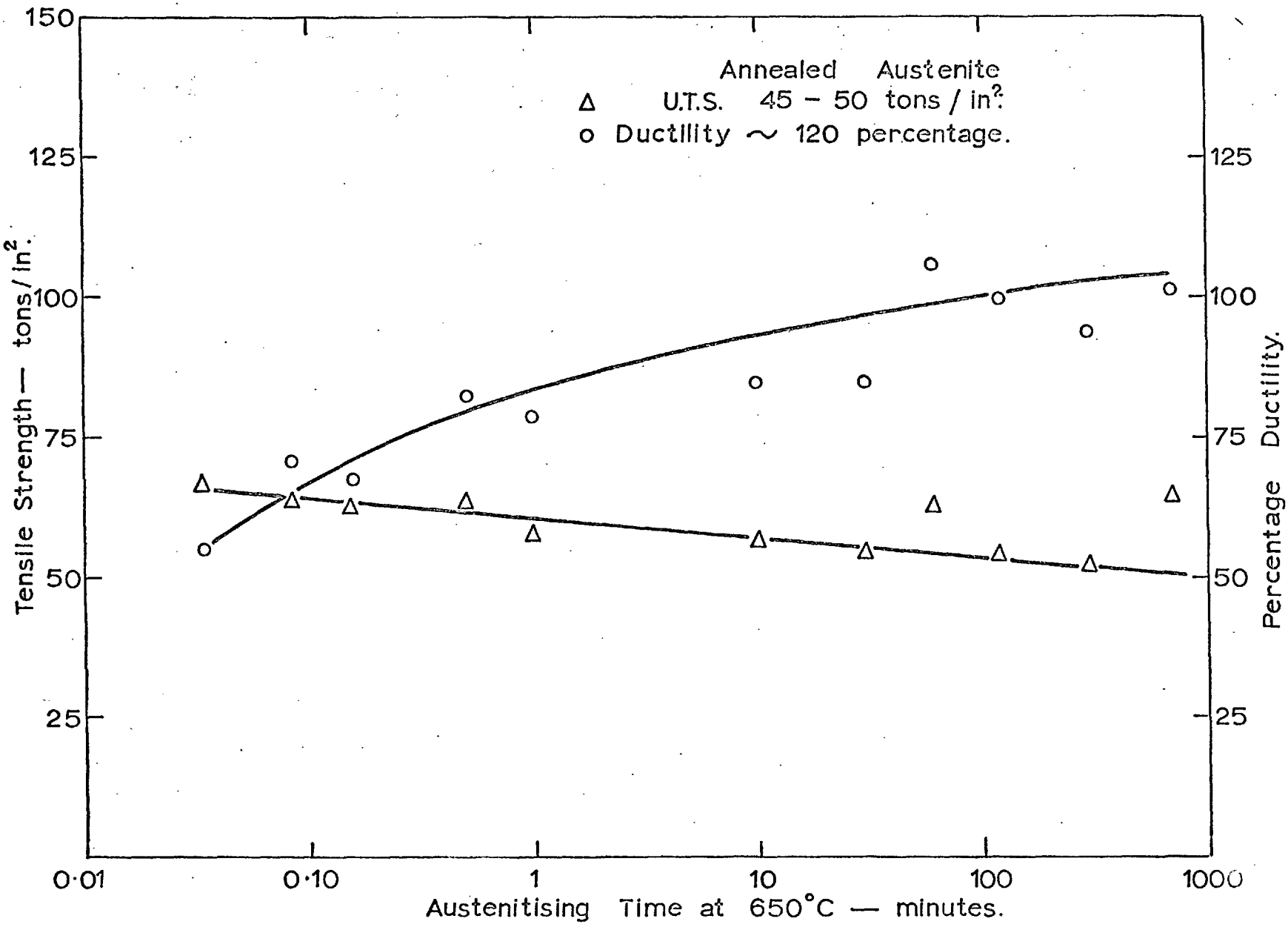

Fig. 3.5. HP1 alloy. Variation of tensile strength and ductility with austenitizing time at 650°C.

Iron-nickel-molybdenum-carbon alloys

Solution treated samples of the iron-nickel-molybdenum-carbon alloy (IMM1), after quenching in liquid nitrogen, gave martensitic structures co-existing with about 30 percent retained austenite. The samples were re-austenitized in a salt bath at temperatures between 650°C and 860°C for times ranging from 30 seconds up to 100 hours. Figs. 3.6 and 3.7 show the variation at room temperature of the hardness of the S.T.A. austenite with austenitizing time at 650°C, 755°C and 860°C. For an austenitizing treatment of about 1 minute the hardness value is about 280 - 300 HV. This may be compared with the hardness of about 140 HV for the austenite solution treated at 1240°C for 3 hours (i.e. conventional austenite) and with the hardness of about 365 HV for the martensite-austenite mixture obtained on cooling the solution treated austenite in liquid nitrogen.

For austenitizing at 650°C and 755°C the hardness of the 'reversed' austenite increases by about 20 HV during the first ten minutes of austenitizing. For the 650°C treatment, further increase in the hardness occurs during an austenitizing period of about 100 hours, whereas at 755°C the hardness decreases markedly with time during this period. For austenitizing at 860°C, the hardness decreases comparatively rapidly with increasing treatment times up to about 12 hours, but the hardness after this time has still not reached the value of 140 HV characteristic of the conventional austenite.

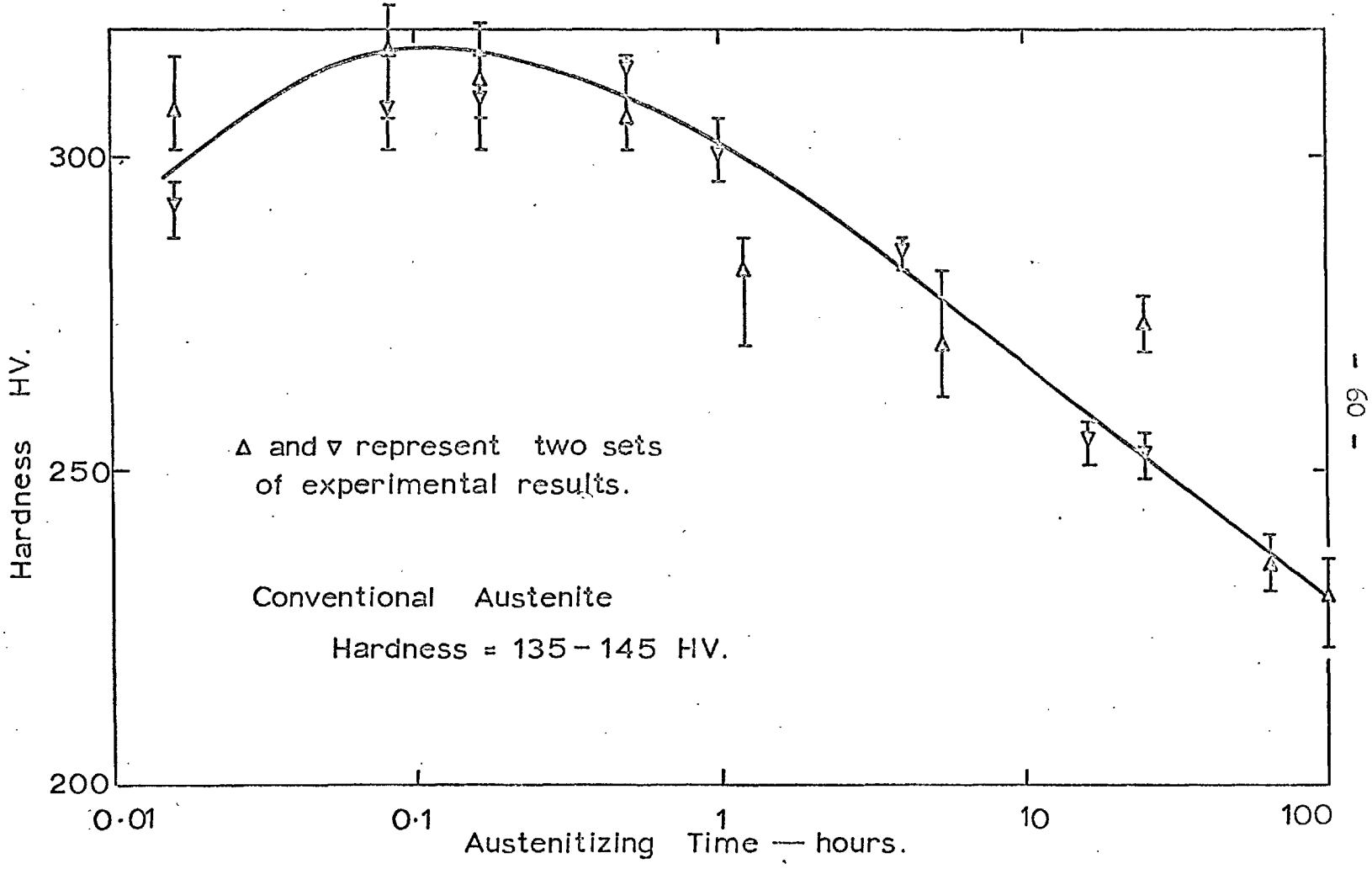

Fig. 3.6. Fe-Ni-Mo-C(INN1) alloy. Variation of hardness with austenitizing time at 755°C.

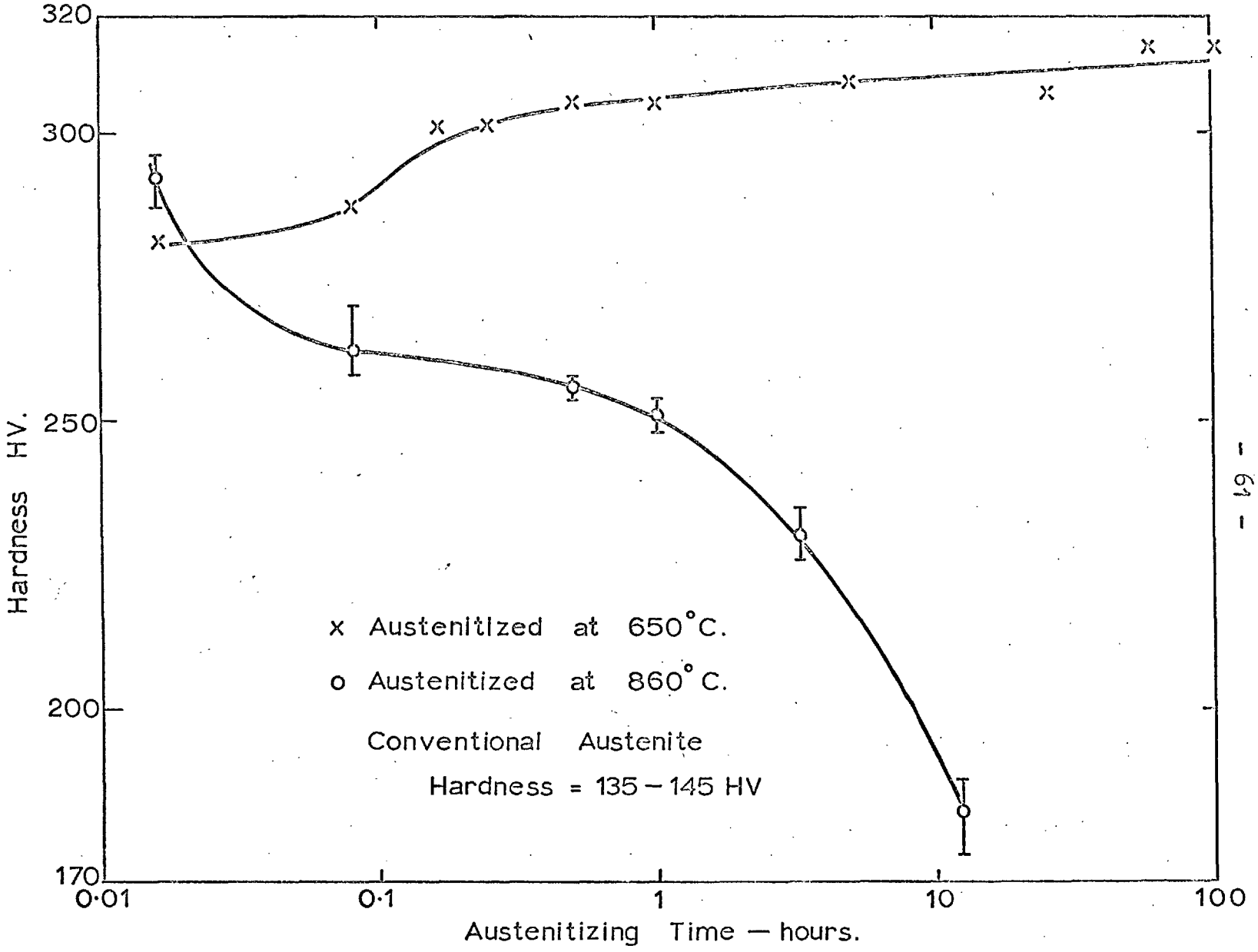

Fig.3.7. Fe-Ni-Mo-C (INM1) alloy. Variation of hardness with austenitizing time at (a) 650°C (b) 860°C.

In the iron-nickel-molybdenum-carbon alloy (INM1) it was found that the specimens became ferromagnetic with increasing austenitizing time. Using a simple magnetic test, the specimens noticeably showed ferromagnetism after a period of time which varied with temperature as shown in Table 3T-4.

TABLE 3T-4

Austenitizing temperature	Austenitizing time
860°C	After 20 minutes
755°C	After 90 minutes
650°C	After 4 hours.

A Sucksmith-type magnetic balance (See Chapter 2) was used to study the amount of ferromagnetic phases (ferrite and/or carbides) formed on prolonged soaking of the iron-nickel-molybdenum-carbon alloy (and also of the iron-nickel-carbon alloy austenitized at 650°C) at an austenitizing temperature of 700°C. Solution treated specimens of these alloys were cooled to liquid nitrogen temperature to produce a structure of martensite co-existing with retained austenite. They were then rapidly austenitized for various times from a few seconds up to about eleven hours at temperatures shown in Table 3T-5.

In view of the fact that the austenite itself gives a magnetic response, it should be emphasized that, with the method

TABLE 3T-5

Effect of time of austenitizing on ferromagnetic response.

Iron-nickel-molybdenum-carbon alloy (INM1). Amount of martensite at -196°C = 70% Temperature of austenitizing = 700°C		Iron-nickel-carbon alloy (INM1) Amount of martensite at -196°C = 85% Temperature of austenitizing = 650°C	
Time of austenitizing	'Equivalent' ferromagnetic content-percent	Time of austenitizing	'Equivalent' ferromagnetic content-percent
1 second	2.5	1 second	6.6
2 seconds	2.3	2 seconds	6.1
	2.6		
5 "	2.1	5 "	6.1
	2.1		
10 "	2.0	15 "	5.8
	1.8		
30 "	2.1	30 "	5.4
	2.1		5.8
1 minute	1.6	1 minute	5.5
	1.7		
	2.0		
5 minutes	2.0	5 minutes	4.4
	2.1		5.2
10 "	2.0	10 "	4.9
	2.0		5.0

TABLE 3T-5 (Continued).

Time of austenitizing	'Equivalent' ferromagnetic content-percent	Time of austenitizing	'Equivalent' ferromagnetic content-percent
30 minutes	2.0	30 minutes	4.5
	2.3		4.6
			4.9
60 "	2.2	60 "	4.6
	2.2		4.9
			4.9
4 hours	2.3	4 hours	4.3
	2.4		4.4
10 "	39.3	12.5 "	4.3
	40.3		6.1
Conventional austenite	2.1	Conventional austenite	6.0
	2.3		6.0
	2.4		6.4

of calibration used, (Chapter 2, section 2.42), the magnetic response of the conventional austenite is equivalent to about 2% ferromagnetic phase in the iron-nickel-molybdenum-carbon alloy (IMM1) and about 6% in the iron-nickel-carbon (INN1) alloy.

The results of these tests indicate that in the time range up to four hours, there is no evidence of any ferromagnetic phases (within the limits of accuracy of the experiments); in other words, the magnetic response of the S.T.A. austenite is the same as that of the original annealed austenite. In case of the iron-nickel-molybdenum-carbon alloy (IMM1), however, a pronounced development of ferromagnetism occurs for austenitizing times of more than four hours. This effect complicated the study of the effects of relatively longer times of austenitizing on the strength of S.T.A. austenite. It was, therefore, decided, at least for the iron-nickel-molybdenum-carbon alloys, to study the effects of rapid austenitizing only for short times - say about a minute.

3.14 - Effect of initial amount of martensite on the yield stress of S.T.A. austenite.

Some experiments were carried out to study the relationship between the strength of S.T.A. austenite and the amount of martensite in the structure prior to austenitizing. Tensile samples of the iron-nickel-carbon alloy (INN2) were heated for

3 hours in vacuum at 1200°C and water-quenched. They were then cooled to selected sub-zero temperatures to give various amounts of martensite. The samples were then re-austenitized for 1 minute at 650°C and quenched in water. Tensile tests were carried out; and the values of the 0.2% yield stress, corresponding to the various amounts of martensite are shown in Table 3T-6 and Fig. 3.8. The yield stress value for austenite produced by annealing at 1200°C for 3 hours is 9-11 tons/in.^{2}

TABLE 3T-6

Amount of martensite and 0.2% yield stress of S.T.A. austenite.

Quenching temperature	Percentage martensite present prior to austenitizing	0.2% yield stress of S.T.A. austenite ton/in^2
-25°C	13.0, 15.0, 18.0	14.0, 15.2, 15.5
-36°C	16.5, 18.0, 20.0	16.0, 16.7, 17.7
-50°C	34.0, 35.0, 38.0	19.7, 20.2, 20.3
-55°C	45.0, 48.0	20.0, 21.0
-60°C	48.0, 50.0, 55.0	20,5, 21.4
-70°C	60.0, 64.0	25.0, 25.2, 25.2
-86°C	81.0, 85.0	26.4, 27.0
-115°C	89.0, 90.0	29.2, 29.2
-196°C	95.0, 97.0	29.2, 29.0

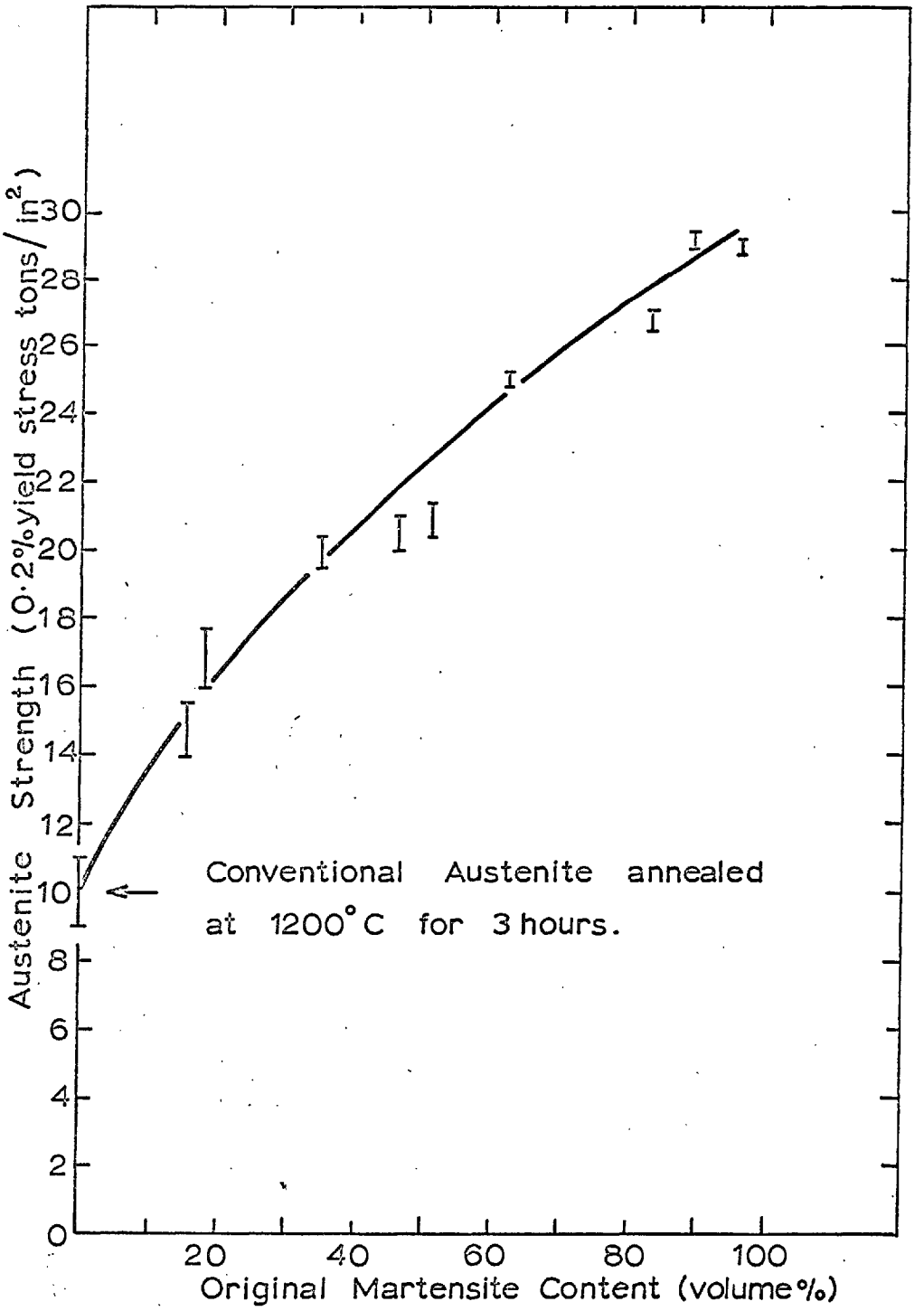

Fig. 3.8. Fe-Ni-C(INN2) alloy. Plot showing effect of amount of martensite on yield stress of S.T.A. austenite.

In order to reduce the uncertainty in the amount of martensite, as measured by the 'point-count' metallographic technique, a large numbers of counts, as many as 1000, were made and, in some cases, the experiment was triplicated for tensile tests and 'point-counts'. The average amount of martensite, formed on quenching to a pre-selected temperature, was taken as the simple arithmetic average of all the values of the amount of martensite from each group of about 1000 counts. Beacuse of the large number of counts made, the probable error (the range in which there was 95% probability that the true value lay) in the amount of martensite, for a specimen containing approximately 50 percent of martensite is estimated to be ± 2.5% (C3).

The points on the graph (Fig. 3.8) appear to lie on a curve rather than a straight line. The graph indicates that the strengthening achieved in the S.T.A. austenite is greater per percent martensite in the range approximately 0-25% martensite than in the range 25-95% martensite. These results are in good agreement with the work done by Krauss (C.4) on an iron-33.5% nickel alloy.

3.15 - Structural changes Characteristics of short-time rapidly austenitized structures.

(i) Optical microscopy

Optical microscopical study of the S.T.A. austenite shows that most of the original martensite plates, on reversion

to austenite, break down into fragments appearing within the original martensite plates. Fully annealed samples of iron nickel-carbon alloy (HP1) were quenched to -41°C and the resulting structure, containing a small amount of martensite co-existing with a large amount of retaining austenite, was rapidly austenitized at 650°C for 10 minutes followed by quenching in water. After grinding off the surface by about 0.002", the samples were polished and etched. Fig. 3.9a shows a typical optical micrograph of S.T.A. austenite present in the matrix of retained austenite. Edmondson and K**O** (C.5) have referred to this effect as a "ghost" structure. The structural mechanism of reversion is characterised by the "banded" appearance (Fig. 3.9a) of austenite fragments in each martensite crystal; the fragments are much smaller than the original martensite crystal.

(ii) Electron microscopy

Electron microscopical evidence for the "banded" appearance of S.T.A. austenite fragments on reversion is furnished **in** Fig. 3.9b. Samples of iron-nickel-molybdenum-carbon alloy (INM1) were quenched to -155°C to produce a small amount of martensite existing with retained austenite. They were then rapidly austenitized at 750°C for 1 minute. The micrograph shows a "banded" structure within the region of the original martensite plate; in this micrograph areas of retained austenite adjoin the reversed austenite. Observations of the

Fig. 3.9a. HP1 alloy. 'Ghost' structure of martensite in austenite X800

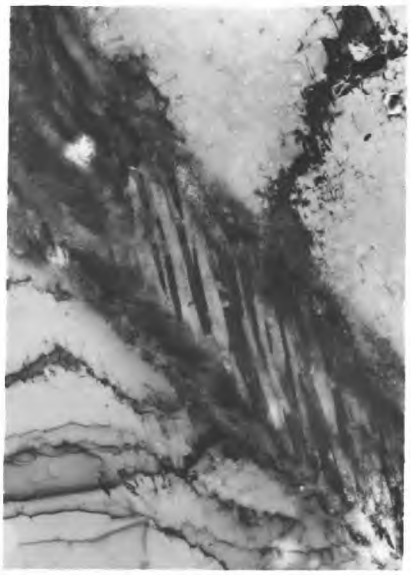

Fig. 3.9b. INM1 alloy. Structure showing "banded" nature of S.T.A. austenite X10,000

Fig. 3.10a. INN2 alloy. Structure showing fragments of S.T.A. austenite within original martensite plate. Carbon replica X4,000

Fig. 3.10b. Conventional martensite. Carbon replica X10,000

existence of the S.T.A. austenite in relation to the original mixture of martensite and retained austenite were not always possible, particularly in samples containing large amounts of original martensite.

Fig. 3.9b shows the "banded" nature of the fragments (0.1 - 0.5 microns thick) of S.T.A. austenite which are separated from one another by irregular, but sharp boundaries.

The carbon replica technique was used to obtain further evidence of the fragmentation effect. Samples of the iron-nickel-carbon alloy (INN2), solution treated at 1200°C for 3 hours and water quenched, were cooled to about -50°C to obtain a mixture of martensite and retained austenite. They were rapidly austenitized at 650°C for 1 minute followed by water-quenching and final polishing to remove oxide scale. Carbon replicas from these samples showed the fragmentation effect within the original martensite crystals (Fig. 3.10a). In comparison with the S.T.A. austenite, Fig. 3.10b shows a conventional martensite plate (in the same alloy as in Fig. 3.10a) replicated on carbon film.

Another structural feature of interest observed in the transmission electron microscopical study of the S.T.A. austenite is the formation of platelets of S.T.A austenite, comparable in size with the original martensite plate, which do not show "banded" fragments but contain a high dislocation density (Fig. 3.11). It may be recalled that the structure before reversion

shows both twinned and untwinned martensite crystals (Fig. 3.1C).

(iii) Crystallographic relations

Frequently the fragments of the S.T.A. austenite tend to be aligned approximately transversely across the original martensite plates (Figs. 3.9a, 3.9b and 3.10a). In other cases the fragments lay more nearly parallel to the length of the original martensite plates (Figs. 3.9a and 3.12). These fragments usually terminate within the original martensite plate.

Attempts were made to study the crystallographic relations between the fragments of the S.T.A. austenite. In some cases it was difficult to obtain a simple diffraction pattern from the areas of the fragmented S.T.A. austenite, especially if the fragments lay along the length of the original martensite; for fragments of the S.T.A. austenite aligned across the original martensite plate, orientation relations were established by electron diffraction method.

Solution treated samples of the iron-nickel-molybdenum -carbon alloy (INM1) alloy, were quenched to -196°C and the resultingstructure (martensite and retained austenite) was rapidly austenitized at 750°C for one minute followed by quenching in water. Fig. 3.13a shows the "banded" fragments of the S.T.A. austenite lying across the original martensite plate.

A selected area diffraction examination of the fragments (Fig. 3.13b) shows a composite diffraction pattern from

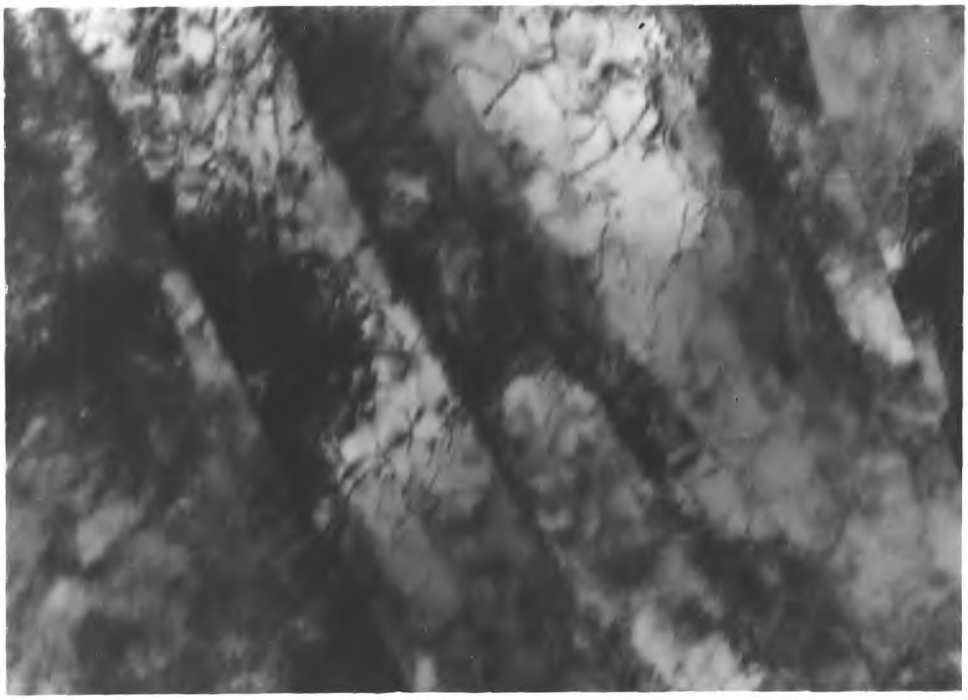

Fig. 3.11. Fe-Ni-C (INN1) alloy. Plates of S.T.A. austenite with high density of dislocations. Retained austenite can be seen between two S.T.A. austenite plates X29,000

Fig. 3.12. Fe-Ni-Mo-C (INM1) alloy, showing fragments of S.T.A. austenite nearly parallel to the original martensite plate X40,000

Fe-Ni-Mo-C (INM1) alloy

Fig. 3.13a. Fragments of S.T.A. austenite are seen. Note irregular nature of the boundaries X40,000

Fig. 3.13b. S.A.D. of fig. 3.13a. foil orientation {110}

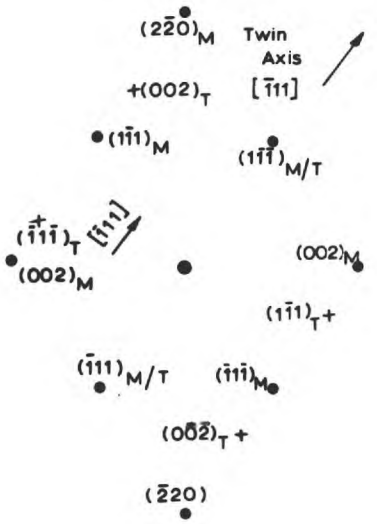

Fig. 3.13c. Indexing the fragmented twin spots (crosses); twinning about $[\bar{1}11]$ axis lying in the plane of the diffraction pattern.

the fragments of the S.T.A. austenite. Indexing of the diffraction pattern (Fig. 3.13C) reveals that the fragments bear a twin relation to one another. Krauss (C.4) has termed these fragments "reversal twins". They terminate within the boundaries of the original martensite plate and unlike annealing twins, the reversal twins have irregular boundaries.

(iv) Dislocation structure of the S.T.A. austenite.

In addition to the formation of the "banded" structure on rapid austenitizing the S.T.A. austenite has been observed to contain a high density of dislocations. Fig. 3.14a shows a complex dislocation configuration in the iron-nickel-molybdenum -carbon alloy (INM1) heated to 750°C for one minute followed by quenching in water. Fig. 3.14b is an electron micrograph from a thin foil of the iron-nickel-carbon alloy (INN1) austenitized at 650°C for 5 seconds. Both the micrographs show areas predominantly populated by a high density of tangled dislocations. In addition, these micrographs show boundaries in the structure. It has not been established that these boundaries are formed on rapid austenitizing and is probable that some of them correspond to the original martensite boundaries.

With increasing time of austenitizing, there is an apparent decrease in the density of dislocations. For example, Figs. 3.15a and 3.15b, are electron micrographs of the iron-

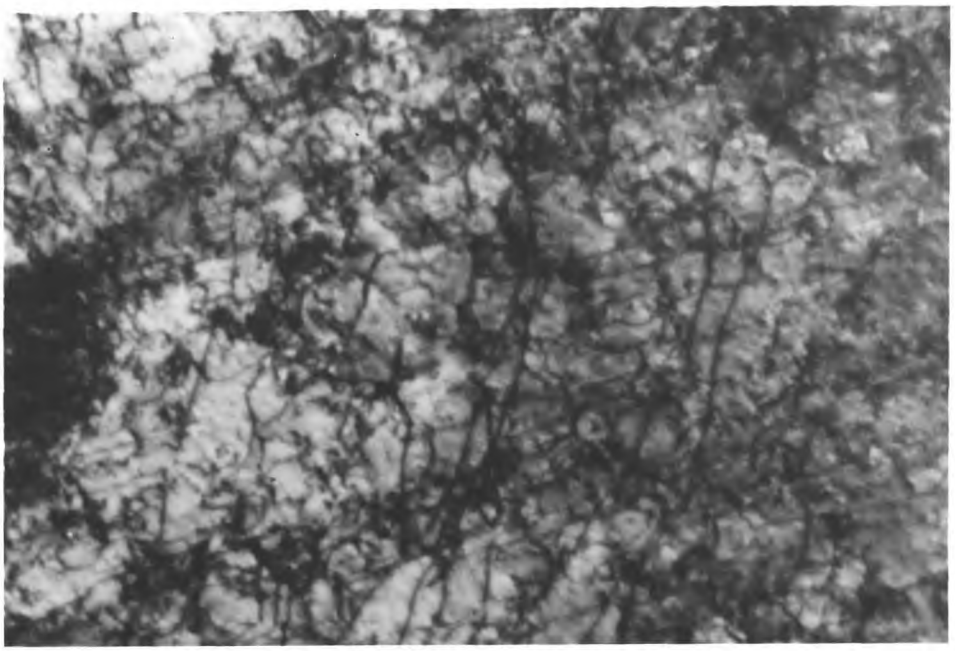

Fig. 3.14a. Fe-Ni-Mo-C(INM1) alloy. Alloy austenitized for one minute at 750°C. showing high density of tangled dislocations X60,000

Fig. 3.14b. Fe-Ni-C(INN1) alloy austenitized for 5 seconds at 650°C. showing high density of dislocations and sub-boundaries X80,000

nickel-carbon alloy (INN1) rapidly austenitized at 650°C for 10 minutes and 40 minutes respectively. For the latter treatment, Fig. 3.15b, the dislocations tend to align themselves in cell 'walls'. The micrograph also shows areas relatively free of dislocations. The effect of the time of austenitizing on the recovery of the original austenite will be further discussed in section 3.17.

In contrast to the highly complex dislocation network in the S.T.A. austenite, slowly heated samples of the iron-nickel-carbon alloy (INN1) have been studied to determine the dislocation arrangements. Fig. 3.16 shows a transmission electron micrograph of a specimen slowly heated in vacuum to 900°C for one hour. In addition to the lower dislocation density in the annealed austenite than in the S.T.A. austenite, the dislocations in the former structure appear to be straight or gently curved.

The value of the dislocation density for the S.T.A. austenite, obtained by applying the Smith and Guttman method (see Chapter II) to the micrographs of Figs. 3.14a and 3.14b, is approximately 10^{10} lines/cm^2. This may be compared with a value of about 10^9 lines/cm^2. (Fig. 3.16) for the fully annealed austenite. The value of the density of dislocations in the annealed austenite, appears to be high. One of the factors probably contributing to this apparent high value is the

Fe-Ni-C (INN2) alloy.

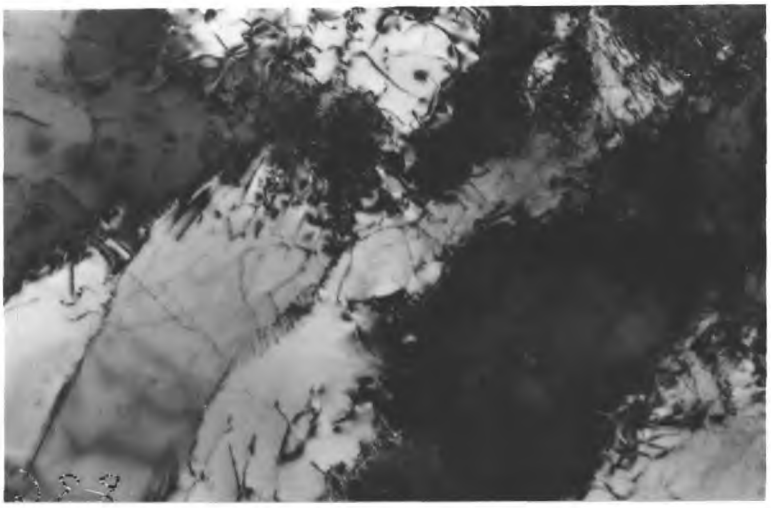

Fig. 3.15a. Austenitized for 10 minutes at 650°C. Areas of both high and low dislocation density are seen. X22,000

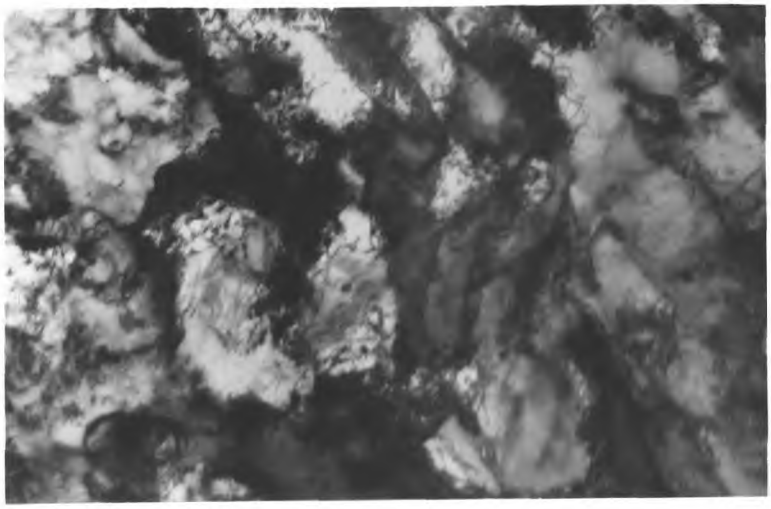

Fig. 3.15b. As fig. 3.15a but austenitized for 40 minutes. Note formation of cell 'walls' X10,000

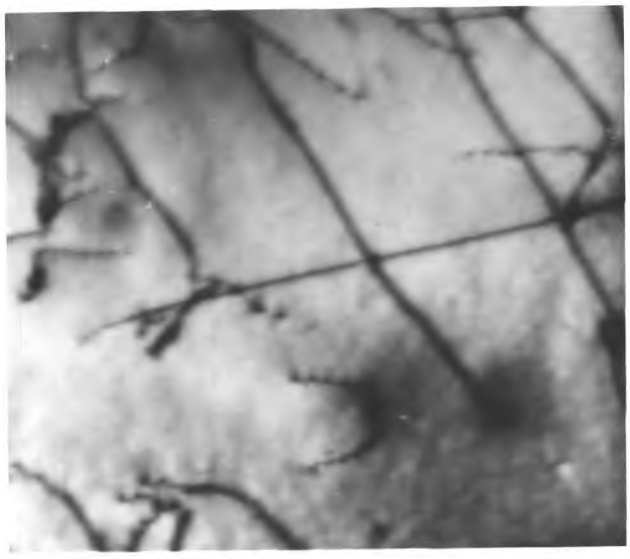

Fig. 3.16. Austenite annealed at 900°C for one hour X80,000

buckling (during handling) of the thin foil of the annealed austenite.

In the foregoing results, it has been established that on 'shock' heating, a martensite plate reverts to austenite with altered internal defects - "banded" structure and high dislocation density. It has also been found that rapid austenitizing brings about lattice distortion in the retained austenite. Fig. 3.11, showing dislocations in the retained austenite (situated between two S.T.A. austenite plates), is indicative of this effect.

Some microhardness tests were also done on the retained austenite co-existing with the S.T.A. austenite. Solution treated samples of the iron-nickel-molybdenum-carbon alloy (INM1) were cooled to -145°C to produce about 30 percent martensite. They were then heated for 1 minute at 650°C and quenched in water. Optical microscopical examination showed (Fig. 3.17) that the areas of the original martensite plates were still visible as dark etching areas although the structure was fully austenitic. The microhardness measurements (Fig. 3.17) indicate that the lattice distortion of the retained austenite is at a maximum in the near vicinity of the original martensite plate, and that more remote areas of retained austenite remain undistorted. The microhardness values for the S.T.A. austenite regions (e.g. Area C in Fig. 3.17), and retained austenite,

remote from an original martensite plate, (e.g. Area A in Fig. 3.17) are in reasonable agreement with the [redacted] hardness values reported in Fig. 3.7.

(v) Shear-type nature of reversion.

The shear-type nature of the reverse transformation has been observed by the surface relief effects.

Samples of the iron-nickel-carbon alloy (INV2) were cooled to -51°C to produce about 35 percent of martensite and were given a fine diamond polish. The samples were rapidly austenitized at 650°C for one minute and were then repolished on $\frac{1}{4}$ micron diamond paste to remove any oxide scale. Polishing after the austenitizing did not destroy surface relief effects, if any, were present, caused by rapid austenitizing.

The results of the interferometry experiments indicate (Fig. 3.18b) that reversion appeared to occur, within the limit of the resolution, with each martensite plate shearing as one unit. Fig. 3.18a shows an interferogram of the iron-nickel-carbon alloy, containing a small amount of martensite, before reversion.

Although the transmission electron microscopical investigation has shown that most of the martensite plates, on reversion, are divided into fragments, the interferometry technique, however, gave no evidence of small fragments of the

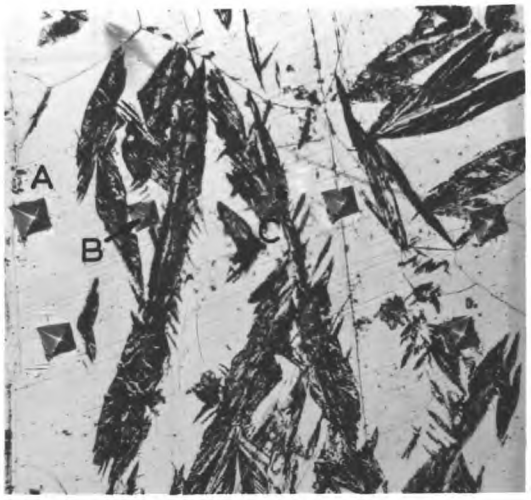

Fig. 3.17. INI alloy. Results of microhardness tests. Figures below in brackets are microhardness values. Load = 30 gm. X600
A(135), B(223), C(268)

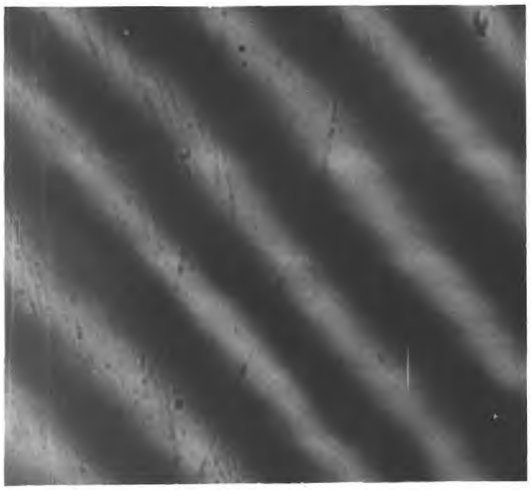

Fig. 3.18a. Interferogram of polished specimen containing martensite/austenite mixture. Fe-Ni-C (INN2) alloy X96

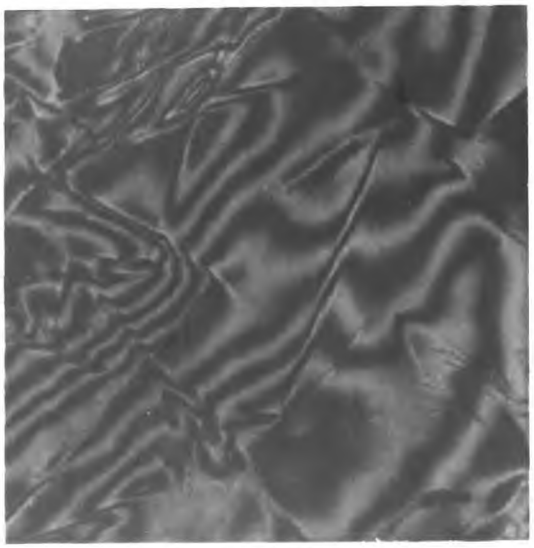

Fig. 3.18b. As fig. 3.18a, but after reversion X96

S.T.A. austenite having their own sector of relief. This was probably because the fragments were so small that, within the resolution of the technique, the relief due to individual fragments, within the original martensite plate, could not be detected.

However, the results of the direct carbon replica technique, suggest (Fig. 3.10a) that surface relief accompanies each fragment formed, within the original martensite plate, on reversion.

3.16 Tempering during reversion

The structure of the austenite produced by rapid austenitizing has been shown to contain a high dislocation density and the possibility that these dislocations might act as sites for carbide precipitation during austenitizing treatments was given special attention, since such a phenomenon might play an important role in contributing to the observed enhanced strength.

It may be recalled here that the original (conventional) martensite before austenitizing is not 'virgin' martensite, but a slightly 'tempered' structure, presumably containing fine precipitate particles. Furthermore, during heating for austenitizing some tempering is expected to occur. This has been demonstrated by carrying out some 'short-time' isothermal tempering treatments to indicate the possible degree of tempering

during continuous heating. A tempering temperature of 550°C was chosen and the hardness changes that accompany the short-time tempering of the iron-nickel-molybdenum-carbon alloy (IMM1) are shown in Table 3T-7.

TABLE 3T-7

Short-time tempering of martensite.

Hardness of conventional martensite/austenite mixture = 365 HV.

Time of tempering at 550°C - seconds	Hardness HV
2	345
5	340
30	330

Electron microscopical examination was carried out on a sample of this alloy tempered at 550°C for 15 seconds, in an attempt to throw light on carbide precipitation that might influence the structure of the austenite that forms on rapid austenitizing to a temperature such as 750°C. Selected area diffraction Fig. 3.19b, gave evidence for the existence of cementite particles, but transmission electronmicrographs, however, did not reveal the presence of such particles. This was possibly because, considering the short-time (15 seconds) used for tempering (at 550°C), their size was too small to be observed.

Fe-Ni-Mo-C (INM1) alloy

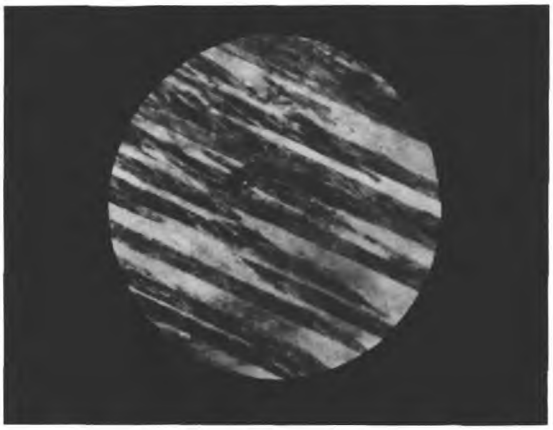

Fig. 3. 19a. Conventional martensite tempered at 550°C for 15 seconds X30,000

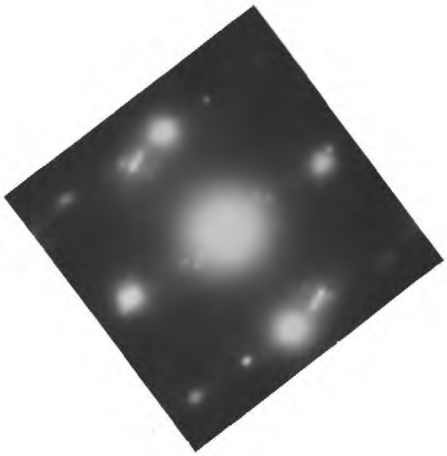

Fig. 3. 19b. S. A. D. of fig. 3. 19a. $(100)_{ferrite}$ orientation

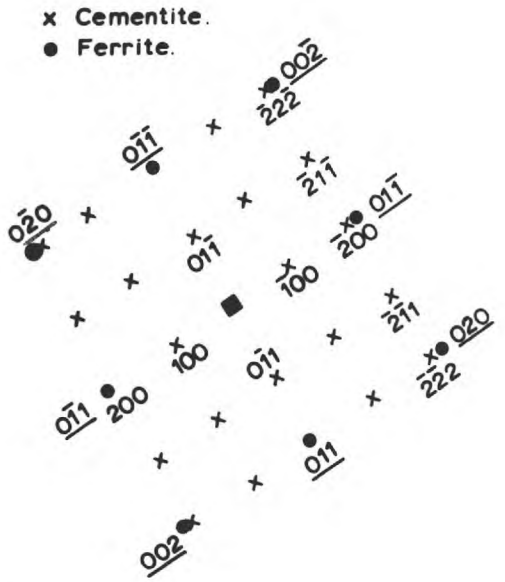

Fig. 3. 19c. Indexing of cementite reflections in matrix of ferrite. $[0\bar{1}1]_{ferrite} \parallel [100]_{cementite}$

While evidence for the cementite particles in short-time tempered martensite has been obtained by electron diffraction, it has not been possible to detect any carbide particles in the S.T.A. austenite containing a high density of dislocations. It is probable that the carbides, although they exist in the ferrite + carbide region of the equilibrium diagram, will tend to redissolve on heating to the austenite region. However, despite the lack of positive evidence, it is considered that the presence of small carbide particles in the S.T.A. austenite is still a possibility.

3.17 Changes with time and temperature of austenitizing - recovery

The manner in which the mechanical properties vary with austenitizing time (Figs. 3.2, 3.3 and 3.4) suggests that recovery processes and possibly recrystallization occur progressively as the time of treatment is increased. The hardness changes in the S.T.A. austenite as a function of annealing time and temperature for the three iron-nickel-carbon alloys have already been shown in Figs. 3.2, 3.3 and 3.4; only a small decrease in hardness occurs during the initial recovery process. The rapid softening displayed by the curves is indicative of recrystallization.

The results of electron microscopical examination, Figs. 3.14b and 3.15, of samples austenitized at 650°C for times ranging from a few seconds up to 40 minutes, indicate that samples austenitized for 10 minutes and 40 minutes (Fig. 3.15) have a lower dislocation density than the samples treated for only a few seconds.

The nature of the process by which the dislocation content is reduced, as austenitizing time increases, seems to be, Fig. 3.15b, by a process where dislocations have polygonized into sub-grains. Some areas in the micrograph show relatively large grains co-existing with small sub-grains. There is, however, no evidence for the existence of high angle boundaries between the grains.

The activation energy (Q) for the process of recovery of the annealed austenite was determined from the time (t) to reach a given fraction of the recovery process (as deduced from the fractional change in hardness during austenitizing).

$$\frac{1}{t} = A \exp\left[-\frac{Q}{RT}\right]$$

where A is a constant; R is the universal gas constant and T is the absolute temperature. Data are given in Table 3T-8.

TABLE 3T-8

Activation energy of 'recovery' process

(Reference: Figures 3.3 and 3.4)

Alloy	Fraction of recovery (ΔH)	Activation energy kcal/mol.
Iron-nickel-carbon alloy (INN1)	0.1	159
	0.5	160
	~ 0.9	160
Iron-nickel-carbon alloy (INN2)	0.1	157
	0.5	153
	~0.9	150

The value of the activation energy is much larger than the activation energy for the self diffusion of iron along the grain boundaries of austenite, which is reported to be 41 kcal/mol (C.6). It appears, therefore, that atom-by-atom transfer of iron (or nickel) across the migrating interface does not control the recovery process under study.

CHAPTER 3.2

The Structure and Properties of Martensite and Tempered Martensite Produced from S.T.A. Austenite

3.21 Synopsis

A study has been made of the difference in mechanical properties between martensite produced by conventional and by rapid austenitizing treatments and of the extent to which these differences are preserved during tempering. Structural studies of tempered martensites, both conventional and that produced from S.T.A austenite, have shown that the internal structure of martensite has a pronounced effect on the morphology of the carbide precipitation.

The early stages of the decomposition of martensite in an iron-nickel-molybdenum-carbon alloy (INM1) have been examined by means of thin-foil electron microscopy. The first precipitate observed is cementite. A substantial increase in strength (secondary hardening) has been found to be associated (at peak hardness) with the presence of molybdenum-carbide (Mo_2C). The average martensite plate size in the S.T.A. martensite was smaller than that in the conventional martensite.

The orientation relationships between the ferrite matrix and the precipitates - cementite and molybdenum-carbide - have been established.

3.22 Effect of time of austenitizing on the hardness of martensite.

Experiments were carried out to study the effects of the time of rapid austenitizing on martensite obtained by refrigeration of the reversed austenite. Specimens of the iron-nickel-carbon alloy (INF1) after the standard heat treatment (800°C for 1 hour followed by water quenching and cooling in liquid nitrogen), were rapidly austenitized at 600°C for various times followed by quenching in water and cooling in liquid nitrogen. The values of the hardness of the quenched samples, which contained a mixture of S.T.A. martensite (about 85 percent), S.T.A. austenite, and austenite retained from the first quench in liquid nitrogen, are listed in Table 3T-9.

The table shows that the hardness of the martensite/austenite mixture formed after austenitizing at 600°C for about one minute is greater than that of the conventionally produced martensite/austenite mixture. Longer austenitizing times, ($\sim$50 hours) followed by quenching in liquid nitrogen give a hardness nearly the same as that of the conventional structure. This is in good agreement with the results obtained (Fig. 3.3) in section 3.13, where the time for complete recovery of the austenite at 600°C was found to be nearly the same; viz. about 80 hours.

TABLE 3T-9

Hardness of martensite/austenite mixtures obtained after various times of austenitizing.

Iron-nickel-carbon alloy (INV1)

Hardness of conventional martensite/austenite mixture = 440 - 450 HV.

Time of austenitizing at 600°C followed by quenching in liquid nitrogen	HV (Load 5kgms)
15 seconds	494
1 minute	487
5 minutes	487
25 "	483
2 hours	473
5 "	475
13.5 "	473
24.0 "	466
50.0 "	450
80.0 "	454

3.23 The two martensites - strength and plate size.

It has been shown in the previous section (3.22) that short-time austenitizing treatments followed by quenching in liquid nitrogen gives a structure of S.T.A. martensite and austenite of greater hardness, by about 40 HV, than that of a conventionally produced martensite/austenite mixture. Further experiments, employing different alloys, were done to study the strength enhancement in the S.T.A. structure. Solution treated samples of iron-nickel-molybdenum-carbon alloy (BISM1) were quenched to produce a mixture of martensite (about 81 percent) and retained austenite. They were then austenitized at 750°C for one minute followed by quenching in water and cooling in liquid nitrogen to produce S.T.A. martensite co-existing with S.T.A. austenite and conventional austenite. (See section 3.27). Hardness and tensile tests were carried out on both conventional and S.T.A. structures. (Table 3T-10).

TABLE 3T-10

Iron-nickel-molybdenum-carbon alloy (BISM1).

Quenched structure	Amount of martensite at -196°C.	Hardness HV.	1.0% yield stress tons/in^2
Conventional martensite/austenite mixture	~ 81 percent	420-436	61-71
S.T.A. martensite + S.T.A austenite + conventional austenite	~ 85 percent	463-473	74-80

It must be emphasized here that the structure obtained after quenching either conventional or S.T.A. austenite in liquid nitrogen is, in fact, a martensite/austenite mixture and, in order to study the strength of martensite only, it was essential to separate the strength contribution of the austenite. Samples of the iron-nickel-molybdenum-carbon alloy (BISRA1), containing either conventional austenite or S.T.A. austenite/conventional austenite mixture, were cooled to various sub-zero temperatures (i.e. $-122^{\circ}C$, $-135^{\circ}C$ and $-196^{\circ}C$) to produce different amounts of conventional martensite/conventional austenite and S.T.A. martensite/S.T.A. austenite/conventional austenite mixtures respectively. In view of the fact that, for structures containing relatively small amounts of martensite, a wide scatter in the hardness was observed, it was decided to carry out tensile tests for 1.0% yield stress and plot these values against the amount of martensite calculated by metallographic 'point-count' technique. On extrapolating the plots (assuming a linear relationship), Fig. 3.20a, to a limit of 100 percent martensite (conventional or S.T.A.), the strength of the latter structure, independent of the strength contribution from the austenite, can be estimated. Fig. 3.20a shows superior strength of the S.T.A. martensite over the conventional one.

The choice of 1.0% yield stress, instead of 0.2%, was necessary because it was found that in these tests, and

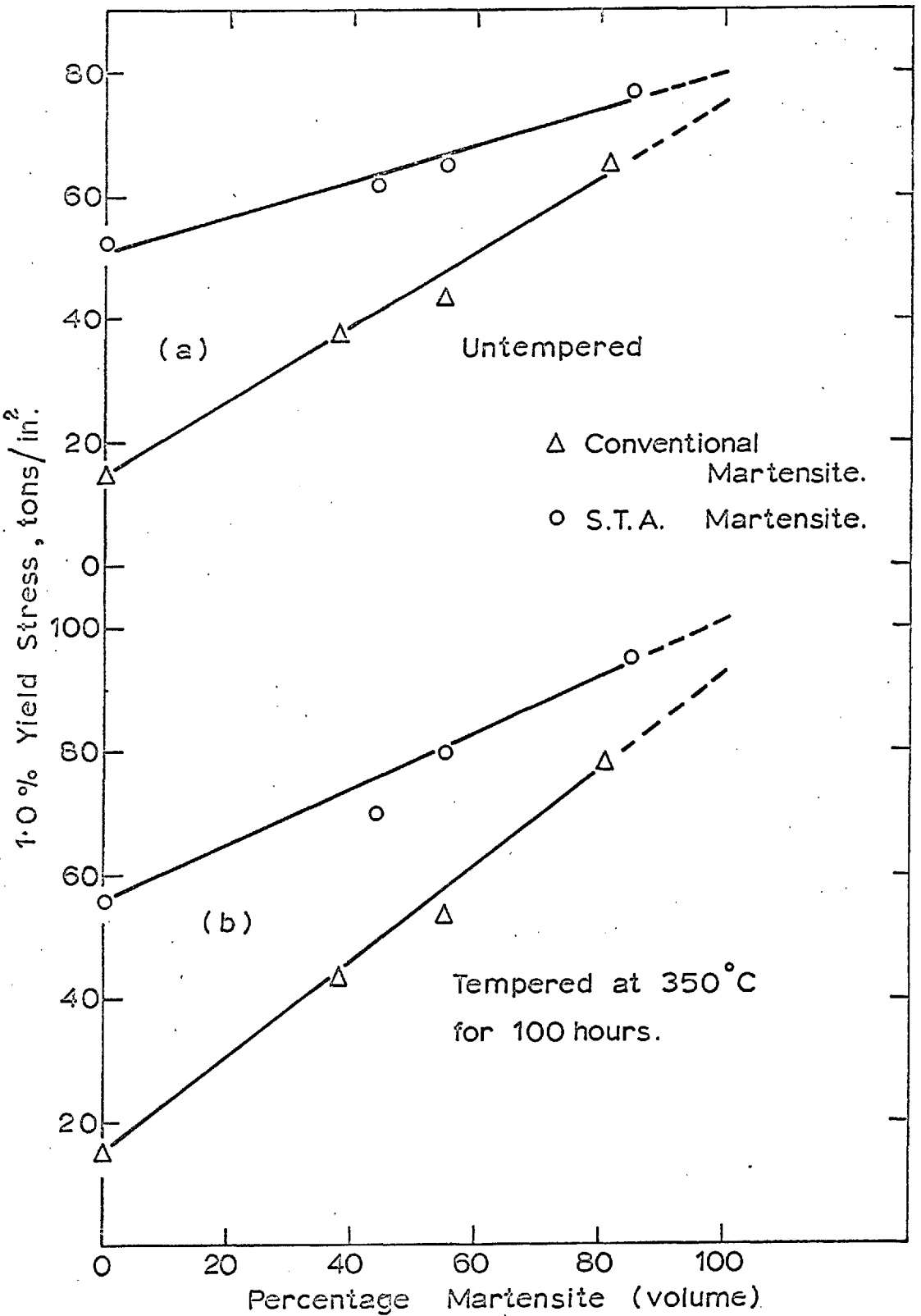

Fig. 3.20. Fe-Ni-Mo-C(BISM1) alloy. Plot of amount of martensite, conventional and S.T.A., versus yield stress. Extrapolation gives strength of martensite independent of that of austenite.

indeed in all tensile tests involving martensite structure, 1.0% strain gave consistent values (within experimental error) of the yield stress. The scatter in the values of 0.2% yield stress was due to the ill-defined initial slope of the stress-strain curve.

Measurements of the dimensions (length and width) of the martensite plates were made using optical microscopy. The total number of martensite plates measured in the case of conventional martensite (INM1 alloy) was about 1500 and for the rapidly heat treated steel about 1000 martensite units were measured. The average plate width and length of the two types of martensite plates are listed in Table 3T-11.

TABLE 3T-11

Dimension of Plates. (microns)	Conventional martensite	S.T.A. martensite
Average width	5.5	4.0
Average length	32	42
Maximum width	20	12
Maximum length	180	180

Optical microscopical observations made on the two types of martensites, Fig. 3.21, show refined crystals of the S.T.A. martensite.

Fe-Ni-Mo-C (INM_1) alloy

Fig. 3.21a. Conventional martensite X550

Fig. 3.21b. S.T.A. martensite structure, showing narrower martensite plates (c.f. fig. 3.21a) X550

Histograms relating the number of the martensite plates (conventional or S.T.A) of a certain range of widths (or lengths) are shown in Figs. 3.22 and 3.23. In the lower range of thickness, there are more plates of S.T.A. martensite than of conventional martensite (Fig. 3.22). The number of relatively thicker plates in the case of conventional martensite is more than in the case of S.T.A. martensite. Although the number of plates with maximum length is the same in both types of martensites, Fig. 3.23, the conventional martensite appears to have more plates in the lower range of length.

3.24 Properties of S.T.A. martensite and conventional martensite after tempering.

Hardness

Some experiments were made on the iron-nickel-carbon alloy (INN1) for the purpose of studying the effects of tempering on the S.T.A. martensite. Samples were initially cooled to $-196^{\circ}C$ to produce martensite and then either austenitized for 1 minute at $600^{\circ}C$ or given a conventional treatment of 1 hour at $800^{\circ}C$. They were then cooled again to $-196^{\circ}C$. After this treatment the hardnesses were approximately 440 HV with conventional austenitizing and 480 HV with short-time austenitizing. These samples were then tempered at $190^{\circ}C \pm 1^{\circ}C$ in a silicone oil bath (MS. 550). Values of the hardness VS

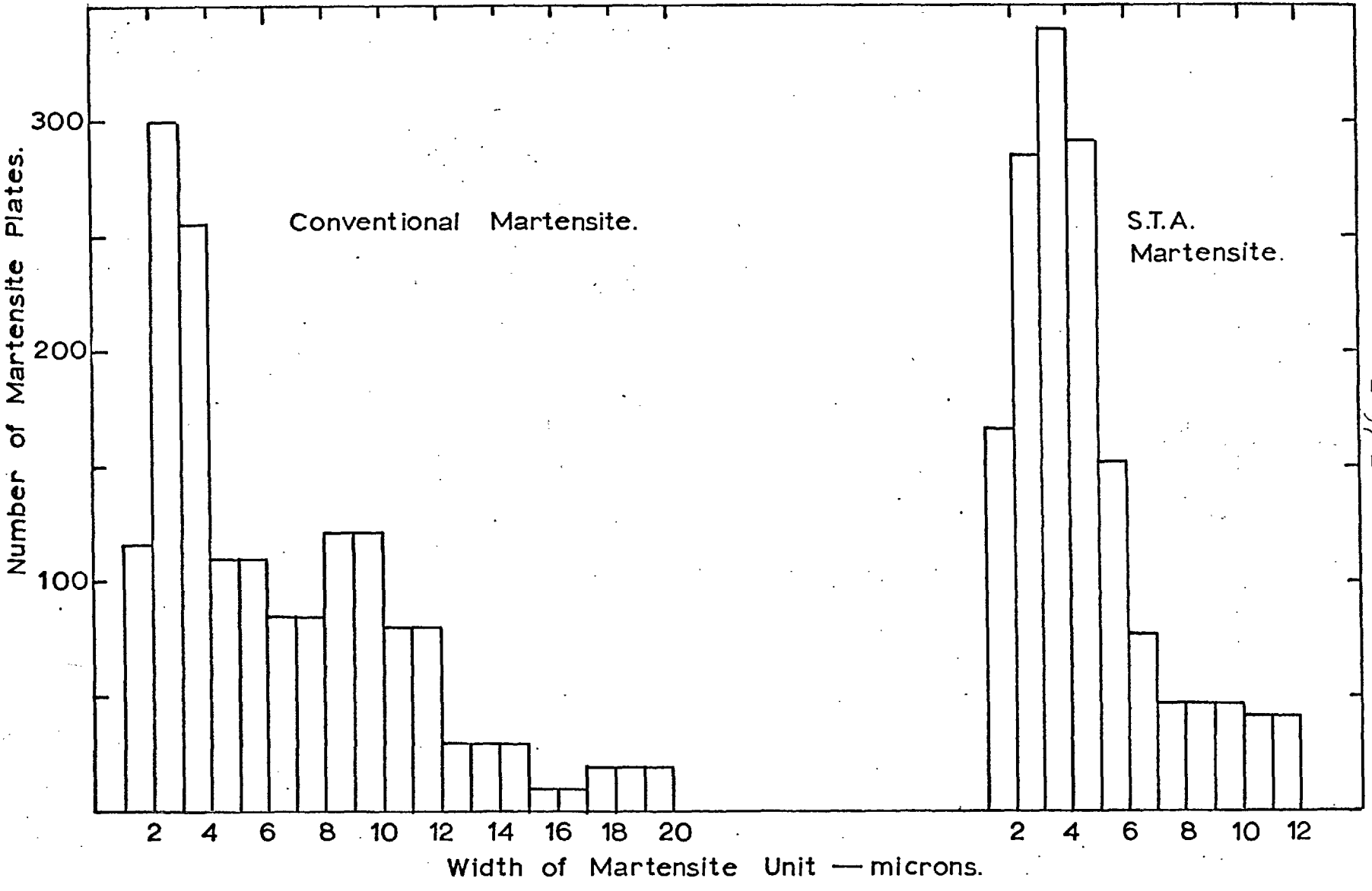

Fig.3.22.Fe-Ni-Mo-C(INM1)alloy.Histograms relating the number of martensite plates (conventional and S.T.A)with their width over one micron range intervals.

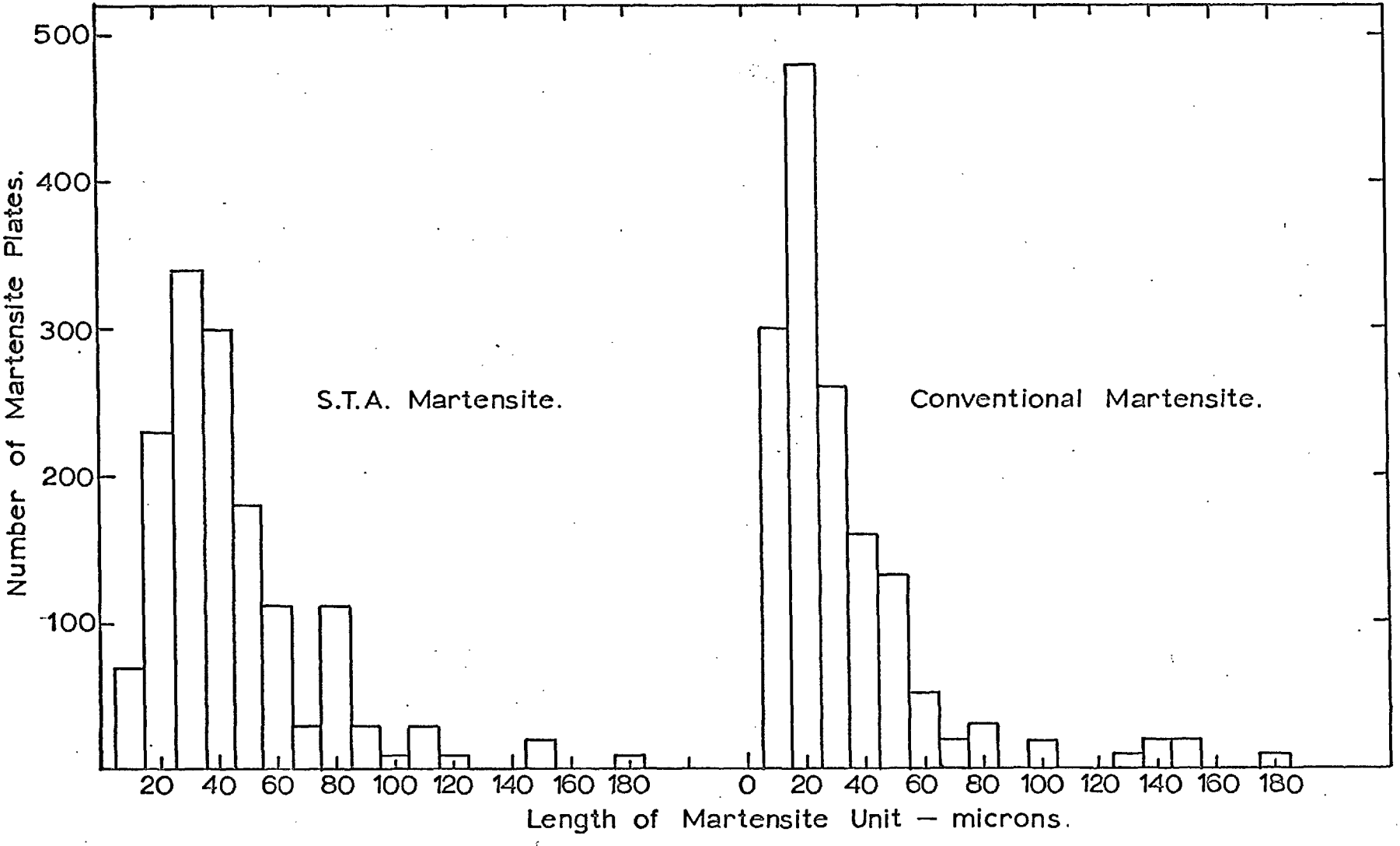

Fig. 3.23. (Fi-Ni-Mo-C) INM1. Histograms relating the number of martensite plates (conventional and S.T.A) with their length over ten micron range interval.

tempering time (on a logarithmic scale) are plotted in Fig. 3.24. For both the conventional martensite and the S.T.A. martensite there is an approximately linear decrease of hardness with log. tempering time in the range of 1 - 350 hours. In comparison with this alloy, the iron-nickel-molybdenum-carbon alloy (INM1), when tempered at 190°C, shows a drop of only about 20 HV during the first hour or so of tempering, Fig. 3.25. In the case of the latter alloy, the hardness of the structure after short-time austenitizing is about 410 HV compared with about 365 HV for the conventional structure. With increasing tempering time (at 190°C) up to about 450 hours, the hardness decreases further to a small extent for the normal structure; in the case of the structure resulting from short-time treatment, virtually no hardness change occurred in this period. There may actually be a trend to slight hardening. The rate of loss of hardness with tempering time is less in the iron-nickel-molybdenum-carbon alloy than in the iron-nickel-carbon alloy.

The results of tempering the iron-nickel-molybdenum-carbon alloy at 350°C (Fig. 3.25) are of special interest in that after an initial softening during the first hour, there is a significant increase in hardness as the tempering time is increased up to about 100 hours. This secondary hardening is slightly greater in this period for tempering of the conventional martensite. Most of the investigators (C.7-8) in the field

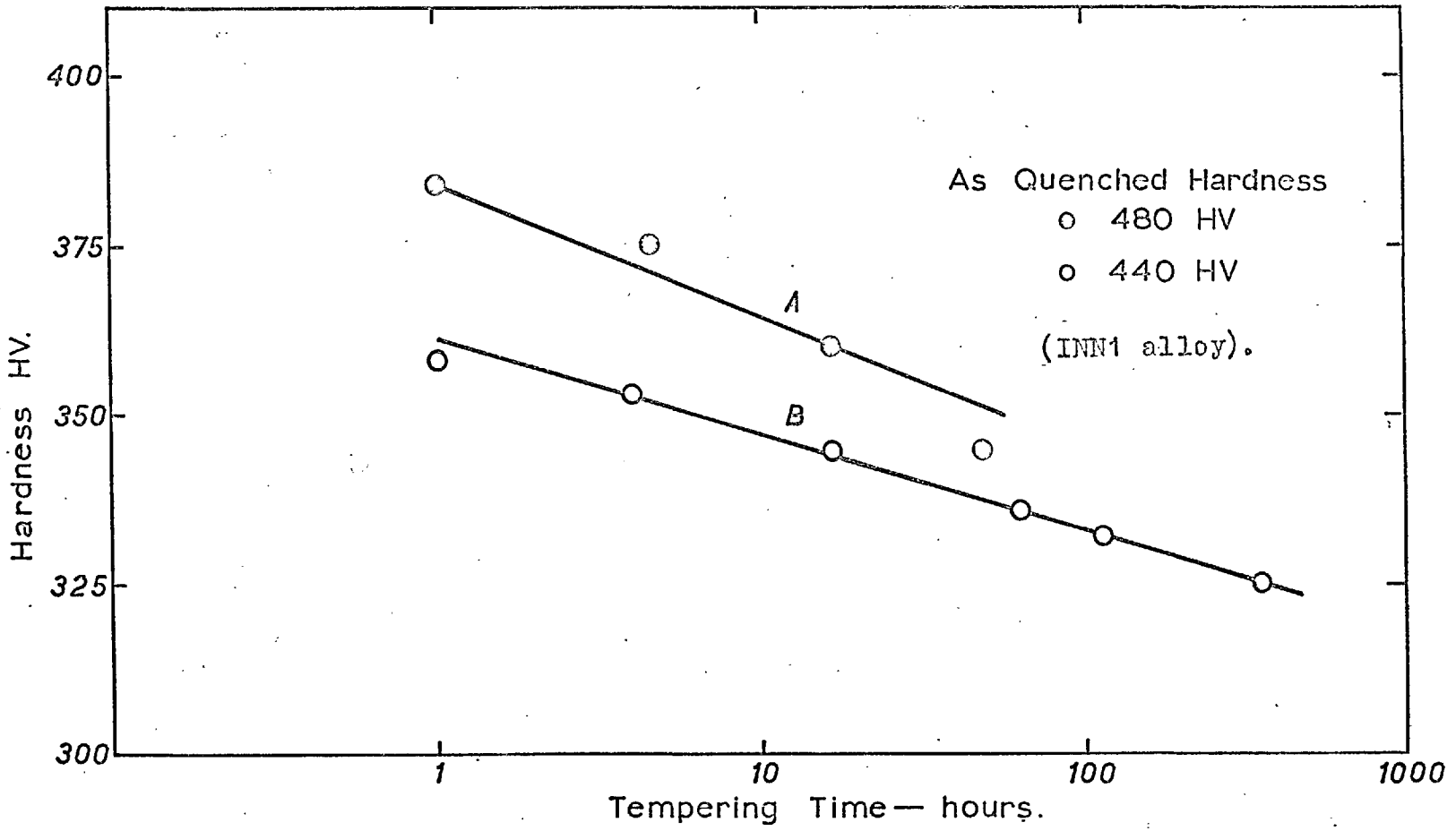

Fig. 3.24. Variation of Hardness with Tempering Time at 190°C.

A. for martensite formed after austenitizing 1 minute at 600°C.

B. for martensite formed after austenitizing 1 hour at 800°C.

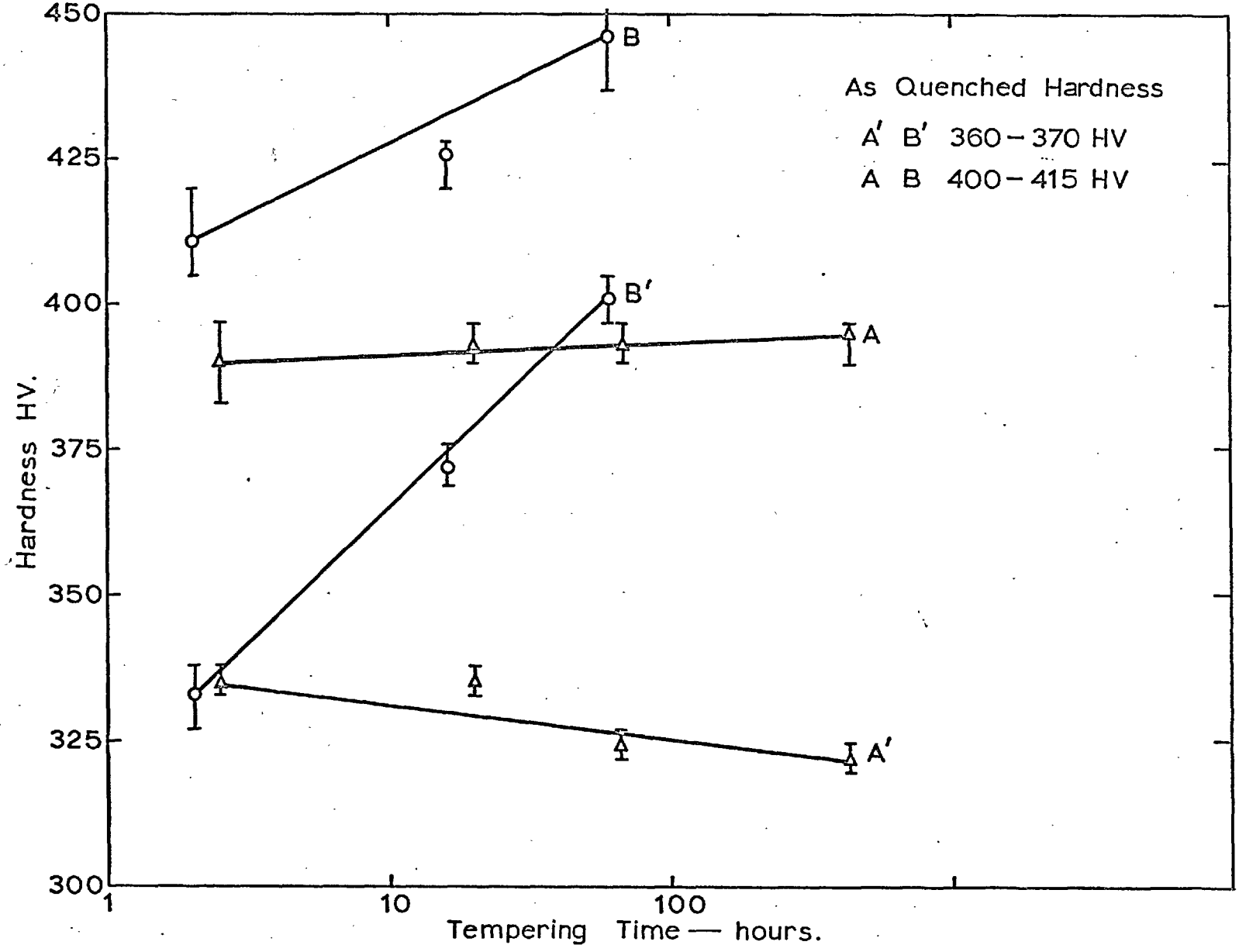

Fig. 3.25. Fe-Ni-Mo-C DM1 alloy. Variation of hardness with tempering time at 190°C (AA') and 350°C (BB')
A'B': for martensite formed after austenitizing 3 hours at 1240°C.
AB: for martensite formed after austenitizing 2 minutes at 700°C (B) and 2 minutes at 650°C (A)

of tempering of molybdenum-steels have employed higher tempering temperatures than 350°C (although their alloys contained less carbon). In the present work, further investigation of the 'secondary' hardening effect was carried out on the iron-nickel-molybdenum-carbon alloy (INM1) employing higher tempering temperatures VIZ 500°C and 550°C.

Samples were rapidly austenitized for one minute at 750°C and cooled to -196°C, and were then tempered at 500°C and 550°C. (In tempering this alloy at 190°C and 350°C, the short-time austenitizing treatments given were not identical with those used for tempering at 500°C & 550°C but are, nevertheless, sufficiently close to take for comparing the tempering behaviour over the range 190°C - 550°C).

Fig. 3.26 shows the changes in hardness with tempering time at 500°C and 550°C of the structures containing austenite together with either conventional or S.T.A. martensite. Comparing their behaviour, the difference of hardness prior to tempering, mentioned earlier, is still present after tempering. At 500°C no significant change in hardness occurs when the S.T.A. martensite was tempered for times up to 200 hours but in the conventional martensite a slight softening occurs after about 100 hours. At 550°C, with both types of martensitic structures, a slight hardening was observed during

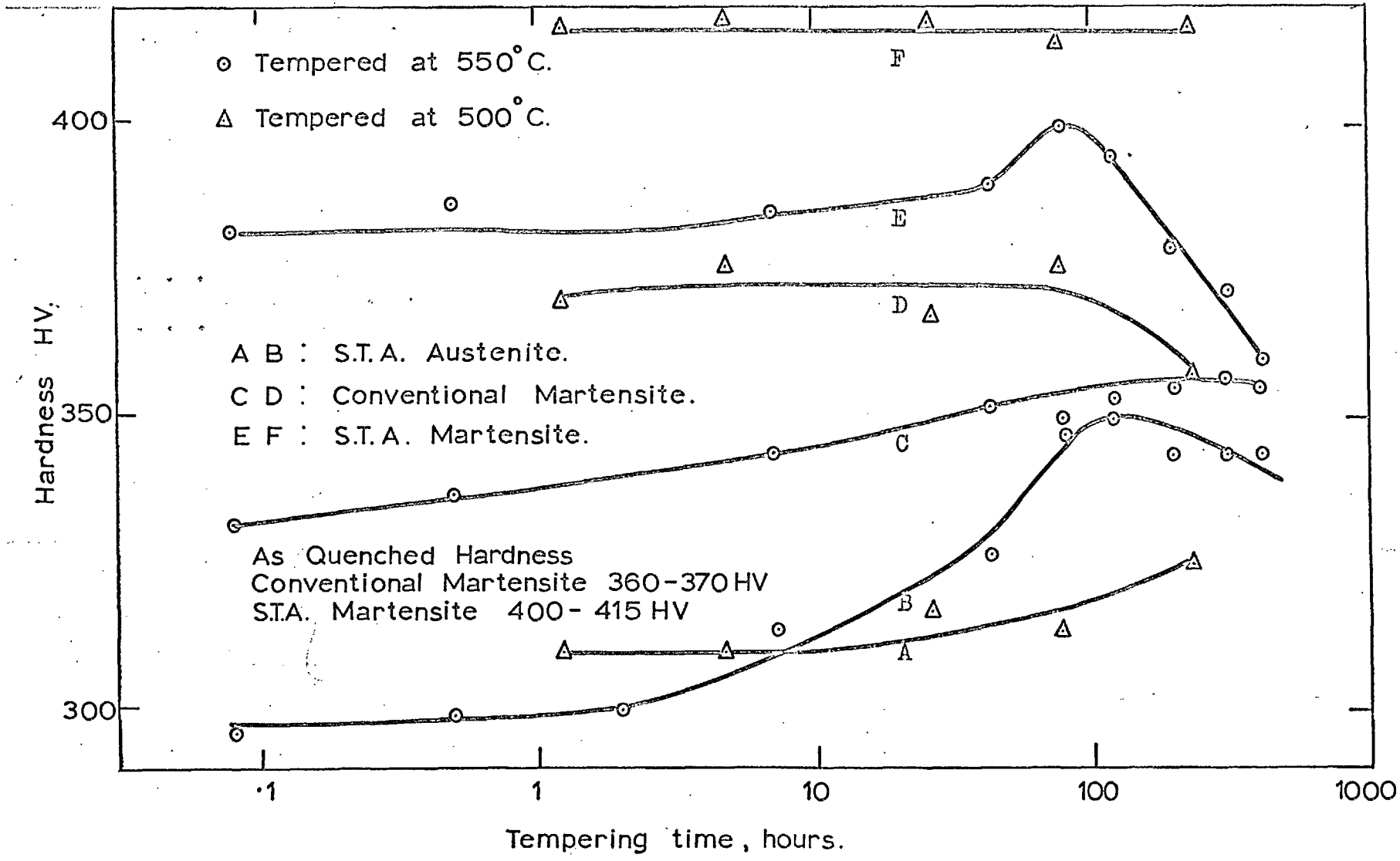

Fig. 3.26. Fe-Ni-Mo-C INM1 alloy. Variation of hardness with tempering time.

tempering, reaching a peak value at about 100 hours. This maximum hardness value was, however, lower than that achieved at 350°C for the same time of tempering.

Fig. 3.27 summarises the variation in tempering behaviour with tempering temperature. The hardness values after 2 hours and 100 hours of tempering at temperatures ranging from 190°C to 550°C are shown for both the martensitic structures. In both types of martensite, when tempered for 2 hours, the highest hardness value was attained at a tempering temperature of 500°C. After tempering for 100 hours at 350°C the secondary hardening effect was very marked with the S.T.A. martensite showing a higher strength level.

Tensile properties.

Measurements of the tensile properties - yield stress, tensile stress and ductility - for various structural conditions in the Fe-Ni-Mo-C alloy (INM1) were made to compare the effects of conventional and short-time austenitizing. The short-time austenitizing was 1 minute at 750°C. The tempering treatments were selected on the basis of the hardness results already shown in Fig. 3.27.

These results (Table 3T-12) show high strength levels maintained on tempering to 350°C - involving a secondary hardening effect. The main point of interest in the tensile

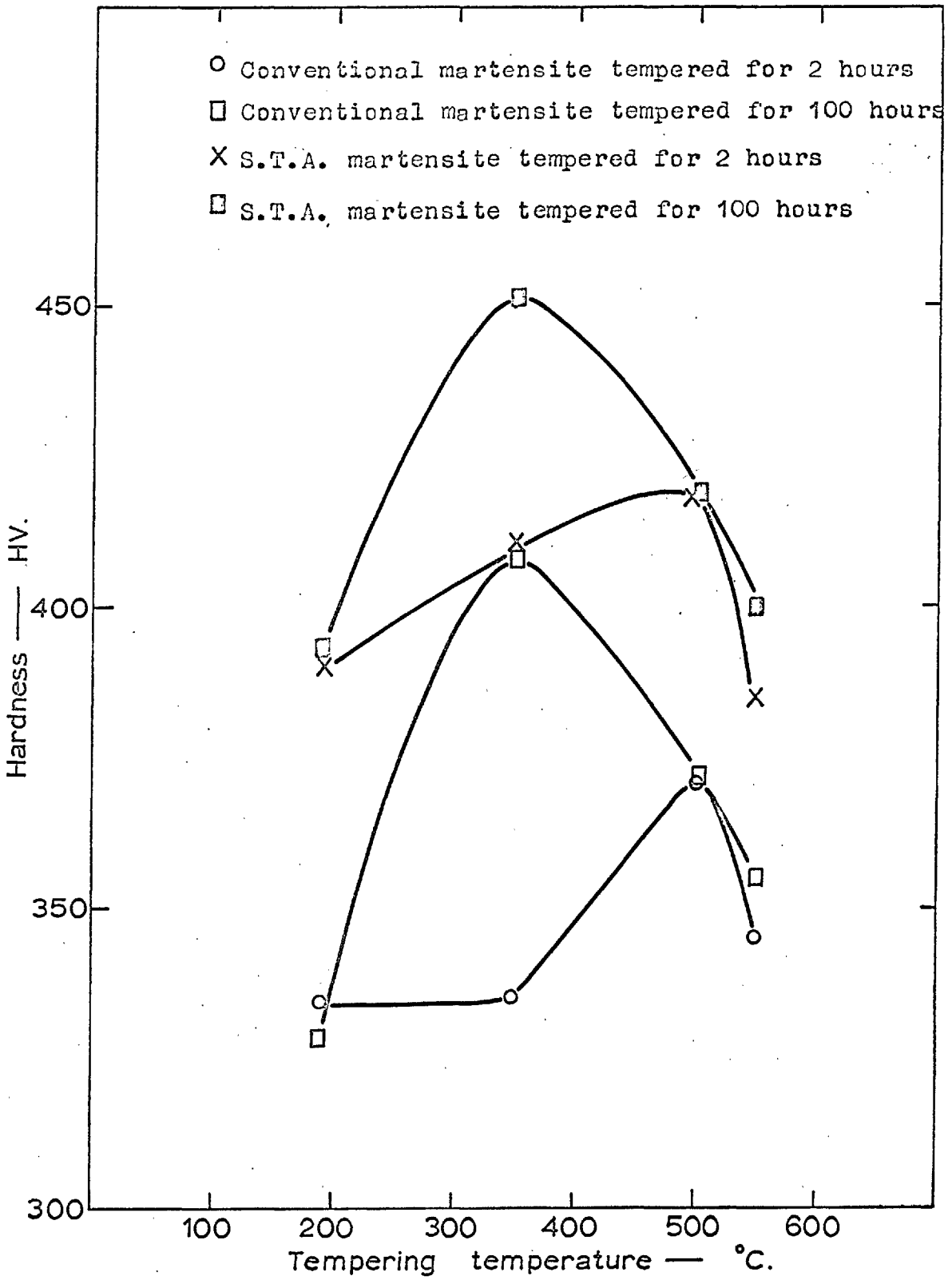

Fig.3.27.Fe-Ni-Mo-C(INM1)alloy.Variation of hardness with tempering temperature.

results is the enhancement in the strength of the tempered S.T.A. martensite (co-existing with austenite); for example, the yield stress, approximately 77 tons/in^2, of untempered S.T.A. martensite increases to approximately 94 tons/in^2 for S.T.A. martensite tempered at 350°C for 100 hours; tempering of the S.T.A. martensite at 550°C for 2 hours lowers the yield stress but the value is still greater than that of conventional martensite. Thus for a given tempering treatment, the S.T.A. martensite gives a higher strength value than that of the conventional martensite but with slightly less ductility. The highest yield stress obtained in the present investigation was from tempering S.T.A. martensite for 100 hours at 350°C. This is in excellent agreement with the hardness curves of Fig. 3.27.

3.25 "Tempering" of S.T.A. austenite.

Referring back to Fig. 3.26, it should be noted that considerable hardening occurs when S.T.A. austenite in the iron-nickel-molybdenum-carbon (INM1) alloy is 'tempered' (Plot 'A' and 'B' of Fig. 3.26); the effect occurs more rapidly and to a greater extent at 550°C than at 500°C. The contribution of this hardening in the observed enhanced strength of the tempered martensite plus austenite structures was given special attention. It should be recalled that the structures referred to as S.T.A. martensite and conventional martensite, are both,

TABLE 3T-12

Tensile properties of tempered structures Fe-Ni-Mo-C alloy. (BISRA)

Treatment	Tensile property		
	1.0% yield stress (tons/in^2)	Ductility % on 1.5"	T.S. (tons/in^2)
Conventional martensite (untempered)	61.5 - 71.0	-	-
S.T.A. martensite (untempered)	74.5 - 79.5	8	-
Conventional martensite tempered 2 hours at 350°C	64.5 - 70.1	9 - 12	79 - 84
S.T.A. martensite tempered 2 hours at 350°C	88.3 - 90.7	6 - 8	94.3-97.5
Conventional martensite tempered 100 hours at 350°C	89.9	6	97.5
S.T.A. martensite tempered 100 hours at 350°C	93.6	-	-
Conventional martensite tempered 2 hours at 550°C	63.5 - 69.0	10 - 12	79.5 - 80.5
S.T.A. martensite tempered 2 hours at 550°C	76.0 - 78.6	6 - 7	80.5 - 81.5

in fact, a mixture of martensite with as much as 30% of austenite.

Tensile specimens of the iron-nickel-molybdenum-carbon alloy (BISM1) in both the conventional austenite and the S.T.A. austenite conditions were quenched to -122°C, -135°C and -196°C to form varying amounts of both types of martensites. These specimens, in different tempered conditions, were then tested to determine the 1.0% yield stress. Figs. 3.28 and 3.20b show plots of 1.0% yield stress against the amount of martensite - both conventional and S.T.A. - tempered for various times and temperatures. The most important feature of these experiments is that on extrapolating the graphs to a limit where the structure is 100 percent martensitic, the tempered S.T.A. martensite shows superior strength as compared with the tempered conventional martensite. A comparison of the behaviour of the two martensites tempered at 350°C and 550°C, for a period of two hours shows, Fig. 3.28, a greater difference in the strength level in the case of the 350°C tempering.

3.26 Structural observations of tempered martensites.

Optical microscopical observations were made to study the structural features of martensites (BISM1 alloy), both conventional and S.T.A., after tempering. The tempering treatments were selected on the basis of the hardness results shown

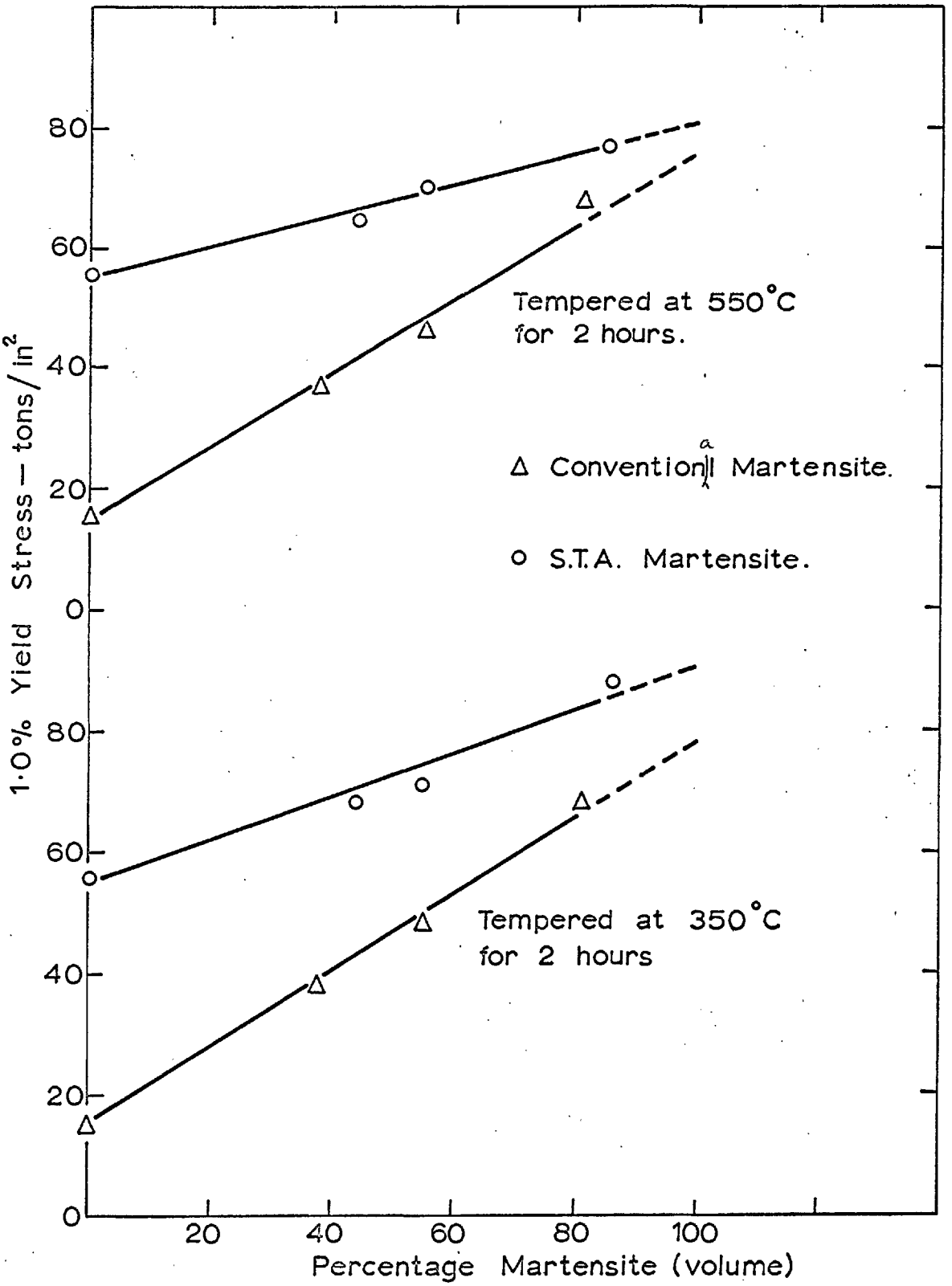

Fig. 3.28. Fe-Ni-Mo-C(BISM1) alloy. Plot of amount of martensite, conventional and S.T.A., versus yield stress. Extrapolation gives strength of martensite independent of that of austenite.

in Fig. 3.27. Conventional martensite (BISM1 alloy) was tempered at 350°C for 100 hours (peak hardness). Carbide precipitation occurs along the original twins across the midrib (Fig. 3.29a). Fig. 3.29b is an electron micrograph showing the same mode of precipitation as shown in Fig. 3.29a. A dark field transmission electron-micrograph for the area in Fig. 3.29b is shown in Fig. 3.29c.

In comparison with the conventional martensite, the S.T.A. martensite (BISM1 alloy), tempered at 350°C for 100 hours, shows (Fig. 3.30a) ill-defined boundaries of the S.T.A. martensite plates with no evidence of a midrib. It is difficult to observe the nature of precipitates in the optical micrograph. However, the electron micrograph (Fig. 3.30b), indicates in addition to the small size of the tempered S.T.A. martensite plates (c.f. tempered conventional martensite plates Fig. 3.29b), that the precipitation in the S.T.A. martensite occurs along the interface of the martensite plates. Although quantitative observations were not made, it appeared in the electron microscope that the number of the S.T.A. martensite plates showing internal twinning was less than that in the case of conventional martensite. Fig. 3.30c (S.T.A. martensite in BISM1 alloy, tempered at 350°C for 100 hours) is one of the few areas showing precipitation along the internal twin boundaries. Fig. 3.30c also suggests that carbide precipitation may have

Fe-Ni-Mo-C(BISM1) alloy
Conventional martensite tempered 350°C for 100 hrs.

Fig. 3.29a. Carbide precipitation along the twin boundaries X650

Fig. 3.29b. Electron micrograph of structure shown in fig. 3.29a X10,000

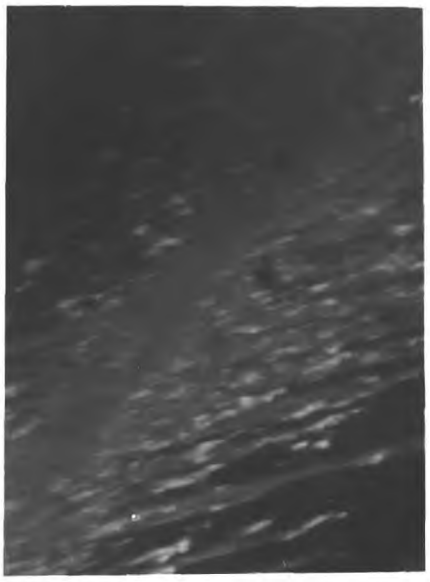

Fig. 3.29c. Dark field transmission using carbide reflection showing precipitation along the original twins X20,000

Fe-Ni-Mo-C.(BISM1) alloy
S.T.A. martensite tempered at 350°C for 100 hours

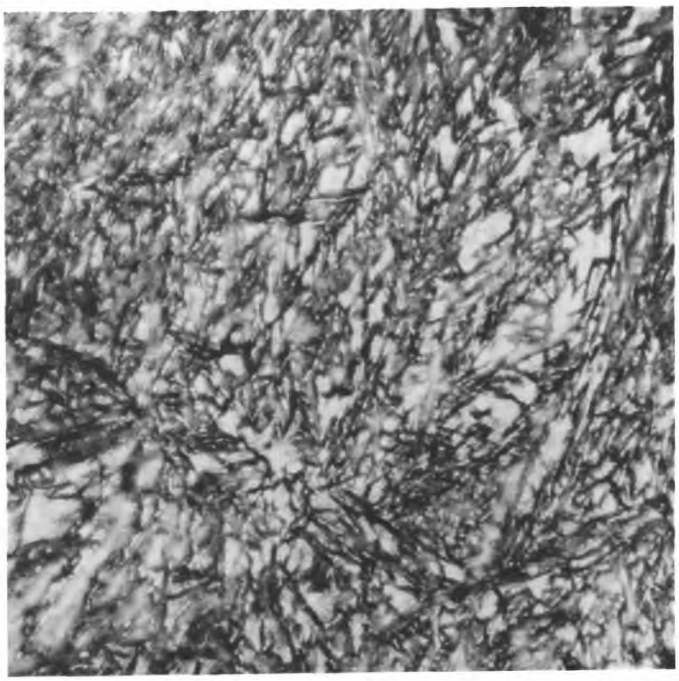

Fig.3.30a.Carbide precipitation along the martensite-austenite interface is seen X850

Fig.3.30b. X40,000

Fig.3.30c. X20,000

Electron micrographs of structure shown in 3.30a. Carbide precipitation is seen along the interface of martensite plates in (b) and (c); (c) also shows precipitation at dislocations

occurred at the dislocations in the austenite surrounding the tempered S.T.A. martensite plates; some features suggestive of coherency strain are also seen.

3.27 Sites for S.T.A. martensite formation.

As already mentioned in section 3.23 the S.T.A. martensite crystals are of considerably smaller width than those of conventional martensite; further evidence on this effect and on the sites for S.T.A. martensite formation has been obtained by optical microscopy. Fig. 3.31 is an optical micrograph of a sample of the iron-nickel-molybdenum-carbon alloy (BISM1) quenched to -122°C from the S.T.A. austenitic condition. The micrograph shows S.T.A. martensite co-existing with S.T.A. austenite and austenite retained from the first quenching. The S.T.A. martensite plates are not only smaller in width than the conventional martensite but also not all of them are formed at the sites originally occupied by conventional martensite. Some plates of the S.T.A. martensite, for instance, are formed in the matrix of retained austenite. These plates are, in general, smaller than the original martensite plates. There are, however, a few plates formed in areas of S.T.A. austenite.

Fig. 3. 31. Fe-Ni-Mo.C(BISM1). Partially transformed S.T.A. martensite co-existing with S.T.A. austenite and retained austenite X540

3.28 Orientation relationship and coherency between precipitate and the matrix.

The early stages of the tempering behaviour of INM1 alloy are associated with the precipitation of cementite. This decomposition of the conventional martensite, tempered at 550°C for 15 seconds, refers to the initial drop in secondary hardness. Fig. 3.19 (section 3.16) shows the diffraction pattern with the cementite reflections (Fig. 3.19c) represented by crosses. The orientation relationship

$$[0\bar{1}1]_{\text{Ferrite}} \parallel [100]_{\text{cementite}}$$

$$[100]_{\text{Ferrite}} \parallel [011]_{\text{cementite}}$$

is in agreement with that determined by Pitsch and Schrader (C.9).

At peak hardness of the tempered martensites (conventional or S.T.A.), precipitates of molybdenum-carbide (Mo_2C) have been detected by electron diffraction examination. The diffraction pattern obtained from the S.T.A. martensitic structure, tempered at 350°C for 100 hours, Fig. 3.32, establishes the following orientation relations.

Fe-Ni-Mo-C (BISM1) alloy
(Tempered S.T.A. martensite)

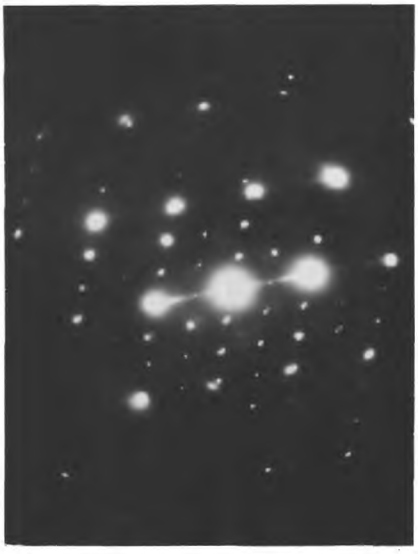

Fig. 3.32a. S.A.D. from tempered S.T.A. martensite in fig. 3.32b.

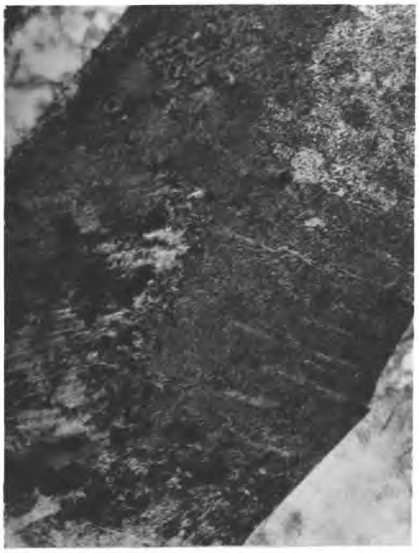

Fig. 3.32b. S.T.A. martensite tempered at 350°C for 100 hours X40,000

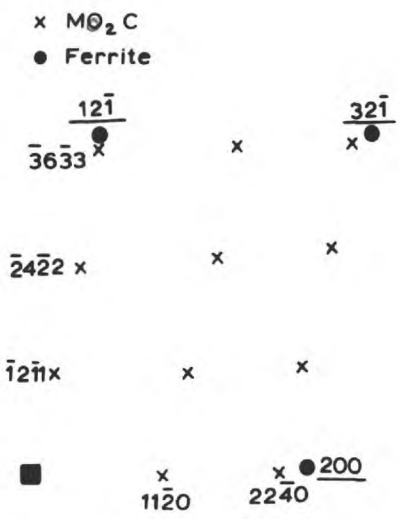

Fig. 3.32c. Indexing of Mo_2C spots (crosses) in ferrite (solid circles) matrix. $(012)_{ferrite}$ foil orientation

Fig. 3.32d. As fig. 3.32b but taken in dark field using carbide reflection in fig. 3.32c. Note fine size of precipitate particles X40,000

Fe-Ni-Mo-C, (BISM1) alloy
(Tempered conventional martensite)

Fig. 3.33a. S.A.D. from tempered conventional martensite in fig. 3.33b.

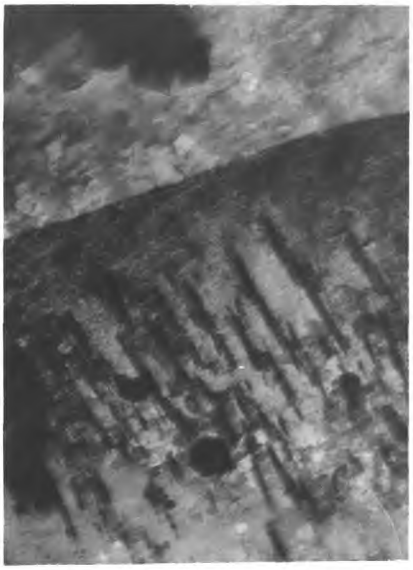

Fig. 3.33b. Conventional martensite tempered at 350°C for 100 hours X30,000

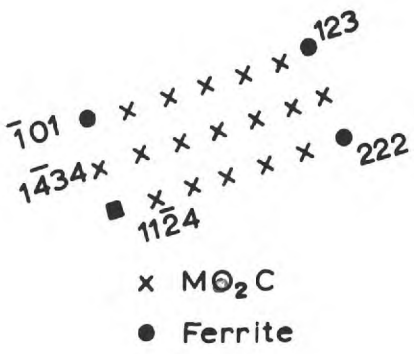

Fig. 3.33c. Indexing of Mo_2C spots (crosses) in ferrite (solid circles) matrix. $(\bar{1}2\bar{1})_{ferrite}$ foil orientation

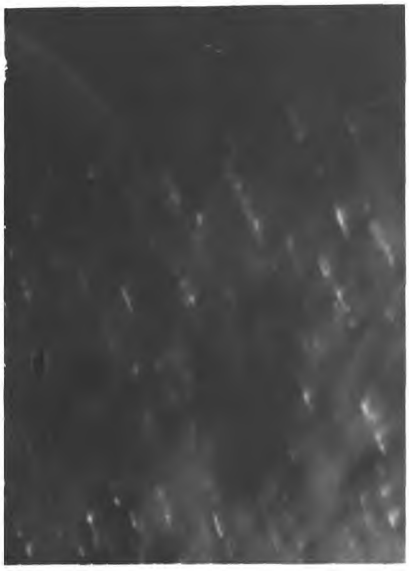

Fig. 3.33d. Dark field transmission using carbide reflection in fig. 3.33c. X40,000

$$(012)_{\text{Ferrite}} \parallel (1\bar{1}04)_{Mo_2C}$$

$$[012]_{\text{Ferrite}} \parallel [\bar{1}\bar{1}03]_{Mo_2C}$$

$$[100]_{\text{Ferrite}} \parallel [11\bar{2}0]_{Mo_2C}$$

Honeycombe et al (3.7) have also reported the same orientation relation in tempered molybdenum-steels. Results obtained on tempering of the conventional martensite at 350°C for 100 hours also support the above crystallographic relation between the molybdenum-carbide and the ferrite Fig. 3.33.

The most significant observation in the present content is the presence of fine molybdenum-carbide precipitates. Using carbide reflection spots under conditions of dark field transmission, the molybdenum-carbide precipitates, in the tempered S.T.A. martensite (Fig. 3.32d), are of finer size than in the conventional martensite (Fig. 3.33d) with the same tempering treatment.

CHAPTER IV

DISCUSSION

4.1. Strength and structure of S.T.A. austenite

It has been shown in the previous chapter (3.1) that as a result of short-time rapid austenitizing, the S.T.A. austenite becomes stronger than the conventional austenite (fig. 3.2). In this section an attempt is made to explain the enhancement in the mechanical properties on the basis of the observed microstructures. Any attempt at relating the observed strength of metals to their microstructures must involve several strengthening mechanisms. Each mechanism must be supported by evidence from observations.

4.2. Characteristics of structure of S.T.A. austenite.

4.21. Ghost structure: Although the interferometry results (section 3.15V) gave no evidence of small fragments of the S.T.A. austenite, (fig. 3.18b), having their own sector of relief, the transmission electronmicroscopy (fig. 3.12) and also direct carbon replicas from the reverted structure (fig. 3.10a) showed that a large number of austenite fragments arise during the reversion at sites originally occupied by a martensite crystal. Following on this, the fragmentation of the martensite crystals was revealed by chemical etching fig. 3.9a. The presence of numerous regions of S.T.A. austenite suggests that the reverse transformation proceeds

gradually, developing from a number of centres within the original martensite plate. Thus in this respect the reverse transformation is not a simple mirror reflection of the direct transformation.

The transformation of martensite to austenite appears to proceed with most of the martensite plates reverting to austenite fragments, figs. 3.9a and 3.12, which are much smaller than the original martensite plate. Some of these observations, e.g. fragments of S.T.A. austenite lying transversely across the original martensite plate (figs. 3.9a and 3.9b), have been reported by other investigators (D.1,D2). In the present investigation a few of the reverted martensite plates showed no evidence of fragmentation occurring within the original martensite plate; instead the reverted plates of the S.T.A. austenite (fig. 3.11) contained a high density of dislocations. It should be noted that the size of these S.T.A. austenite plates is comparable with that of original martensite plates. The occurrence of such S.T.A. austenite plates suggests another mode of reverse transformation i.e. transformation occurring over the entire martensite plate. It is difficult to conceive, in view of the short time of austenitizing employed at 650°C (viz about one minute) that the reversion initiated first with the appearance of the S.T.A. austenite fragments and that these fragments then

disappeared leaving a high density of dislocations in the S.T.A. austenite plate. It must be pointed out that very few such areas were observed.

4.22 Dislocation density: One of the most interesting structural observations made in the present investigation is the presence of a high dislocation density resulting from short-time rapid austenitizing. Fig. 3.14 shows such a structure of tangled dislocations. It is clear from fig. 3.14 that the tangles consist of irregularly curved lengths of dislocation lines sharply kinked at irregular intervals and that no visible obstacle can be observed at these anchoring points. (Despite the lack of evidence for the existence of fine carbide particles in the S.T.A. austenite, if they were present they could act as anchoring points to give rise to tangled and jogged dislocations. This point is further discussed in section 4.24). The occasional presence of round loops in the S.T.A. austenite can also be noticed (fig.3.14b) and this may indicate that as a result of rapid austenitizing at 950°K vacancies are formed, and on subsequent quenching precipitate out in the form of a loop. An estimate of the vacancy concentration (C_v) at 950°K using $C_v = e^{-\frac{E}{RT}}$ (E is the energy of formation per mole of vacancies) is about 10^{-17}. Although this value appears to be too small for vacancies to condense and form loops, it is, however, likely that, in view

of the structural volume changes occurring during the martensite → austenite transformation, the concentration of vacancies in the gamma iron rises at the transformation temperature. The quenching strain could also result in the formation of vacancies (D.3.)

The origin of the tangled nature of the dislocations can be explained on the theory put forward by Kuhlmann-Wilsdorf and Wilsdorf (D.4). According to these workers any point defects "precipitate" at dislocations and will necessarily cause the dislocations to be deflected out of their respective slip planes; since this deflection does not take place uniformly and continuously it will block the glide motion of the dislocations in certain planes only. The result of this process will be dislocation tangling.

It may be suggested that the high density of dislocations produced on rapid austenitizing can originate from the following sources.

(i) Structural volume and shear changes.

(ii) Inherited defects (e.g. dislocations and microstrains) from the original martensite structure.

(iii) Anisotropy of thermal expansion of martensite crystals.

(iv) Condensation of vacancies on certain crystallographic planes in f.c.c. structures.

It should be pointed out that sources (i) and (iii) will cause plastic deformation in both S.T.A. and the retained austenite, while source (ii) is responsible for the dislocated structure of the S.T.A. austenite alone.

(i) Structural volume change: When a region of a martensite crystal tries to change its form but is partly prevented from doing so by the surrounding material of retained austenite, internal stresses are set up. The change of form is a combined volume and shear change due to the martensitic nature of reversion (see section 3.15V). The volume contraction accompanying the reversioncan only be accommodated by the plastic deformation of the softer surrounding retained austenite which, in turn, imposes tensile stresses on the reverted martensite crystal. The whole process results in the formation of a dislocated structure. Since the reversion occurs while the martensite crystal is embedded in the untransformed matrix,dislocations are left at the interface between the transformed (S.T.A. austenite) and the untransformed (retained austenite) regions. This is seen in fig. 4.1.

It should, therefore, be expected that in martensitic transformations where the structural volume change is very small, e.g. pure cobalt (D.5), little (or no)

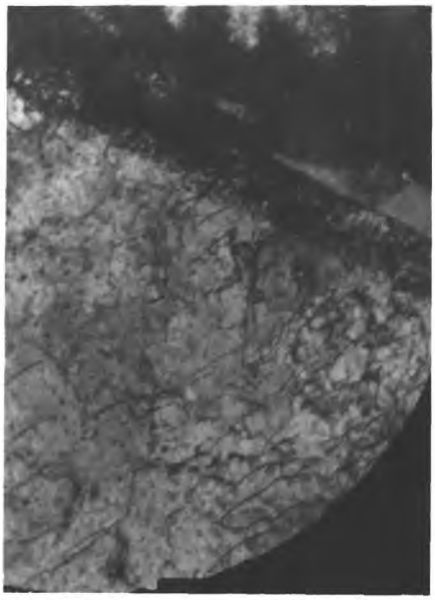

Fig.4.1. IIM1 alloy. S.T.A. austenite co-existing with retained austenite. Dislocations at the interface can be seen. X40,000.

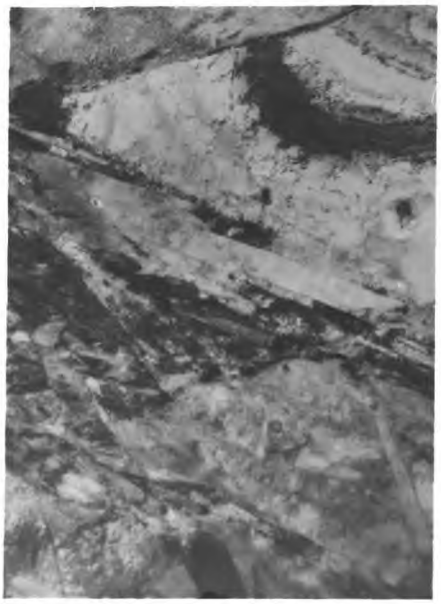

Fig.4.2. BISM1 alloy. Dislocation substructure in S.T.A. martensite plates. Note absence of internal twinning in the plates. X20,000.

hardening should occur on short-time heating to a region where structural changes takes place. Some exploratory tests were carried out using pure cobalt. It was found that with short-time "austenitizing" (30 seconds at 530°C) the specimens had nearly the same hardness as with conventional annealing. However, in view of the absence of detailed information e.g. amount of martensite (c.p.hex.) present prior to reversion*, these results are not conclusive.

(ii) Inherited defects from the original martensite: It has been established (D.7., D.8., D.9) that martensite crystals in steels contain a substructure e.g. dislocations and internal twins. It is, therefore, difficult to ignore the possibility that on rapid reversion, and possibly after some recovery, the substructure of the parent phase (martensite) is inherited by the S.T.A. austenite. The presence of dislocations in the reverted structure has been discussed. It is however, difficult to say authoritatively whether the dislocations in the S.T.A. austenite are due to the constraining effect of the distorted retained austenite or from the inherited dislocation structure

* In the transformation of pure cobalt (M_S = 480°C and 0.3 percent structural volume change (D.5) occurring from the direct transformation of f.c.c. $\rightarrow$ c.p.hex.) the amount of martensitic phase depends critically (D.6) on the thermal history.

of the parent phase. In principle, rapid austenitizing of a single crystal of martensite and subsequent microscopical observation could throw some light on this point.

(iii) Anisotropy of thermal expansion of martensite crystal:

In crystalline structures, belonging to the hexagonal and the tetragonal crystal systems, the thermal expansion varies with the direction in the crystal. In a crystal of a cubic metal, on the other hand, no such effect can exist because the thermal expansion is the same in all the principal crystallographic directions. It would be expected therefore, that as a result of reversion of a martensite crystal (b.c.t), in the matrix of austenite, anisotropic thermal expansion of the tetragonal structure may set up stresses in both the phases; here the relative volume of each phase may be of importance (see section 4.3). Three additional effects must also be considered.

1. The difference in the thermal expansion occurs not only from phase to phase but also from grain to grain and stresses may be set up even if both the phases present were cubic.

2. Each crystal of martensite has many neighbours, usually of different orientation. A preferred orientation would show deformation to a lesser degree than a structure in which crystals are oriented at random.

3. Anisotropy of Young's modulus may also cause plastic deformation.

It is very likely that the stresses set up by the anisotropy of thermal expansion of the martensite crystal(s) are nearly negligible since the thermal expansion is dependent on the temperature difference and not on the rate at which the temperature changes. Furthermore, if the reversion proceeds via a tempering "path" i.e. martensite (b.c.t.) $\longrightarrow$ ferrite (b.c.c) + cementite (orthohombic) $\longrightarrow$ austenite (f.c.c.), the accompanying loss in tetragonality would lessen the effects of anisotropy of thermal expansion.

(iv) Condensation of vacancies on certain crystallographic planes in f.c.c. metals: Since Sietz (D.10) studied the interaction between vacancies and dislocations, evidence (D.11) has become available to indicate the profound influence which vacancies can have on the plastic properties of metals. Kuhlmann-Wilsdorf (D.12) suggested that dislocations can be generated in f.c.c. metals by the condensation of vacancies on the $\{110\}$ planes. This would result in an edge dislocation forming part of a prismatic dislocation. They have also suggested vacancy condensation on $\{111\}$ planes resulting in the formation of sessile type (Frank partial) dislocations with $\frac{1}{3}$ $[111]$ Burger's Vector. Although the stacking fault energy of a material is an important parameter in the transformation of a Frank partial, the ease with which a Shockley partial is nucleated must also be considered. Smallman and

Eikum (D.13) have reported Frank sessile loops in a high stacking fault material by quenching pure aluminium from 600°C into an oil bath. Probably the accompanying quenching stresses were too low for nucleation of a Shockley partial to occur.

In view of the fact that the energy for the formation of vacancies in iron is about 3.5eV, it is probable that only a small number of dislocations are produced by vacancy condensation on certain planes in austenitic steels with the austenitizing temperatures used in this investigation.

Thus it can be concluded that the predominant source of dislocations produced on rapid austenitizing is the structural volume change.

4.23 Reversal twins and sub-boundaries.

The fragmented nature of the reversed austenite has been observed in the present investigation (section 3.15ii). These fragments, when lying transversely across the reverted plate, are twin-related with respect to one another. The twins differ from annealing twins in that they commonly have irregular boundaries and in addition, they contain a dislocation sub-structure, fig. 3.13a. On the basis of these observations, two possible mechanisms by which reversal twins can form are suggested.

(i) Coalescence of the original twins in the martensite plates:

During the reversion, stresses at the original twin boundaries are relieved by thickening of two (or more) adjacent original microtwins (60 - 500Å thick); the resulting twins (reversal twins) have thicknesses varying from 0.1 - 0.5 micron. This mechanism of twin-coalescence is consistent with the following observations.

(a) The reversal twins are always formed within the original martensite plates which show internal twinning. Although twins have been reported (D.14) in 16/12 stainless steel, which contains no internal twins in the martensite needles before reversion, it is, however, possible that these twins may be stacking faults. The reported reversal twins in 16/12 stainless steel have straight boundaries. Moreover, in 16/12 stainless steel numbers of such twins occur in the form of 'bundles' apparently appearing like stacking faults.

(b) It has been well established (D.15) that the thickening of a twin requires much less energy than that required to form it. The necessary energy for twin-coalescence is probably supplied by stress relief at the original twin boundaries, overall lowering of the twin boundary energy and the thermal energy during austenitizing. Any increase in one of these factors, e.g. thermal energy of austenitizing, would be expected to lead to eventual disappearance of reversal twins.

No reversal twins were observed in specimens austenitized for relatively longer periods, say about half an hour.

(ii) Cross slip during reversion: The irregular nature of the boundaries of the reversal twins (fig. 3.13a) can be explained by the occurrence of cross-slip, a phenomenon very common in materials of high stacking fault energy. In a thermally cycled sample, where much of the cross slip i.e. localized change of slip plane, must have occurred at the temperature of austenitizing and the slip is expected to be relatively coarse. Fig. 3.13 shows this effect and emphasizes the irregularity of the cross slip segments.

At the temperature of austenitizing where cross slip is likely to be enhanced, it is probable that two (or more) adjoining twins in the original martensite plate form a 'band' with cross slip occurring at the narrow ends. Since cross slip segments are well-known for their zigzag nature, it is of interest to note that the ends of almost all the 'bands' are very jogged.

If the above process of reversal twin formation is accepted, no reversal twins would be expected in the rapidly-austenitized structure of low stacking fault energy materials.

It is difficult to comment with certainty regarding the nature of certain boundaries and sub-boundaries in the S.T.A. austenite, fig. 3.14b. It is, however, probable

that the straight and long boundaries are the original boundaries of martensite plates. The presence of irregular sub-boundaries can be accounted for by phenomenon of cross-slip.

4.24 Tempering during reversion: Electron microscopical study, both darkfield and diffraction pattern, gave no evidence for the presence of carbide particles in the austenite. It may be recalled here that the martensite before reversion is a slightly tempered structure (even at room temperature) presumably containing fine carbide particles. In view of this and the occurrence of some additional tempering occurring during the period of reversion, it is suggested that the presence of fine carbide particles in the austenite is a possibility. Sastri (D.16), working on a plain carbon eutectoid steel (initially in the tempered condition) austenitized at 850°C for 4 seconds, showed that an essentially pearlitic structure was formed on cooling and claimed a good degree of homogenization. In the present investigation, however, unless the carbides redissolved on austenitizing (a typical time of austenitizing used was one minute), the possible presence of fine carbides cannot be ruled out. As already mentioned (section 4.22), these carbides could have an anchoring effect and cause tangling of dislocations.

4.3 Contribution of various strengthening mechanisms in the S.T.A. austenite.

Fig. 3.2 shows the enhancement in the mechanical properties (yield stress and hardness) of the rapidly austenitized structure. Austenitizing treatments, involving relatively low temperatures and short times (e.g. about one minute), result in an appreciable increase in the strength. Furthermore, it has been shown (section 3.14 fig. 3.8) that the degree of strengthening due to rapid reversion depends upon the initial amount of martensite present in the structure prior to austenitizing.

Effect of initial amount of martensite on the yield stress of S.T.A. austenite.

The effect of the initial amount of martensite on the yield stress of the reverted structure can be explained by considering the structure as a mixture of two "phases" viz S.T.A. austenite and conventional austenite. The increase in the average dislocation density with varying amounts of mixture of the two austenites can be suggested schematically in the following figure.

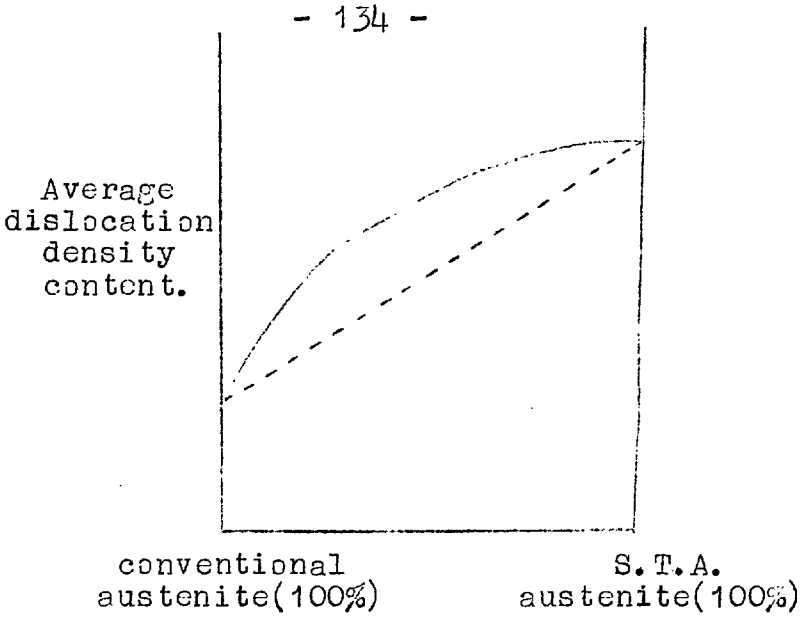

Schematic diagram showing change in average dislocation density with varying amounts of mixture of austenite "phases"

The dotted line in the figure shows the increase in the average dislocation density assuming the structure to be a mixture of S.T.A. and retained austenite, with each "phase" having a constant dislocation density. The dislocation density of the retained austenite does not, however, remain constant and its average dislocation density includes, in addition to the dislocations produced on reversion, the dislocations introduced in the retained austenite on direct transformation. Structural observations made by Edmondson and Ko (D.16A) suggest that the plastic deformation in the retained austenite during the reverse transformation is not so extensive as during the direct transformation. The number of dislocations in the retained austenite, after reversion,

will vary with the amount of retained austenite and this will, probably, affect the form of the dotted line in the figure. Although the exact form of the curve is not known, the suggested full curve (in the figure) represents the probable trend of dislocation content of the mixture of conventional and S.T.A. austenites.

It can be inferred from fig. 3.8 that a relatively small amount of martensite phase (20 - 30%) causes considerable strengthening of the reverted austenite while further increase in the martensite phase brings about a relatively smaller amount of strengthening per percent of initial martensite phase.

It can be seen from fig. 3.8 that the maximum yield strength of the S.T.A. austenite obtained by rapid austenitizing (with an initial amount of martensite of about 90 percent) is about 3 times the strength of the annealed austenite. In the following section various possible sources contributing to this strength increase are discussed in the light of the observed structural features.

Quantitative relationships for strengthening in S.T.A. austenite.

The relationship between the grain size and flow stress was first given by Hall and Petch (D.17 and D.18) in the following form:

$$\sigma_f = \sigma_0 + Kd^{-\frac{1}{2}} \quad - - - - - - \quad (1)$$

where 'σ_f' is the flow stress; 'σ_0' is the friction stress and is a measure of the resistance to dislocation movement; 'd' is the grain size; and 'K' is a function of the stress necessary to activate a dislocation source.

Detailed investigations of the friction stress (σ_0) have shown that it is a function of temperature, interstitials and precipitates (D.19) and strain (D.20). If all these factors are considered, the flow stress (σ_f) is given by

$$\sigma_f = \sigma_{f(T)} + \sigma_{f(Ath)} + Kd^{-\frac{1}{2}}$$

where $\sigma_{f(T)}$ is the thermal component and $\sigma_{f(Ath)}$ the athermal component which varies with density of dislocations and precipitates in a manner proposed by Conrad (D.21). The expression for flow stress then becomes

$$\sigma_f = \sigma_{f(T)} + \alpha_1 \mu b \rho^{\frac{1}{2}} + \alpha_2 \mu b \lambda^{-1} + Kd^{-\frac{1}{2}} \quad - - - - \quad (2)$$

in which α_1 and α_2 are constants, μ the shear modulus of iron, b the Burgers vector, ρ the dislocation density and λ the precipitate spacing. In equation (2), the second and third terms represent the dislocation density and precipitate strengthening respectively. Although a term involving strengthening due to solid solution alloying (e.g. by carbon, nickel, molybdenum) must also be added to the equation (2),

it may be emphasized that, in using this equation to account for the increase in the strength of the S.T.A. austenite, no attempt is made to discuss the effects of alloying elements on the strength of S.T.A. austenite; this is because solid solution strengthening will occur to the same extent in both conventional and S.T.A. austenites unless the amount of carbon in solution in the S.T.A. austenite is reduced by the presence of carbide precipitates.

The theoretical model for the $d^{-\frac{1}{2}}$ term in equation (2) relies upon dislocation pile-ups forming at the grain boundaries. However, models based on a process of dislocations interacting and forming tangles (a characteristic structural feature of the S.T.A. austenite) show that the flow stress is proportional to the square root of the dislocation density and this has been experimentaly established (D.22-D.25). It appears that although the flow stress may be a function of grain size, the term involving dislocation density ($\alpha_1 \mu b \rho^{\frac{1}{2}}$) is consistent with both current theories and experimental results. Because of this the dislocation contribution was considered more significant than the grain size term ($d^{-\frac{1}{2}}$). Moreover, in section 3.12b it has been shown that the size of the original grains of the austenite remains unaltered on rapid heating (compare fig. 3.1a and 3.1b). Therefore the term $d^{-\frac{1}{2}}$ and also the term $\sigma_{f(T)}$, which

is negligible at room temperature (D.19), are omitted in equation (2), which then takes the form

$$\Delta\sigma_f = \alpha_1 \mu b(\rho_1^{\frac{1}{2}} - \rho_2^{\frac{1}{2}}) + \alpha_2 \mu b(\lambda_1^{-1} - \lambda_2^{-2}) \text{ - - - } (3)$$

Local changes in carbon content during austenitizing —— tempering during reversion.

Although the chemical composition of the austenitic alloys used in the investigation was chosen in such a way that the martensite forms on cooling to below $0^{\circ}C$, the possibility of carbide being precipitated from the martensite (and austenite) while reaching the temperature of reversion (or during subsequent cooling) must be considered. Any carbide precipitation from the solid solution can contribute to the strength of the S.T.A. austenite and it may be that the observed high strength of the S.T.A. austenite (particularly in alloys containing strong carbide forming elements, INM1 and BISM1) is in part due to the precipitation and dispersion hardening.

As mentioned earlier, no direct evidence for the existence of carbides in the S.T.A. austenite has been obtained, however, if any carbide precipitation occurs by tempering during heating and if the resolution of this carbide was not complete in the austenite range, then it would be expected that the M_s temperature of the S.T.A. austenite

would be raised due to the reduced carbon content in the solid solution. During the course of experimentation, however, it was noticed that the M_s temperature of the S.T.A. austenite, for BISM1 alloy, was lower than that of the conventional austenite. Due to lack of any positive evidence for the presence of carbide in the austenite after reversion, the possible contribution of the precipitates to the flow stress (σ_f) of the S.T.A. austenite could not be estimated. However, it seems that the most significant term to consider, to account for the increase of about 18 tons/in^2 in yield stress of the S.T.A. austenite over the conventional austenite is the dislocation density term in equation (3).

The value of the density of dislocations for the S.T.A. austenite has been calculated (section 3.15iv) to be about 10^{10} lines/cm^2 in comparison with a value of about 10^9 lines/cm^2 for fully annealed austenite. In order to take into account the 'forest' nature of the dislocations in the S.T.A. austenite, a value of 10^{11} lines/cm^2 can be used to estimate σ_f from the theoretical relationship (equation 3). Krauss (D.26) has also reported the density of dislocations in the reversed austenite to be of the order of 10^{11} lines/cm^2. In the annealed austenite the value of the dislocation density (10^9 lines/cm^2) appears to be high, possibly because of the generation of dislocations during foil preparation

and subsequent handling. A value for annealed austenite of 10^8 or even less appears more likely.

The expression

$$\sigma_f = \alpha \mu b \, (\rho_1^{\frac{1}{2}} - \rho_2^{\frac{1}{2}})$$

may be used where α = const $\simeq$ 0.4 (D.27); μ = shear modulus of iron = 12 x 10^6 lb/in^2. b = Burgers vector = 2.5 x 10^{-8}cm, ρ_1 = dislocation density of S.T.A. austenite, 10^{11} lines/cm^2 ρ_2 = dislocation density of conventional austenite, 10^8 lines/cm^2. By substituting these values, 'σ_f', the increase in the flow stress resulting from rapid austenitizing, can be estimated as being about 15 tons/in^2 which is quite close to the observed increase in the yield stress (18 tons/in^2) of the S.T.A. austenite.

Strength of S.T.A. austenite and reversal twins.

The presence of reversal twins in the S.T.A. austenite may limit the movement of the dislocations. A dislocation whose line passes through a twin interface can move easily only if its Burgers vector is identical (an unlikely situation because of the atomic disorder in the interface) on both sides of the interface. Any discontinuity in the magnitude of the Burgers vector of the intersecting dislocation will result in the 'pinning' of the dislocation with the twin interface acting as a barrier to dislocation movement.

Kelly and Nutting (D.28) have claimed that there is a small strengthening (in martensite) due to twinning. In view of the fact that the thickness of the reversal twins is about 0.1 - 0.5 microns (c.f. 60 - 500Å in the case of twins in martensite), the number of the twin barrier to the dislocation movement is less. It is therefore justified to say that the presence of the reversal twins contributes slightly to the overall strength of the S.T.A. austenite.

Thus the increase in the strength of the S.T.A. austenite is primarily due to the high dislocation density.

4.4 Mechanism of reversion

The martensitic nature of rapid reversion has been demonstrated by the surface relief effects, fig. 3.18(b). Some sharp tilts in the interference fringes can be observed which are due to the reversal plates of austenite formed martensitically. Carbon replicas taken from reversed austenite plates, fig. 3.10a, indicate that the fragments of S.T.A. austenite present within the original martensite plate have relief sectors of their own. The interferometric technique, fig. 3.18b, however, does not, within the limit of resolution, conclusively establish that each fragment of S.T.A. austenite formed within the original martensite plate is associated with surface tilts. The general appearance of the interference fringes is distorted probably

because of the impingement of several S.T.A. austenite fragments.

A comparison of carbon replicas obtained respectively from a martensitic plate and from an S.T.A. austenite plate, fig.3.10a (c.f. fig.3.10b) shows the absence of a midrib in the S.T.A. austenite structure and this may indicate that the reverse transformation proceeds in only one direction from the plane of nucleation. Although no observation indicating a plane sweeping, on austenitizing, through the original martensite plate was made, Jana and Weyman (D.29), in a recent publication, have shown a partially reversed martensite plate in which a sweeping interface stopped midway. The rate of heating, as employed by them, was $1^{o}C$ per minute and this may mean that the reverse transformation was diffusion controlled. Kessler and Pitsch (D.30) employed both slower ($0.3^{o}C$ per minute) and faster ($100^{o}C$ per second) heating rates and detected a martensitic reversal in both cases.

4.5 Effect of annealing time and temperature.

4.51 Hardness changes

The hardness changes in S.T.A. austenite as a function of time and temperature of austenitizing, ranging between 600 - $670^{o}C$ have been plotted in fig. 3.2 to 3.4 for

the three iron-nickel-carbon alloys. Only a small decrease in hardness is observed during the initial period, [redacted] then, depending upon the temperature of austenitizing, a sudden drop in hardness begins. With a prolonged austenitizing period, the hardness of the reversed austenite reaches the same value as that of the conventionally annealed austenite.

4.52 Structural changes and activation energy.

The microscopical structural changes are reflected in the manner in which the dislocations anneal out with increasing time of austenitizing. For an austenitizing time of about ten minutes, the hardness of the S.T.A. austenite (fig. 3.3) is still substantially higher than that of the conventional austenite. Figure 3.15a shows the microstructure corresponding to this hardness value. There are areas of both high and low density of dislocations. It may be noted that the electron micrograph shows dislocations inside the cells indicating a certain amount of dislocation pinning by the matrix. With increasing time of austenitizing (40 minutes at 650°C) the cell-structure formation is more prominent (fig. 3.15b). Although the dislocation density appears to be high for a structure which has nearly the same hardness as that of the conventional austenite, the high content of dislocations is primarily distributed in the formation of

cell walls, leaving the matrix, in comparison with fig. 3.15a, free of dislocations. It may, therefore, be suggested that the strength of the reverted austenite is largely determined by the dislocation arrangement rather than the dislocation density.

The effect of the alloying elements on the dislocation arrangements in the reverted austenite must also be considered. If carbides are formed during the period of heating to the austenitizing temperature, the effects of the precipitates will be that the particles will hinder slip motion and cause the dislocation multiplication. However, for prolonged soaking times at the austenitizing temperature, the carbides will tend to redissolve.

Thomas et al(D.31) have detected carbides in ausformed austenite (iron-28% nickel 0.3% carbon and iron-25% nickel-4.5% molybdenum-0.28% carbon alloys). According to these investigators the occurrence of carbides depends on the amount, and possibly the temperature, of deformation; high deformations will favour carbide precipitation in austenite.

It is generally accepted that the effect of annealing on the cold-worked metal is to bring about recovery and recrystallization by nucleating new grains at the grain boundaries of the deformed material. The boundaries of the new grains then migrate through the deformed material. The swept area (virtually free of dislocations) is separated from

the deformed region of a high-angle boundary (D.32). The microscopical investigation of the S.T.A. austenite on prolonged soaking showed no signs of the presence of high-angle (recrystallization) boundaries, though the S.T.A. austenite contained a high density of dislocations. However, some boundaries were seen e.g. fig. 3.15b which are possibly the original boundaries of the martensite plates. The absence of high-angle (recrystallization) boundaries indicates that the effect of austenitizing time on the reverted structure is basically a recovery process wherein the dislocations polygnize themselves to form sub-grains without migration of the grain boundaries. Microstructural evidence to support this view is furnished in figure 3.15b. The micrograph (iron-nickel-carbon INN1 alloy) shows the structure of a specimen austenitized at 650°C for 40 minutes (from figure 3.3, the hardness after this treatment is nearly the same as that of the conventionally annealed austenite).

The activation energy (section 3.17) for the process of recovery of the annealed austenite by rapid austenitizing has been calculated to be about 155 Kcal/mol for the iron-nickel-carbon alloys (HP1, INN1 and INN2). Although this value is much larger than the activation energy for the self diffusion of iron along the grain boundaries of austenite (41 Kcal/mol D.37), values of the order of 90 Kcal/mol have been reported by Krauss and Cohen (D.33) for

iron-nickel alloys containing impurity-level amounts of carbon. They believe that the annealing of reversed austenite is the same as the annealing of cold-worked metals in that both the processes involve recovery and recrystallization. Following the idea of Lucke and Detert(D.34), Krauss and Cohen (D.33) proposed that the high activation energy results from the preferential segregation of the carbon atoms at the grain boundaries. In alloys containing higher amounts of carbon, as in the present investigation, it would, therefore, be expected that a higher concentration of solute atoms can build up at certain regions than at others. Cottrell (D.35) has suggested that such segregation is possible around a dislocation. Thus at the temperature of austenitizing a high density of dislocations can provide sites for carbon segregation.

The effect of impurities (tin in zone-refined lead) on boundary migration has been well demonstrated by Aust and Rutter(D.36). They have concluded that very small impurity concentrations can dramatically retard boundary migration. Earlier, Lucke and Detert(D.34) had postulated that dissolved impurities retard a moving boundary through an elastic attraction of impurity atoms towards the 'open' structure of the boundary (or dislocations); the boundary must then either drag the impurity atoms along - so that its speed is limited by the diffusion rate of the impurity atoms - or else

the boundary can break away if the impurity concentration is small enough or the temperature is high enough. A revised version of Cahn's theory (D.32) on boundary migration predicts that the velocity of boundary migration is an inverse function of solute concentration and that a lower diffusivity of the solute will lead to a stronger boundary drag.

With the amount of segregation varying from boundary to boundary (or uneven along any boundary) the net effect is that the boundary would be less mobile than would be anticipated if there was no segregation, in which case the activation energy will provide atom-by-atom transfer of iron (or nickel) across the migrating interface.

The high activation energy, therefore, possibly involves carbon segregation and clustering at the sub-boundaries (and dislocations) thus retarding the mobility of the grain boundaries.

4.6. S.T.A. and conventional martensite - tempered and untempered.

The structural changes in the austenite, e.g. increase in the dislocation density, accompanying short-time rapid austenitizing treatments have already been discussed. The increased strength of the S.T.A. austenite seems to be mainly dependent on the dislocation content. Any possible effect of inheritence of the austenite sub-structure on the strength of S.T.A. martensite (both in the tempered and untempered conditions) is discussed in this section.

Kurdjumow (D.38) pointed out that tempering is essentially an ageing phenomenon in that it is a process of precipitation from super saturated solid solution. The fundamental difference between normal ageing and tempering lies in the mode of formation of the super saturated solid solution. In the latter case the parent phase is a product of shear transformation. As shown by Kelly and Nutting (D.39) shear transformation in steels gives rise to two kinds of microstructure: low-carbon martensite is in the form of needles containing dense dislocation networks, while high-carbon martensite is in the form of internally twinned plates.

The tempering of martensite has been the subject of many studies since it plays an important part in the production of high strength steels. In plain carbon martensitic steels, tempering generally proceeds by a three-stage process (D.40). On tempering below about 200°C, ϵ-carbide is precipitated leaving the matrix containing about 0.25% carbon. The ϵ-carbide is not a stable phase and on tempering at higher temperatures, or for longer times at lower temperatures, cementite is precipitated. This is known as the third stage of tempering, the second stage has been identified as the transformation of retained austenite to non-martensitic products. It should be stressed that these stages are not confined to definite temperature ranges, but are both time and temperature dependent, and vary in different alloys.

In the tempering of alloy steels the first three stages are essentially the same as in plain carbon steels. During the fourth stage cementite gradually dissolves and alloy carbides start to precipitate (D.41). Honeycombe et al (D.42) have reported in situ transformation of cementite to alloy carbides. Cementite may also be present along with the alloy carbides (D.43). Houndremont et al (D.44) showed that secondary hardening was due to the precipitation of alloy carbides.

It may be recalled here that the strength of the two types of structures investigated (both in the tempered and untempered conditions), in fact, represents the strength of mixtures of phases in that the structure prior to tempering is a mixture either of conventional martensite + conventional austenite or of S.T.A. martensite + S.T.A. austenite + conventional austenite. The strength of the martensite, tempered or untempered, was, therefore, determined by extrapolating plots of yield stress versus amount of martensite to 100 percent martensite (figs. 3.20 and 3.28).

4.61. Factors contributing to the increased strength of the untempered S.T.A. martensite.

It was observed that in the iron-nickel-molybdenum-carbon alloy (BISM1), the S.T.A. martensite showed a slightly higher strength than the conventional martensite. The difference in the 1.0% yield stress (extrapolated values) of the two martensites in this alloy is only about 6% and this is discussed below on the basis of the structural study. It may be mentioned that since no extrapolation of the values of ductility of the two martensites was done, no comment can be made on this aspect. The factors contributing to the strengthening of ferrous martensite can be briefly mentioned.

Carbon is the most important factor in the strengthening of martensites; the yield strengths achieved vary from 80,000 lbs/in^2 for 0% carbon (extrapolated value) to 280,000 lbs/in^2 for 0.8% carbon in iron-nickel-carbon alloys (D.45), the strengthening due to the nickel (about 10,000 lbs/in^2) being negligible for the relatively high amounts of nickel. If any precipitation occurs as a result of auto-tempering or sub-zero tempering, it will be the amount of carbon remaining in solution which will mainly determine the strength of martensite. The results of Kelly and Nutting (D.46) have shown that carbon in solution is responsible for nearly half the strength of high carbon martensite.

The ageing experiments of Winchell and Cohen (D.45) suggest that carbon can diffuse rapidly in the b.c.t. structure and the virgin martensite undergoes temperature-dependent ageing above about -60^{0}C provided the carbon content is more than 0.2%. The influence of this rapid migration of carbon on the mechanical properties of the martensite can be appreciable. Kelly and Nutting (D.46) found that in plain-carbon steels a considerable increase in hardness occurs due to carbon precipitation during the quench.

Kelly and Nutting (D.46) have shown that the effect of substitutional solid solution hardening, involving

non-carbide forming elements (e.g. nickel) on the overall strength of martensite is very small. With strong carbide formers as substitutional elements (and with appreciable amounts of carbon), clustering may give rise to chemical hardening (D.47). However, Kelly and Nutting(D.46) have suggested that a large increase in the yield stress of martensite would not be expected.

In low-carbon steels the lath martensite contains a high density of dislocations(D.48). By comparing the strength of fine grained low-carbon ferrites and the strength of low-carbon martensites, Kelly and Nutting(D.46) have shown that the contribution of the dislocation sub-structure to the strength of carbon-containing martensites is relatively small. The proposal that internal twinning is partly responsible for the strength of high-carbon martensites was put forward by Kelly and Nutting(D.48), although the proposal has met some opposition(D.45). With regard to the relative effects of dislocations and twinning on the strength of martensite, Kelly and Nutting have discussed work on carbon-free iron-nickel alloys(D.46). In these alloys when the martensitic structure changes from laths containing a high density of dislocations to internally twinned plates there is no appreciable change in strength. If the twins have no effect on the strength, it can be

argued that the internally twinned martensite should be weaker than lath martensite. They conclude that the similarity in the strength of the two structures indicates that the twins provide a strengthening effect.

In the present work when accounting for the increase in the strength of S.T.A. martensite over that of conventional martensite, the effect of solid solution hardening, both by interstitial and substitutional elements, on the strength of the two martensites is not considered, since it will cause the same degree of strengthening in both cases. In the case of any sub-zero tempering (see section 2.54), it is assumed that the carbon precipitation will occur to the same extent in the two martensites.

The experimental observations clearly show (fig. 4.2) that the extent of transformation twinning in the S.T.A. martensite is less than in conventional martensite; it, therefore, appears that the decreased amount of twinning may be of importance from the point of view of the strength of S.T.A. martensite. The large, homogeneous distribution of dislocations in the S.T.A. martensite, fig. 4.2, would make slip difficult because of dislocation interaction.

The fact that the S.T.A. martensite shows more plates in the lower range of thickness than does the conventional martensite (fig. 3.22) is also likely to be

important. The refinement in the S.T.A. martensite plates can effectively enhance the yield stress by increasing the number of martensite boundaries per unit slip path. Phillips and Duckworth(D.49), using plain-carbon martensitic steel, have concluded that the increase in the hardness and tensile strength of martensite, produced after 'shock' austenitizing treatments, results from the fine plate size of the martensite.

Thus the small difference in the strength of the two martensites is due to refinement of the S.T.A. martensite plates and the high density of dislocations in the S.T.A. martensite plates.

4.62. Tempering and the strength of S.T.A. martensite.

Most of the study of tempered structures was done on the alloys containing molybdenum (INM1 and BISM1). Tempering of martensite in the iron-nickel-carbon alloy (INN1), both conventional and S.T.A., produced a gradual decrease in hardness as commonly observed in plain-carbon steels. The structural changes accompanying the variation in hardness in iron-nickel-carbon alloys have been discussed by Wells(D.50) and Tekin and Kelly(D.51). Wells, in particular, employed an alloy of similar composition to that used in the present investigation. Tempering at a low temperature (about 200°C) brings out ϵ-carbide precipitates as long narrow

plates (or laths) in more than one direction or in more than one plane in the martensite plate. On prolonged tempering, the ϵ -carbide dispersion coarsens and the precipitate becomes less coherent with the ferrite matrix. As the carbon continues to come out of solution and forms cementite at 300 - 400°C, an overall decrease in hardness results (fig. 3.24). The cementite precipitates as platelets on the fine twin interfaces. No carbide is nucleated on the austenite/martensite interface. In the later stages of tempering, the twins disappear and this leads to a further reduction in hardness.

In comparison with the tempered iron-nickel-carbon alloy (INN1) martensite, the effect of tempering on molybdenum-containing alloys (INM1 and BISM1) is somewhat different. Although molybdenum is a strong carbide former its diffusion rate in iron is considerably slower than that of carbon. As a result, there is an initial drop in hardness during isothermal tempering, fig. 3.25, associated with the precipitation of cementite (fig. 3.19c). With continued ageing, secondary hardening occurs from the precipitation of Mo_2C (figs. 3.32 and 3.33). The marked increase in hardness due to secondary hardening of both the martensites with increasing tempering temperature comes to a maximum at about 350°C (fig. 3.27) depending upon the tempering time, while

above this temperature there is a gradual softening. The hardness in the S.T.A. samples is greater than that of conventionally treated samples. No structural study in the overaged conditions was carried out; however, the softening after secondary hardening has been attributed to the growth of alloy carbide(D.43).

The structural study of the tempered martensite in iron-nickel-molybdenum-carbon alloys (INM1 and BISM1) has provided some basis for explaining the higher strength of tempered S.T.A. martensite (about 10%, extrapolated value) over that of conventional martensite in the peak hardness condition.

In view of the high defect content of the S.T.A. martensite and the precipitation of molybdenum carbide on these imperfections, fig. 3.30b, (which are suitable sites for nucleation) the tempered S.T.A. martensite (350°C for 100 hours) has shown finer precipitate particles than in the case of conventional martensite (figs. 3.33d and 3.32d). It may be pointed out here that the molybdenum atom is approximately 10 percent larger than an iron atom and for this reason may be expected to segregate to the dislocations and grain boundaries (fig. 3.30(b) and (c)). Assuming that the total volume of the precipitates is the same in both the martensites (and remains constant), the finer precipitates in the

case of S.T.A. martensite will be relatively closely spaced. Measurements have not been made of the size and spacing of the precipitate particles. However, from figs. 3.30b and 3.32d, the size of the precipitate particles can be approximately estimated as being about 50 - 125Å. Thomas et al(D.52), in work on an ausformed Fe-Ni-Mo-C alloy have calculated that the size of the molybdenum carbide (MoC) particles would have to be less than about 70Å for the particles to be cut by the dislocations. In view of the uncertain value of the particle size in the present work, it is difficult to predict the nature of the interaction of the precipitate particles with the dislocations; however, it seems that some cutting may occur.

In the case of conventional martensite (tempered at 350°C for 100 hours), the size of the precipitate particles (fig. 3.33d) is approximately 500 - 1000Å and it is likely that the Orowan mechanism(D.53) is operative whereby the dislocations pass between the precipitate particles, leaving encircling loops of dislocations around the particles; this mechanism involves relatively less energy than that required for the shearing of particles.

There are a few areas in the austenite region of the tempered S.T.A. structure, fig. 3.30c, showing narrow white regions with dark contrast on either side; these areas

may be interpreted as elastic coherency strains around precipitates. Kelly and Nicholson(D.54) have suggested that small coherent precipitates are usually sheared by dislocations and alloys containing such precipitates are characterized by a high initial yield stress. Payson(D.43) has attributed secondary hardening in alloy martensites to coherent precipitates of alloy carbide. However, in the present work, these effects were not detected in the martensite regions.

Thus, the factors contributing to the increased strength of S.T.A. martensite, tempered at 350°C for 100 hours, are the refinement in precipitate particle size, associated with precipitation of alloy carbide (Mo_2C) at dislocations in the S.T.A. martensite and possibly at the martensite/austenite interface.

Conclusions

The main results and conclusions from the present investigation of iron-nickel-carbon and iron-nickel-molybdenum alloys, austenitic at room temperature, are summarized below:

(1) The reverted austenite (S.T.A. austenite) produced by rapid heating of martensitic structure for short austenitizing times has been shown to have a higher strength than the conventionally annealed austenite. The degree of strengthening increases with increasing amounts of martensite present prior to austenitizing. The relationship between the amount of martensite and final strength of austenite is not linear. For relatively short times of austenitizing - about a minute - the yield stress and hardness are increased by a factor of 3 - 4.

(2) It is suggested that the enhancement in strength is primarily due to an increase in dislocation density resulting from structural volume changes.

(3) In most cases fragments of S.T.A. austenite have been observed in areas originally occupied by martensite plates. The fragments lay in two directions with respect to the initial martensite plates, in one case transversely across the original martensite plates and in the other case along the martensite plate. In the former orientation, the

fragments of the S.T.A. austenite have been shown to be twin related with respect to each other. The occurrence of fragments (of S.T.A. austenite) has been confirmed by carbon replica techniques. A few plates of S.T.A. austenite, comparable in size with the original martensite plate, have been observed containing a high density of jogged dislocations, suggesting a different mode of reversal.

(4) Interferometric techniques have established that the reversion is of martensitic nature - at least with the rate of heating employed in the present investigation.

(5) With increasing time of isothermal austenitizing in the range 600 - 700°C, the changes in hardness in the iron-nickel-carbon alloys are of sigmoidal form and, on the evidence of the structural study, it is suggested they arise from recovery processes involving a relatively high activation energy (i.e. ~ 150 Kcal/mol). In the iron-nickel-molybdenum-carbon alloys, the effects of relatively long times of austenitizing in the range 650 - 850°C are complicated by the occurrence of phase changes.

(6) S.T.A. martensite has a higher yield stress than the conventional martensite - both in the tempered and untempered conditions.

(7) In the untempered condition, the difference in the yield stress of the S.T.A. conventional martensite (~ 6%)

has been attributed to the refinement in the plate size and to the occurrence of less twinning as compared with the conventional martensite.

(8) The effects of tempering of the S.T.A. and conventional martensite in iron-nickel-molybdenum-carbon alloys have been studied in relation to the observed secondary hardening occurring in both the martensites. The higher secondary hardness of the S.T.A. martensite over that of the conventional martensite has been attributed to the finer dispersion of the particles of the alloy carbide. The tempering of S.T.A. martensite in iron-nickel-molybdenum-carbon alloys is primarily associated with alloy carbide precipitation at dislocations and at the martensite/austenite interface, while in the case of conventional martensite precipitates of alloy carbide occur along the twins.

Some suggestions for future work.

The more responsive nature of the austenite, than of the martensite, to rapid austenitizing, from the point of view of strengthening, has been established in the present investigation. It appears that the microstructure of the parent phase (martensite), prior to austenitizing, is of considerable importance with regard to the final strength of the reverted austenite. It will, therefore, be of interest to study the effects of rapid austenitizing on austenitic stainless steels since the microstructure of the martensite in these steels is distinctly different from that observed in this investigation. To this end, some research is being done in the Metallurgy Department of Imperial College. Similar work on some martensitic steels is also underway.

Study of dispersion hardening combined with rapid austenitizing in alloys belonging to ageing system, is an avenue of interest from both the academic and industrial points of view. A combination of rapid austenitizing followed by ausforming of carbon-containing austenitic commercial steels may result in better mechanical properties than either of these methods individually.

Acknowledgements

The author wishes to express his gratitude to Dr. D.R.F. West whose interest, guidance and encouragement has contributed to the successful completion of this work and to Professor J.G. Ball for the provision of research facilities. Thanks are also due to Miss J. Jonasdottir for proof reading.

The author also records his thanks to the Ministry of Technology for support of the work, including the provision of a bursary, and also th International Nickel Limited (Birmingham) and British Iron and Steel Research Association (Sheffield) for supply of material.

The author is also grateful to his colleagues in the group for stimulating discussions and to the permanent staff of the Metallurgy Department for their co-operation.

Appendix A

(The author is indebted to Dr. M.G. Hocking of the Metallurgy Department, Imperial College, for the following calculations).

Approximate calculations for carbon from 0.1 cm thick sample containing 0.4% of carbon and heated to about 1200°C for three hours in

a. Sealed evacuated silica tube (at pressure $\sim 10^{-4}$ mm.Hg).

b. Vacuum furnace with continuous pumping (i.e. unsealed). Vacuum of 10^{-5} - 10^{-4} was maintained.

If 'D' is the diffusion coefficient of carbon in iron ($\sim 10^{-6}$ cm^2/sec), 't' is the time (seconds) of heating and 'L' is the half thickness (cm) of the specimen, the value of the function $\frac{Dt}{L^2}$ is equal to

$$\frac{10^{-6} \times 10800}{0.05^2} \simeq 4$$

From the standard charts*, the value of the ratio $\frac{C_m - C_o}{C_s - C_o}$ corresponding to the value of $\frac{Dt}{L^2}$ (=4) is 0.9999

$$\text{i.e. } \frac{C_m - C_o}{C_s - C_o} \simeq 1$$

* Reference: Darken and Gurry "Physical Chemistry of Metals" page 447.

where C_m = mean carbon content of the sample, C_s = concentration of the carbon at the surface of the specimen after heating to 1200°C for 3 hours. C_o = initial carbon concentration (C_o = 0.4% = 400 ppm). We have

$$C_m - C_o = C_s - C_o \quad (C_o = 400 \text{ ppm})$$

$$\text{or } C_m = C_s$$

Thus the mean concentration of the carbon in the sample after three hours of heating at 1200°C equal the surface concentration.

a. <u>Sealed in silica tube:</u>

Volume of the evacuated silica tube = 100 c.c.

Weight of the specimen = 100 gms.

Assuming the reaction

$$2C + O_2 = 2CO$$

goes to completion i.e. all the oxygen (at pressure 10^{-4}mm. Hg) in the silica tube is used up by the carbon to form Co. The partial pressure of CO (pCO) will, therefore, be 2 x pO_2 $\simeq$ 2 x 10^{-7} atmosphere.

From the universal gas equation

$$pV = nRT.$$

p = partial pressure of CO = 2 x 10^{-7} atm.

V = volume of the tube filled with CO = 0.1 litre

n = number of moles of CO

R = gas constant = 0.08 litre. atm/deg°K.

T = absolute temperature = 1500°K.

the value of n can be calculated

$$n = \frac{2 \times 10^{-7} \times .1}{.08 \times 1500} \simeq 10^{-10} \text{ moles of Co}$$

$$\simeq 10^{-9} \text{ gm of carbon.}$$

Thus the silica tube can be filled with CO at 10^{-7} atm and only 10^{-9} gm of carbon will be lost from the initial concentration of 0.4% carbon. C_s will remain equal to C_m.

b. Unsealed samples: Carbon is not volatile and so it can escape as CO. When the vacuum pump is left connected, all the CO gas will be removed, but the gas cannot form continuously since there is no source of oxygen - assuming no leaks. Back-diffusion of oxygen from the atmosphere through the pump and into the crucible (containing the sample) can be neglected. Hence, again there should be no appreciable loss of carbon.

Appendix B.

Decarburization in the salt bath.

Technical advice received from I.C.I. (Witton, Birmingham) claims that the salts have no carburizing potential. For the prevention of decarburization, however, it was important to add a regenerator (supplied under the commercial name Regenerator "A") if the salt bath is to be used for treatments of more than eight hours duration.

Even with the addition of the regenerator, it was considered advisable to check whether [illegible] any significant decarburization took place during the heat treatments. An ordinary razor blade was immersed in the salt bath at 760°C for about twenty minutes followed by quenching in water. On bending the blade, it broke in a brittle fashion indicating, thereby, that no decarburization had occurred. Thus it can be deduced that no decarburization occurred in the samples used in the investigation during heat treatments in the salt bath.

Appendix C.

The exact carbon content of alloys, as marked with an asterisk in table, is not known. Two sets of analysis were carried out by International Nickel Co. Ltd. The first was done on an as-cast sample and gave 0.42% carbon for INN1 and 0.43% carbon for INN2. It was found that the hardness of the annealed austenite in the latter alloy was significantly higher than that of the former and a repeat chemical analysis was done on fabricated samples. This gave carbon values of 0.37% and 0.30% respectively. A further chemical analysis for carbon in INN2 alloy gave values of 0.40, 0.41 and 0.40% (triplicate). The carbon content of INN2 appears to be

between 0.4 and 0.43 while INN1 alloy appears to have a somewhat lower value. The reason for this anomaly is not known. In spite of the uncertainty in carbon figures the results of the investigation are not significantly affected.

Appendix D.

d-spacings (Å) of planes (hk.l) in Mo_2C (c.p. hex).

($c = 4.724$Å; $a = 3.002$Å)

$$\frac{1}{d^2} = .147(h^2+hk+l^2) + 0.0448(l^2)$$

Planes(hk.l)	$\frac{1}{d^2}$	$\frac{1}{d}$
001	0.0448	0.211
$1\bar{1}0, 0\bar{1}0, 100$	0.147	0.383
$\bar{1}00, 010, \bar{1}10$	"	"
$002, 00\bar{2}$	0.1792	0.423
$1\bar{1}1, \bar{1}1\bar{1}, 10\bar{1},$	0.1918	0.438
$\bar{1}01, 1\bar{1}\bar{1}, 01\bar{1}, 0\bar{1}1$	"	"
$0\bar{1}2, 01\bar{2}, 01\bar{2}, 0\bar{1}\bar{2},$	0.3262	0.571
$10\bar{2}, \bar{1}1\bar{2}, 1\bar{1}\bar{2},$	"	"
$\bar{1}\bar{1}0, 110,$	0.441	0.664
$1\bar{2}0, 2\bar{1}0, \bar{2}10$	"	"
$11\bar{1}, 2\bar{1}1$	0.4858	0.697
$\bar{2}12, 11\bar{2}, 2\bar{1}2,$	0.6202	0.787
$2\bar{1}\bar{2}, \bar{2}1\bar{2}, \bar{1}22$	"	"
$1\bar{1}3, \bar{1}03, 103, \bar{1}13$	0.561	0.741
$20\bar{1}, 021$	0.6328	0.795
$2\bar{1}3$	0.843	.918
302	1.4982	1.21

References.

A.1. Malyshev et al Inst. Fiz. Metal 1958, vol.20, p.339.

A.2. Krauss, G. Acta Met vol.11 June, 1963.

A.3. Phillips and Duckworth N.P.L. report Jan. 1963. MG/E/143/62. (Unpublished).

A.4. R. Phillips et al BISRA report MG/E/111/64. (Unpublished)

A.5. Schmatz and Zackay "Mechanical Properties of deformed metastable austenite". Trans ASM vol.51, 1959 p.229.

A.6. McEvily et al Trans. ASM 56, 1963, p.753.

A.7. Johari and Thomas. Trans ASM, vol 58. 1965, p.563.

A.8. Schmatz et al. NPL. Symposium; Teddington (England) January 1963.

A.9. Raymond. L and Renter. W.G; Acta Met vol.12,1964,p.949.

A.10. Thomas et al. "High Strength Material" by V.F. Zackay. John Wiley and Sones.

A.11. C.G. Bieber; Metal Progress 78, 1960, p.99.

A.12. R.F. Decker NPL Symposium No:15 1964, p.649.

A.13. Krauss and Cohen Trans AIME, vol.224 1962, p.1212.

A.14. Gorback and Malyshev; Fiz. metal. metalloved 17, No-2. 229-233 1964.

A.15. G.Wasserman Arch. Eisenhuttenw, 1932-33 vol-6 p.347.

A.16. V.N. Gridnev et al. Metalloved i Obrabotka metal 1957,p7

A.17. Malyshew. K.A et al. Metalloved i Obrabotka metal 1962 p.21.

A.18. Goldberg and Connor Nature Jan. 1966.

A.19. V.G. Gorback and E.D. Butakova Fiz. metal. metalloved 16. No:2 1963 p.292.

A.20. Dash and N. Brown. Abstract from the Oct. 1965 meeting. Detroit; AIME.

A.21. S. Jana and C.M. Wayman Trans AIME vol.239 August 19[illegible] p-1187.

A.22. Kessler and Pitsch Acta Met vol.15, 1967 p.401.

A.23. Golochina. Ya. M: Probl metallography metal Physics Moscow, 7, p-281 1961.

A.24. B.Edmondson and T.Ko; Acta Met. vol.2. March 1954,p-235.

A.25. B.K. Sokolov and V.G. Gorbach; Inst fiz, metal, Akad, Nauk. SSSR 22 1959.

A.26. Krauss and Shapiro Unpublished.

A.27. Cohen M; "Phase Transformations in solids" John Wiley; N.Y. 1951, p.588.

A.28. Kessler and Pitsch. Acta Met 13, p-871, 1963.

A.29. Wechsler et al J. Metals 5. 1953 p-1503.

A.30. Kuhlmann-Wilsdorf et al "Strengthening mechanisms in solids p-137 A.S.M. Ohio 1962.

A.31. Breedis Trans AIME. 1960 p-218.

A.32. Thomas and Krauss Trans. AIME August 1967 vol.239 p-[illegible]

B.1. O.A. Ankara Ph.D. Thesis Metallurgy Dept. Imperial College; London S.W.7. 1964.

B.2. Recrystallization, Grain Growth and Texture A.S.M. Oct.1965 p-592.

B.3. Report no: 302 June '65. Edgar. C. Bain Lab.; U.S. Steel Corporation Research Centre; Monroeville, Pn. U.S.A.

B.4. K. Hozelitz "Ferromagnetic Properties of Metals and alloys". O.U.P. 1952.

B.5. J. Crangle and W. Sucksmith; JISI, 168, 1951 p-141.

B.6. Winchell and Cohen; Trans AIME vol.55 No:2 June '62.

B.7. Bollman; Phys Review 1956, 103 p-1588.

B.8. Smith and Guttman; J. Metal; N.Y. vol.5. p-81 1953.

C.1. Winchell. P.G. (Communication).

C.2. Kelly. P.M. and Nutting. N: J.I.S.I March 1961, vol.197 p-199.

C.3. Gladman and Woodhead. J.I.S.I. 194, p-189, 1960.

C.4. Krauss. G.; Acta Met, vol-11 p-499 June 1963.

C.5. Edmondson and Ko, Acta Met, vol-2 March 1954.

C.6. Leymonie. C and Lacombe. P.L.; Acta Met 1959 vol.56 p-74.

C.7. Honeycombe.R.W.K.,J.I.S.I. vol-204 Nov.1966 p-1114.

C.8. Tanino et al. J.I.S.I. August vol-205 August 1967 p-874.

C.9. Pitsch and Schrader. Arch. Eisenh. 1958, 29. p-485.

D.1. As A.19.

D.2. As C.4.

D.3. Takamura et al Am. Phys. Soc. Series II 5, 182, 1960.

D.4. D.Kuhlmann-Wilsdorf and Wilsdorf. "Electron microscopy and strength of crystals by Thomas and Washburn. Interscience, N.Y. p-583.

D.5. E.O. Hall; "Twinning and diffusionless transformation in metals" Butterworths Sc. Pub. 1954.

D.6. Ogilvie, G.J; Thesis; Leeds University, 1951 (Cross reference from D.5).

D.7. As B.6.

D.8. Special Report no: 93 I.S.I. May 1965.

D.9. As C.2.

D.10. Seitz. F; Advanc Phys; 1. p-43 1952.

D.11. Cottrell. A.H; Symposium on "Vacancies and other point defects in metal and alloys" Institute of metals. Monograph no:23 1957.

D.12. Kuhlmann-Wilsdorf.D; Phil Mag; vol.3. p-125 1958.

D.13. Smallman and Eikum "Lattice defects in quenched metals" Ed. by Cotterill et al. Academic Press 1965 p.591.

D.14. As A.31.

D.15. As D.5.

D.16. Sastri A.S. Ph.D. Thesis 1963. Metallurgy Dept. Imperial College. London. S.W.7.

D.16A. As A.24.

D.17. Hall.E.O; Proc. of Phyc Soc. 1951, 64(9) No:381B.

D.18. N.J. Petch JISI. 1953, 174 p-25.

D.19. Heslop J; and Petch N.J; Phil Mag 1956, 1, 866.

D.20. Petch and et al Phil Mag 1962 7, 45.

D.21. Conrad.H; "Iron and its dilute solid solution" AIME Proc of conference (Michigan) Oct. 23 1961.

D.22. A.R. Cox Private Communication.

D.23. A.S.Keh and S.Weissmann; As D.4.

D.24. Edigton and Smallman; Acta Met 1964 12, p-1313.

D.25. Van Thorne and Thomas ibid 1963 11, p-881.

D.26. As C.4.

D.27. As D.4. p-231.

D.28. Kelly and Nutting Proc. Roy. Soc.1960, 259A, p-45.

D.29. As A.21.

D.30. As A.22.

D.31. Thomas et al "High Strength Materials" Proc of Barkeley; Ed. by V.F. Zackay, John Wiley & Sons. p-251.

D.32. R.W. Cahn; "Physical Metallurgy" North-Holland Pub. Co; Amsterdam 1965, p-925.

D.33. As A.13.

D.34. K. Lucke and K. Detert. Acta Met, 1957, vol.5. p-628.

D.35. A.H. Cottrell; Report on "Strength of Solids" Proc. Phys. Soc. 1948, p-30.

D.36. Anst and Rutter "Recovery and Recrystallization of metals" John Wiley & Sons. N.Y. 1963 p-131.

D.37. As C.6.

D.38. G.V. Kurdjumow J.I.S.I. 195 (1960) p-26.

D.39. As C.2.

D.40. Werner, Averbach and Cohen. Trans ASM, 49 1957, p-823.

D.41. E. Smith and J. Nutting JISI, 187 1957 p-314.

D.42. R.W.K. Honeycombe et al. JISI. Nov.1966 vol.204 p-1114.

D.43. P.Payson Trans ASM SI (1959) p-60.

D.44. Hondremont et al. Trans AIME. 216 (1953) p-260.

D.45. As B.6.

D.46. As D.8. p-166.

D.47. A.Kelly and M.E. Fine Acta Met 1957 vol.5,p-365.

D.48. Kelly and Nutting Proc. Roy. Soc. 1960 259A, p-45.

D.50. M.G.H.Wells. Acta Met. vol.12, 1964 p-389.

D.51. "Precipitation from Iron-base alloys". Met. Soc. Conference vol-28.Cleveland, Ohio Oct.1963. Ed by Speich and Clark.

D.52. As D.31.

D.53. Orowan. E. "A Symposium on internal stresses" Inst of Metals 1948, London. p-451.

D.54. A.Kelly and R.B. Nicholson. "Precipitation Hardening". Prog. in Material Soc. vol.10. p-151.